

Université d'Ottawa • University of Ottawa



Université d'Ottawa - University of Ottawa

FACULTÉ DES ÉTUDES SUPÉRIEURES
ET POSTDOCTORALES

FACULTY OF GRADUATE AND
POSTDOCTORAL STUDIES

SHEN, Jiacheng

AUTEUR DE LA THÈSE - AUTHOR OF THESIS

M.A.Sc. (Chemical Engineering – spec.: Environmental Engineering)

GRADE - DEGREE

Chemical Engineering

FACULTÉ, ÉCOLE, DÉPARTEMENT - FACULTY, SCHOOL, DEPARTMENT

TITRE DE LA THÈSE - TITLE OF THE THESIS

Biosorption of Cupric and Cadmium Ions by Corncob Particles

Zdravko Duvnjak

DIRECTEUR DE LA THÈSE - THESIS SUPERVISOR

EXAMINATEURS DE LA THÈSE - THESIS EXAMINERS

Boguslaw Kruczek

Jason Zhang

J.-M. De Koninck, Ph.D.

LE DOYEN DE LA FACULTÉ DES ÉTUDES
SUPÉRIEURES ET POSTDOCTORALES

SIGNATURE

DEAN OF THE FACULTY OF GRADUATE
AND POSTDOCTORAL STUDIES

**BIOSORPTION OF CUPRIC AND CADMIUM IONS
BY CORNCOB PARTICLES**

JIACHENG SHEN

Thesis submitted to the Faculty of Graduate and Postdoctoral Studies
in partial fulfillment of the requirements for the degree of Master in Applied Science

Department of Chemical Engineering
University of Ottawa

© Jiacheng Shen, Ottawa, Canada, 2003



National Library
of Canada

Bibliothèque nationale
du Canada

Acquisitions and
Bibliographic Services

Acquisitons et
services bibliographiques

395 Wellington Street
Ottawa ON K1A 0N4
Canada

395, rue Wellington
Ottawa ON K1A 0N4
Canada

Your file *Votre référence*
ISBN: 0-612-89910-1
Our file *Notre référence*
ISBN: 0-612-89910-1

The author has granted a non-exclusive licence allowing the National Library of Canada to reproduce, loan, distribute or sell copies of this thesis in microform, paper or electronic formats.

L'auteur a accordé une licence non exclusive permettant à la Bibliothèque nationale du Canada de reproduire, prêter, distribuer ou vendre des copies de cette thèse sous la forme de microfiche/film, de reproduction sur papier ou sur format électronique.

The author retains ownership of the copyright in this thesis. Neither the thesis nor substantial extracts from it may be printed or otherwise reproduced without the author's permission.

L'auteur conserve la propriété du droit d'auteur qui protège cette thèse. Ni la thèse ni des extraits substantiels de celle-ci ne doivent être imprimés ou autrement reproduits sans son autorisation.

In compliance with the Canadian Privacy Act some supporting forms may have been removed from this dissertation.

Conformément à la loi canadienne sur la protection de la vie privée, quelques formulaires secondaires ont été enlevés de ce manuscrit.

While these forms may be included in the document page count, their removal does not represent any loss of content from the dissertation.

Bien que ces formulaires aient inclus dans la pagination, il n'y aura aucun contenu manquant.

Canada

ABSTRACT

The effects of various parameters, such as initial pH, biomass concentration, temperature, buffer, agitation speed, and particle size, on the biosorption of cupric and cadmium ions by the corncob particles were investigated. It was found that the uptake of the two ions by the corncob particles increases with the increase of the initial pH in the range of 4.0 – 6.0 for copper and 4.0 – 8.3 for cadmium, temperature, and initial ion concentration, and with the decrease of particle size and biomass concentration. A modified Langmuir model, which considers the effect of pH on the isotherm, is appropriate for the experimental equilibrium data. The enthalpy changes calculated from the equilibrium constants at various temperatures indicate that the biosorption processes of copper and cadmium on the corncob particles are exothermic. The smaller corncob particles have a higher adsorption rate and uptake, which suggests that the particle size not only affects adsorption kinetics, but also the equilibrium (isotherm).

A novel reversible surface reaction model combined with an effectiveness factor was developed. An experimental procedure was designed to determine four constants (the effectiveness factor, the maximum adsorption capacity, the forward and backward rate constants) in the model. Two regression constants in each step of the procedure were obtained to avoid the uncertainty of nonlinear regression. The intrinsic forward and backward rate constants were determined to be 1.082 l/(mmol.min) and 0.472 min⁻¹ for copper, and 2.88 l/(mmol.min) and 0.184 min⁻¹ for cadmium based on the elimination of external and intraparticle diffusions. The other two constants, the maximum adsorption capacity, q_m , and the effectiveness factor, η , in the model, were determined as a function of initial pH and particle size. These two parameters increase with the increase of initial

pH, and the decrease of particle size. A simple external diffusion model can only describe the solute change in the solution for the initial 5 minutes, which suggests that biosorptions of copper and cadmium by the corncob particles are controlled first by the external diffusion of metal ions, and then the intraparticle diffusion of metal ions.

In addition, a preliminary study on competitive biosorption of copper and cadmium ions from their mixture by the corncob particles was conducted. The experiments show that the uptake of copper ions in the mixture increases with the increase of total metal ion concentration. However, the uptake of cadmium first increases, reaches a maximum point, and then decreases with the increase of total metal ion concentration (inversed U-shaped isotherm). To describe these inversed U-shaped isotherms, a new competitive adsorption model has been proposed and its parameters were estimated.

The pH at zero charge point of the corncob particles was measured (pH_{zcp} 4.97) by applying the primary equilibrium method of H^+ and OH^- . The pH_{zcp} is used to distinguish the chemical free energy from the solvation and coulombic free energies in the James-Healy model. The calculated results indicate that the chemical and solvation free energies contribute much to the adsorption free energy. The chemical free energy is constant, while the solvation free energy increases with the increase of the pH. However, their effects are opposite (with opposite signs). The adsorption free energy will increase with the pH value during biosorption processes of cupric and cadmium ions on the corncob particles.

RÉSUMÉ

Les effets de certains paramètres tels que le pH initial, la concentration de biomasse, la température, la solution tampon, la vitesse d'agitation et la dimension particulaire sur la biosorption d'ions de cuivre et de cadmium sur des particules d'épi de maïs ont été investigués. La prise de deux ions par les particules d'épi de maïs augmente avec l'augmentation du pH initial, de la température et de la concentration d'ions initiale, et avec la diminution de la dimension particulaire et de la concentration de biomasse. Un modèle de Langmuir modifié prenant en considération l'effet du pH sur l'isotherme, ajuste bien les données expérimentales. Les changements d'enthalpie, calculés à partir de constantes d'équilibre, avec la température indiquent que les biosorptions de cuivre et de cadmium sur des particules d'épi de maïs sont des procédés exothermiques. Les particules d'épi de maïs démontrent un taux d'adsorption et une prise plus élevés, ce qui suggère que la dimension particulaire non seulement affecte la cinétique d'adsorption, mais aussi l'équilibre (isotherme).

Un modèle novateur de réaction de surface combiné avec un facteur d'efficacité a été développé. Une procédure expérimentale a été conçue afin de déterminer quatre paramètres (le facteur d'efficacité, la capacité maximale d'adsorption, les constantes de taux directe et inverse) dans le modèle. À chaque étape de la procédure, deux paramètres ont été utilisés afin d'éviter l'incertitude de la régression non linéaire. Les constantes intrinsèques de taux directe et inverse sont $1.082 \text{ l}/(\text{mmol}\cdot\text{min})$ et 0.472 min^{-1} pour le cuivre, et $2.88 \text{ l}/(\text{mmol}\cdot\text{min})$ et 0.184 min^{-1} le cadmium basé sur l'élimination de diffusions externe et intraparticulaire. Les deux autres paramètres (la capacité maximale d'adsorption, q_m et le facteur d'efficacité η) dans le modèle ont été déterminés en tant que

fonction du pH initial et de la dimension particulaire. Les deux paramètres augmentent avec une augmentation du pH initial et avec une diminution de la dimension particulaire. Un modèle simple de diffusion externe ne peut que décrire le changement de soluté en solution pour les 5 premières minutes, ce qui suggère que les biosorptions de cuivre et de cadmium sur des particules d'épi de maïs soit contrôlée premièrement par la diffusion externe d'ions de métaux, et ensuite par la diffusion intraparticulaire d'ions de métaux.

De plus, une étude préliminaire a été entreprise, portant sur la biosorption compétitive d'ions de cuivre et de cadmium à partir de leur mélange sur des particules d'épi de maïs. Les expériences ont démontré que la prise d'ions de cuivre dans le mélange augmente avec l'augmentation de la concentration totale d'ions de métaux. Par contre, la prise de cadmium augmente initialement, atteint un point maximal et ensuite diminue avec l'augmentation de la concentration totale d'ions de métaux. Afin de décrire l'isotherme de ce dernier, un nouveau modèle d'adsorption compétitive a été proposé et ses paramètres ont été estimés.

Le pH au point de charge nulle de particules d'épi de maïs a été mesuré (pH_{zcp} 4.97) en appliquant la méthode d'équilibre primaire de H^+ et de OH^- . Le pH_{zcp} est utilisé afin de distinguer l'énergie libre chimique des énergies libres coulombique et de solvatisation dans le modèle de James-Healy. Les résultats calculés indiquent que les énergies libres chimique et de solvatisation contribuent beaucoup à l'énergie libre d'adsorption. L'énergie libre chimique est constante, alors que l'énergie libre de solvatisation augmente avec une augmentation de pH, mais leurs effets sont opposés (signes opposés). L'énergie libre d'adsorption augmentera avec le pH au cours des procédés de biosorption d'ions de cuivre et de cadmium sur des particules d'épi de maïs.

TABLE OF CONTENTS

ABSTRACT	I
RÉSUMÉ	iii
TABLE OF CONTENTS	v
LIST OF FIGURES	ix
LIST OF TABLES	xii
ACKNOWLEDGMENTS	xiv
NOMENCLATURE	xv
CHAPTER ONE	
INTRODUCTION	1
1.1 Biosorbents	1
1.2 Sources of Copper and Cadmium Ions as Pollutants in the Environment	4
1.2.1 Copper	4
1.2.2 Cadmium	5
1.3 Objectives	6
CHAPTER TWO	
METHODS FOR THE REMOVAL OF METAL IONS FROM WASTEWATER	9
2.1 Chemical Precipitation	9
2.1.1 Chemical Precipitation Principle	9
2.1.2 Chemical Precipitation for Cupric and Cadmium Ions	10
2.2 Ion Exchange	11
2.2.1 Principle of Ion Exchange	11
2.2.2 Ion Exchange for Cupric and Cadmium Ions	12

2.3 Adsorption	12
2.3.1 Principle of Adsorption	12
2.3.2 Adsorption Process	14
2.3.3 Adsorption of Copper and Cadmium Ions	17
CHAPTER THREE	
LITERATURE REVIEW OF BIOSORPTION	
AND ADSORPTION MODELS	18
3.1 Biosorption by Agricultural By-Products	18
3.2 Competitive Adsorption of Metal Ions	21
3.3 Adsorption Models	22
3.3.1 Equilibrium Models	22
3.3.2. Kinetic Models	25
CHAPTER FOUR	
DEVELOPMENT OF NOVEL EQUILIBRIUM	
AND KINETICS MODELS	32
4.1 A Modified Langmuir Model Including Effect of pH	32
4.2 An Equilibrium Model for Competitive Adsorption	33
4.3 A Reversible Surface Reaction Model Combined with an Effectiveness Factor	34
4.3.1 The Model Development	35
4.3.2 The Solution of Model	37
4.3.3 The Determination Strategy of Model Parameters and Design of Experiments	38

CHAPTER FIVE	
EXPERIMENTAL	39
5.1 Materials and Methods	39
5.1.1 Materials	39
5.1.2 Analytical Method	42
5.2 Experimental Technique	42
5.2.1 Equilibrium of Adsorption (Adsorption Isotherm)	42
5.2.2 Kinetics of Adsorption	46
5.2.3 Measurement of pH at Zero Charge Point of Corncob Particles	46
CHAPTER SIX	
RESULTS AND DISCUSSIONS	48
6.1 Effect of pH on Adsorption Isotherms	48
6.2 Effect of pH on Adsorption Isotherms for Copper and Cadmium in Mixture	57
6.3 Effect of Temperature on Adsorption Isotherms	63
6.4 Effect of Agitation Speed on Kinetics of Adsorption	70
6.5 Effect of Particle Size on Kinetics of Adsorption	76
6.6 Effect of Initial pH on Kinetics of Adsorption	81
6.7 Effect of Biomass Concentration on Kinetics of Adsorption	86
6.8 Effect of Initial Metal Ion Concentration on Kinetics of Adsorption	90
6.9 Effect of Pretreatment of Corncob Particles with Sodium Hydroxide	95

6.10 The Estimation of Free Energies of Adsorption at Various pH Values and 25°C	96
CHAPTER SEVEN	
CONCLUSIONS AND RECOMMENDATIONS	102
7.1 Conclusions	102
7.2 Recommendations	103
REFERENCES	105
APPENDIX	
One Example of Determination of Parameters in Eq. (4.19)	112

LIST OF FIGURES

Figure 5.1: Corncob Particles Composition	40
Figure 5.2: Relationship between Bulk Densities and Size of Corncob Particles	40
Figure 5.3: Copper Concentration Comparison Before and After Membrane Filtration	45
Figure 5.4: Cadmium Concentration Comparison Before and After Membrane Filtration	45
Figure 6.1: Effect of pH on Adsorption Isotherms for Copper in Water Solution (mixed size particles)	49
Figure 6.2: Effect of pH on Adsorption Isotherms for Copper in Water solution (0.21 mm size particles)	49
Figure 6.3: Effect of pH on Adsorption Isotherms for Copper with MES (mixed size particles)	50
Figure 6.4: Effect of pH on Adsorption Isotherms for Cadmium in Water Solution (mixed size particles)	50
Figure 6.5: Effect of pH on Adsorption Isotherms for Cadmium in Water solution (0.21 mm size particles)	51
Figure 6.6: Effect of pH on Adsorption Isotherms for Cadmium with HEPES (mixed size particles)	51
Figure 6.7: Effect of pH on Adsorption Isotherms for Cadmium with MES (mixed size particles)	52
Figure 6.8: Effect of pH on isotherms of copper with MES (using Eq. 4.7)	56
Figure 6.9: Effect of pH on isotherms of cadmium with HEPES (using Eq. 4.7)	56
Figure 6.10: Effect of pH on Adsorption Isotherms for Copper in Mixture (mixed size particles, mol. ratio 1.77)	58
Figure 6.11: Effect of pH on Adsorption Isotherms for Cadmium in Mixture (mixed size particles, mol. ratio 1.77)	58
Figure 6.12: Effect of pH on Adsorption Isotherms for Copper in Mixture (mixed size particles, mol. ratio 1.00)	59

Figure 6.13: Effect of pH on Adsorption Isotherms for Cadmium in Mixture (mixed size particles, mol. ratio 1.00)	59
Figure 6.14: Temperature Effect on Adsorption Isotherms for Copper with MES (mixed size particles, pH 5.5)	64
Figure 6.15: Temperature Effect on Adsorption Isotherms for Cadmium with HEPES (mixed size particles, pH 7.6)	64
Figure 6.16: Effect of Temperature on Equilibrium Constant K_c for Copper	68
Figure 6.17: Effect of Temperature on Equilibrium Constant K_c for Cadmium	68
Figure 6.18: Effect of Agitation Speed on Copper Concentration in Solution	71
Figure 6.19: Effect of Agitation Speed on Cadmium Concentration in Solution	71
Figure 6.20: Effect of Agitation Speed on Copper Concentration in Solution (Eq. 3.11)	73
Figure 6.21: Effect of Agitation Speed on Cadmium Concentration in Solution (Eq. 3.11)	73
Figure 6.22: The Relationship between External Diffusion Coefficient and Reynolds Number	74
Figure 6.23: Effect of Corncob Particle Size on Copper Concentration in Solution	77
Figure 6.24: Effect of Corncob Particle Size on Uptake of Copper	77
Figure 6.25: Effect of Corncob Particle Size on Cadmium Concentration in Solution	78
Figure 6.26: Effect of Corncob Particle Size on Uptake of Cadmium	78
Figure 6.27: Effect of pH on Copper Concentration in Solution (corncob concn. 10 g/l)	82
Figure 6.28: Effect of pH on Uptake of Copper (corncob concn. 10 g/l)	82
Figure 6.29: Effect of pH on Copper Concentration in Solution (corncob concn. 20 g/l)	83
Figure 6.30: Effect of pH on Uptake of Copper (corncob concn. 20 g/l)	83

Figure 6.31: Effect of pH on Cadmium Concentration in Solution (corncob concn. 10 g/l)	84
Figure 6.32: Effect of pH on Uptake of Cadmium (corncob concn. 10 g/l)	84
Figure 6.33: Effect of Corncob Concentration on Copper Concentration in Solution	87
Figure 6.34: Effect of Corncob Concentration on Uptake of Copper	87
Figure 6.35: Effect of Corncob Concentration on Cadmium Concentration in Solution	88
Figure 6.36: Effect of Corncob Concentration on Uptake of Cadmium	88
Figure 6.37: Effect of Corncob Concentration on Cadmium Concentration in Solution (initial concentration of cadmium 5 mg/l)	89
Figure 6.38: Effect of Initial Concentration on Copper Concentration in Solution (initial pH 4.8)	92
Figure 6.39: Effect of Initial Concentration on Uptake of Copper (initial pH 4.8)	92
Figure 6.40: Effect of Initial Concentration on Copper Concentration in Solution (initial pH 5.9)	93
Figure 6.41: Effect of Initial Concentration on Uptake of Copper (initial pH 5.9)	93
Figure 6.42: Effect of Initial Concentration on Cadmium Concentration in Solution (initial pH 7.6)	94
Figure 6.43: Effect of Initial Concentration on Uptake of Cadmium (initial pH 7.6)	94
Figure 6.44: Effect of NaOH Pretreatment on Adsorption Isotherms of Copper	96
Figure 6.45: The Relationship between Free Energies and pH for Copper	101
Figure 6.46: The Relationship between Free Energies and pH for Cadmium	101

LIST OF TABLES

Table 6.1: Parameters: q_m and K_l of Langmuir Model (Eq. 4.1) for Copper at Various pH Values	54
Table 6.2: Parameters: q_m and K_l of Langmuir Model (Eq. 4.1) for Cadmium at Various pH Values	54
Table 6.3: Parameters: q_{mzcp}, k, K_0, and n of Eqs. 4.3, 4.6 for Copper	57
Table 6.4: Parameters: q_{mzcp}, k, K_0, and n of Eqs. 4.3, 4.6 for Cadmium	57
Table 6.5: Metal Ion Data	62
Table 6.6: Interaction Factors: δ_1, δ_2, ε_1, and ε_2 of Isotherms (Eqs. 4.8, 4.9) in Mixture of Copper and Cadmium at Various pH Values	62
Table 6.7: Parameters: q_m and K_l of Langmuir Model (Eq. 3.1) for Copper with MES at pH 5.5 and Various Temperatures	65
Table 6.8: Parameters: q_m and K_l of Langmuir Model (Eq. 3.1) for Cadmium with HEPES at pH 7.6 and Various Temperatures	65
Table 6.9: The Relationship Between Specific Area and Size of Corncob Particles ($m = 10$ g/l)	72
Table 6.10: Parameters: η and q_m in Eq. 4.19 for Copper at Various Corncob Particle Sizes ($k_{ads} = 1.082$ l/(mmol.min), $k_{desH} = 0.472$ min⁻¹)	80
Table 6.11: Parameters: η and q_m in Eq. 4.19 for Cadmium at Various Corncob Particle Sizes ($k_{ads} = 2.88$ l/(mmol.min), $k_{desH} = 0.184$ min⁻¹)	80
Table 6.12: Parameters: η and q_m in Eq. 4.19 for Copper at Various pH ($k_{ads} = 1.082$ l/(mmol.min), $k_{desH} = 0.472$ min⁻¹)	85
Table 6.13: Parameters: η and q_m in Eq. 4.19 for Cadmium at Various pH ($k_{ads} = 2.88$ l/(mmol.min), $k_{desH} = 0.184$ min⁻¹)	85
Table 6.14: Parameters: η and q_m in Eq. 4.19 for Copper at Various Corncob Concentrations ($k_{ads} = 1.082$ l/(mmol.min), $k_{desH} = 0.472$ min⁻¹)	90

**Table 6.15: Parameters: η and q_m in Eq. 4.19 for Cadmium
at Various Corncob Concentrations
($k_{ads} = 2.88 \text{ l}/(\text{mmol}\cdot\text{min})$, $k_{desH} = 0.184 \text{ min}^{-1}$)**

91

ACKNOWLEDGMENTS

I would like to express my sincere gratitude to Dr. Z. Duvnjak for his support, guidance and financial assistance throughout this project.

I also would like to express my gratitude to my laboratory colleagues E. Martinez, Hasan Atiyeh, and S. Kumarappan for their help in the laboratory.

My Sincere thanks to technicians of Department of Chemical Engineering, Mr. L. Tremblay, G. Nina, and F. Zioldo for their technical assistance during the experiments.

NOMENCLATURE

Symbols

- a coefficient for regression (-)
- a_i constant of multiply- components isotherm derived from the corresponding individual Langmuir isotherm equations
- a_m specific area of the particle (m^2/m^3)
- b coefficient for regression (-)
- b_j constant of multiply- components isotherm derived from the corresponding individual Langmuir isotherm equation (-)
- c coefficient for regression or solute concentration (mmol/l) in the bulk solution
- c_H proton concentration in solution (mmol/l)
- c_o initial solute concentration in suspension (mmol/l)
- c_e solute equilibrium concentration in solution (mmol/l)
- c_s solute concentration at the surface of adsorbent (mmol/g)
- D integrate constant (-)
- D_e effective diffusion coefficient (m^2/s)
- D_i diameter of impeller (m)
- D_m molecule (or ion) diffusion coefficient (m^2/s)
- D_p pore diffusion coefficient (m^2/s)
- D_s surface diffusion coefficient (m^2/s)
- d coefficient for regression (-)
- d_p average particle size (m)
- E_1 activation energies for forward reactions (J/mol)

- E_2 activation energies for reverse reactions (J/mol)
- e elementary charge (1.60×10^{-19} C)
- erf error function
- F Faraday constant (96485 C/mol)
- K equilibrium constant (-)
- K_{chem} specific chemical equilibrium constant (-)
- K_e equilibrium constant (-)
- K_{coul} coulombic equilibrium constant (-)
- K_{solv} solvation equilibrium constant (-)
- K_{sp} solubility product of insoluble salt (-)
- K_L coefficient in McKay and Allen Model (l/g)
- K_1 Langmuir constant (l/mmol)
- K_t equilibrium binding constant corresponding to the maximum binding energy ($K_t = \exp(-\Delta G_{\text{max}}/RT)$) (l/mol)
- k constant for regression (-)
- k_1 rate constant of pseudo-first sorption or the frequency (or preexponential) factor (-)
- k_2 rate constant of pseudo-second order sorption or the frequency (or preexponential) factor (g/(mmol.min))
- k_{ads} forward rate constant ($k_1 \exp(-E_1/RT)$) (l/(mmol.min))
- k_{des} backward rate constant ($k_2 \exp(-E_2/RT)$) (l/(mmol.min))
- k_{desH} backward rate constant ($k_{\text{des}}[\text{H}^+]$) (min^{-1})
- k_F Freundlich constant ($\text{l.mol}^{1-n}/\text{g}$)
- k_f mass transfer coefficient between bulk solution and solid surface (m/s)
- k_p point value of the mass transfer coefficient (m/s)

- I ionic strength (mol/l)
- M initial quantity (gram) of adsorbent in the suspension (g/l)
- M_s adsorbent quantity in McKay and Allen Model (g/l)
- N Avogadro's constant ($6.022 \times 10^{23} \text{ mol}^{-1}$)
- n agitation speed or a constant for regression (round per second)
- q uptake on adsorbent at equilibrium (mmol/g)
- q_∞ uptake of metal ion at equilibrium or a constant for regression (mmol/g)
- q_m maximum adsorption capacity in adsorbent or a constant for regression (mmol/g)
- q_{mzcp} constant for regression (-)
- q_{m0} constant for regression (mmol/g)
- q_{mzcp} no charged activated site at pH_{zcp} . (mmol/g)
- q_t differential surface capacity per unit binding energy (mol/kJ)
- R general gas constant (J/(K.mol))
- r radial distance from the center of the particle sphere (m)
- r_{ion} ion radius (m)
- r_w water radius (m)
- S_s specific area of adsorbent in McKay and Allen Model (m^2/m^3)
- T absolute temperature (K)
- v water volume in the beaker (l)
- x metal ion radius plus water molecular diameter (m)
- y thickness of the diffusion sublayer or penetration depth of solute (m)
- z 1 (for 1:1 background electrolyte) (-)
- z_i sign and number of charges on the adsorbed ion (-)

Greek Symbols

- α ratio of the mass of solute dissolved in the solution to the mass of solute in the adsorbent under equilibrium conditions (-)
- β desorption constant (g/mmol)
- β_j constant for regression (-)
- ΔG change of free energy (kJ/mol)
- ΔG_{ads} change of adsorption free energy (kJ/mol)
- ΔG_{chem} change of chemical free energy (kJ/mol)
- ΔG_{coul} change of coulombic free energy (kJ/mol)
- ΔG_{solv} change of solvation free energy (kJ/mol)
- ΔH enthalpy change (kJ/mol)
- ΔS entropy change (J/(mol.K))
- δ interaction factor, which is regressed for competitive isotherm (-)
- ε particle porosity or interaction factor, which is regressed for competitive isotherm (-)
- $\varepsilon_{\text{bulk}}$ dielectric constant of solvent (water) (-)
- ε_{int} dielectric constant of interface (-)
- ε_0 dielectric constant of vacuum (8.85×10^{-12} C/(vm))
- ε_p particle porosity (-)
- ε_{ads} dielectric constant of adsorbent (-)
- η effectiveness factor (-)
- η_i interaction factor estimated from competitive adsorption data (-)
- κ Dabye length (m^{-1})
- μ_l viscosity of water ($\text{N}/(\text{m}^2 \cdot \text{s})$)

- σ charge density (C/m^2)
- ρ_b particle bulk density (kg/m^3)
- ρ_l density of water (kg/m^3)
- ρ_p particle density (kg/m^3)
- τ tortuosity factor of particle (-)
- ψ_o surface potential of surface plane o of electrical double layer or the surface potential of cell wall (v)
- ψ_β surface potential of inner Helmholtz plane β of electrical double layer (v)

Subscripts

- 1 first type composition (e. g. copper)
- 2 second type composition (e. g. cadmium)
- o surface plane of electrical double layer
- d outer Helmholtz plane of electrical double layer
- β inner Helmholtz plane of electrical double layer

CHAPTER ONE

INTRODUCTION

1.1 Biosorbents

People are concerned about the fate of heavy metal ions in the environment. With increasing industrial activities, more and more wastewater containing heavy metal ions is being discharged into streams and rivers. It is well known that heavy metal ions can cause various diseases in humans and animals, retard the growth of plants and agricultural crops, and even cause gene mutation. Unlike organic pollutants, heavy metal ions cannot be degraded by microorganisms in the soil, rivers, and activated sludge in wastewater treatment plants. This is the reason why chemical and physical treatments become the main methods for removal of heavy metal ions from wastewater. Among them, the adsorption process has been widely applied to purify various industrial and municipal wastewaters. However, traditional adsorbents, such as activated carbons, are expensive, and their applications are limited.

A recent progress in adsorbents is a low-cost biosorbent development. These biosorbents can be classified in two groups: living and nonliving biosorbents. The properties and process parameters of living biosorbents, such as algae, have been widely investigated. However, because of their certain inherent disadvantages, the use of living organisms for metal ion removal and recovery from wastewater is not feasible in all situations. For example, toxic metals and other compounds in industrial effluents may damage the growth and maintenance of an active microbial population. Moreover, the provision of some essential elements, such as carbon, nitrogen and phosphorus as energy

resources, is required to sustain microbial life and multiplication. These conditions are not often met in the industrial environment. Finally, acid or alkali solutions, which are used to regenerate the saturated biosorbents and recover valuable metal ions, may kill the microorganisms. Because of these factors, many efforts have been made for the use of nonliving biomass as biosorbents.

The advantages of nonliving biosorbents include (Volesky, 1987; 1990a):

1) No biomass growth. Nonliving biomass is neither subject to toxicity limitations of cells nor requires costly nutrients in feed solutions to keep their life and multiplication. Nonliving biosorbents will not produce a large amount of sludge, creating a disposal problem for the environmental protection. Moreover, the process with nonliving biosorbents is not governed by the physiological constraints of microbial cells.

2) Short contact time. Like ion exchangers, nonliving biomass adsorbs metal ions fast, usually requiring from a few minutes to a few hours, which means that a small column can treat a large volume of wastewater.

3) Wide operation conditions. Because the cells of biosorbents are nonliving, processing conditions are not restricted to those required to maintain the growth of cells. In other words, a wider variation of operating parameters, such as pH, temperature, and metal concentrations, is possible.

4) Possibility of metal ion recovery. Since an adsorption is a reversible process, the metal ions adsorbed on biosorbents can be desorbed and then recovered.

5) No further treatment. If the value and the amount of metal ions recovered are insignificant, and the biosorbent is plentiful, the metal-loading biosorbent can be directly incinerated. Thereby, the regeneration of saturated biosorbents is not required.

Disadvantages of nonliving biosorbents are:

1) Lower adsorption capacity. Compared to activated carbons and ion exchange resins, nonliving biosorbents may possess lower adsorption capacity, which causes early saturation of biosorbents and frequent regeneration. Therefore, operating costs are increased.

2) No potential of genetic modification. Modern genetic engineering makes cell modification possible. However, since the cells of nonliving biosorbents are not metabolizing, the potential for biological process improvement is limited.

3) No biodegradation and no valence state change for metal ions. After a biosorption treatment, metal ions neither be degraded nor change their valence state.

Based on their source, nonliving biosorbents are also grouped in two types: the nonliving microorganisms, such as non-vital algae, fungi, bacteria etc., and the agricultural by-products such as corncobs, peanut shells, soybean hulls and rice hulls etc. Since agricultural wastes are in huge quantities, and have a small monetary value, and in addition, they create a disposal problem in the environment, scientists and engineers are trying to find ways for their utilization. Randall et al. (1978) found that agricultural by-products had natural ion-exchange capability for metal ions. These by-products have three additional advantages over commercial resins besides the common advantages of nonliving biosorbents:

1) Abundant resources. It is estimated that agricultural by-products as a whole exceed 320 million metric tons/year (Wing, 1996).

2) No cultivation. They are by-products from agricultural process, and do not need to be specially cultivated and harvested, unlike algae that should be grown and caught from water.

3) Lower cost. The nonliving biosorbents made from agricultural by-products are wastes from agricultural processes. Consequently, they have a very low cost.

Because of these advantages, nonliving biosorbents made from agricultural by-products have been predicted for wide application prospects.

1.2 Sources of Copper and Cadmium Ions as Pollutants in the Environment

Heavy metal ions come mainly from mining, mineral-processing, extractive-metallurgical operations, and chemical industries. The following text only mentions sources of copper and cadmium ions, which are related to this study, as pollutants in the environment.

1.2.1 Copper

Basically, copper is not distributed widely in natural waters. A survey performed in 15 North American rivers showed that the copper contents ranged from 0.83 to 105 $\mu\text{g/l}$, but as high as 3.0 mg/l had been measured in household waters (Faust and Aly, 1983a). The primary sources of copper in industrial wastewaters are metal-process pickling baths and plating baths. The wastewater discharged from these industries may contain a copper concentration greater than 1.0 mg/l in near areas. Copper may also be present in wastewater from a variety of chemical manufacturing processes employing copper salts or recovery processes, which include ion exchange, evaporation, and

electrodialysis. The acidic corrosion of copper pipes often originates from the wastewaters containing cupric ions.

If people absorb copper in excess, they will suffer from "Wilson's disease" in which the excess of copper is deposited in the brain, skin, liver, pancreas, and myocardium (Volesky, 1990b). Therefore, the environmental protection agency has ruled that the maximum contaminant level for copper is 1.0 mg/l in drinking water (Faust and Aly, 1983b).

1.2.2 Cadmium

Cadmium ions are not especially widespread in natural geological sources. Surface water contents of cadmium in North America ranged from 21 to 130 $\mu\text{g/l}$. However, cadmium may occur in substantial concentrations due to the discharge of wastewater, especially from plating wastes. Cadmium is commonly present in wastewater from metallurgical alloying ceramics, electroplating, photography, pigment works, textile printing, chemical industries, and lead mine drainage. The dominant species of cadmium in aqueous solution are Cd^{2+} , $\text{CdCO}_3(\text{s})$ (Otavite), and $\text{Cd}(\text{OH})_2(\text{s})$ (Faust and Aly, 1983c). Otavite has a solubility of approximately 300 $\mu\text{g/l}$ at a pH value greater than 10. The solubility of $\text{Cd}(\text{OH})_2(\text{s})$ is 44 $\mu\text{g/l}$ at a pH of 10 for an aged form of this solid.

Due to its acute toxicity, cadmium has joined lead and mercury to form a group of heavy metals with the greatest potential hazard to humans and the environment. The maximum contaminant level of this element in drinking water in the U. S. A. must not exceed 0.01 mg/l (Faust and Aly, 1983d).

1.3 Objectives

To design and scale up an adsorption process from laboratory to industrial scale, it is necessary thoroughly to understand the adsorption equilibrium and kinetics. The former rules what degree of reaction can be reached; the latter describes the rate of the process that governs the volume of the reactors or columns. The main factors influencing adsorption equilibrium are the solution pH and temperature. For the adsorption kinetics, more factors should be considered such as agitation speed (for batch experiments), flow rate (for column experiments), particle size of adsorbents, biomass concentration, contact time between metal ions and adsorbents etc. These kinetic factors commonly involve the phenomena of mass transfer and surface reaction on the adsorbent and in the adsorption column. Mathematical models have been widely applied for long time to describe these phenomena quantitatively. As early as 1947, Boyd et al. had proposed three basic adsorption models to describe the corresponding phenomena:

- 1) The external diffusion of metal ions from the bulk solution to the surface of adsorbents.
- 2) The intraparticle diffusion of metal ions in the pores and the surface of adsorbents.
- 3) The chemical reaction on the surface of adsorbents.

Later, the more models with one resistance (film diffusion) and two resistances (film and pore diffusion) to mass transfer have been presented by Furusawa and Smith (1974) and McKay and Bino (1985), respectively. In addition to using a diffusion coefficient to describe mass transfer in the pores, another way is to introduce an effectiveness factor, which is used to estimate the effect of intraparticle diffusion in the particle interiors, into

a rate equation. This method simplifies intraparticle diffusion in the pores since it avoids calculating the distribution of solute concentration in the pores. By applying this concept of the effectiveness factor combined with a surface reaction, the kinetics of the surface reaction in the pores can be described.

On the other hand, apart from the properties of absorbents and their compositions, various process parameters, such as flow conditions, degrees of mixing, and heat and mass transfer of a system, can influence the kinetic rate. Therefore, an apparent kinetic rate takes into account the effects of both the chemical and physical rate processes. If the factors of the physical process cannot be eliminated, the parameters in the kinetic models will change with the operating conditions. An interesting topic in chemical engineering is to determine the intrinsic kinetics rate, which may be thought of as the apparent rate that would exist if all physical rate processes occur at infinitely fast rates (i. e., those effects of the physical factors are eliminated) (Hill, 1977).

The aims in this study were:

- 1) To investigate the various factors affecting biosorption isotherms and kinetics of the adsorption of cupric and cadmium ions by the corncob particles;
- 2) To investigate the competitive biosorption of copper and cadmium ions by the corncob particles;
- 3) To develop a novel competitive adsorption model to describe the inversed U-shaped isotherms;
- 4) To develop a novel reversible surface reaction model combined with an effectiveness factor, and to determine the parameters of model;

5) To estimate the adsorption, chemical, solvation, and coulombic free energies in Ion-Solvent Interaction model (James and Healy, 1972).

CHAPTER TWO

METHODS FOR THE REMOVAL OF METAL IONS FROM WASTEWATER

2.1 Chemical Precipitation

2.1.1 Chemical Precipitation Principle

Chemical precipitation is a process in which undesirable solutes in a solution react with some added chemicals, and form a more dense sludge. The sludge settles down in the bottom of the tank, and is removed. Chemical precipitation usually removes Ca^{2+} and Mg^{2+} in water treatment and heavy metal ions in wastewater treatment.

At a constant temperature, an ionic equilibrium will be reached in a saturated solution of insoluble salts.



According to the mass action law,

$$K = \frac{\{M^{n+}\}^m \{N^{m-}\}^n}{\{M_m N_n\}} \quad (2.2)$$

or

$$K_{sp} = K \{M_m N_n\} = \{M^{n+}\}^m \{N^{m-}\}^n \quad (2.3)$$

where K and K_{sp} are the equilibrium constant and the solubility product of the insoluble salt, respectively, $\{ \}$ denotes the solute concentration in solutions (mol/l).

Chemicals used in precipitation usually include hydroxides, sulfide, and carbonate. However, several of these precipitating compounds are amphoteric and exhibit a point of minimum solubility. For hydroxide, the ionic equilibrium can be expressed as:



$$K_{spM(OH)_n} = \{M^{n+}\} \{OH^-\}^n \quad (2.5)$$

The water ionic product K_w at 25°C is:

$$K_w = \{H^+\} \{OH^-\} = 1 \times 10^{-14} \quad (2.6)$$

Combining Eq. (2.5) with Eq. (2.6) and taking a 10-base logarithm of the resulting equation, it produces:

$$\text{Log}\{M^{n+}\} = 14n - npH - pK_{spM(OH)_n} \quad (2.7)$$

or

$$pH = \frac{1}{n} (14n - pK_{spM(OH)_n} - \log\{M^{n+}\}) \quad (2.8)$$

Equations (2.7, 2.8) can estimate the metal ion concentration or pH value when a chemical precipitation occurs. For example, when the actual metal ion concentration or pH in a solution at equilibrium is greater than the value in the right side of the equations (2.7) or (2.8), theoretically, the chemical precipitation will take place (Chapter 5.2.1 for details).

2.1.2 Chemical Precipitation for Cupric and Cadmium Ions

Copper is precipitated as a relatively insoluble metal hydroxide at an alkaline pH when adding alkalis, usually cheaper calcium hydroxide, or calcium carbonate to the solution. But in the presence of the high concentration of sulfates, calcium sulfate will interfere with the precipitation that causes the difficulty to recover the copper from its sludge. In this situation, more expensive alkalis such as NaOH can be used to obtain the sludge without the calcium sulfate. Cupric oxide has a minimum solubility of 0.01 mg/l between pH 9.0 and 10.3. The precipitation with sulfide at a pH of 8.5 will result in effluent copper concentrations of 0.01 to 0.02 mg/l. It is difficult to achieve low residual concentrations of copper in the presence of complexing agents such as cyanide and ammonia. It is necessary to remove those complexing agents by a pretreatment for a high

removal efficiency of copper. One of the effective methods for removal of copper cyanide is to use the activated carbon adsorption prior to the precipitation.

Cadmium is also removed from wastewater by chemical precipitation in which cadmium forms an insoluble and highly stable hydroxide at an alkaline pH. The amount of cadmium in a solution is approximately 1 mg/l at a pH of 8 and 0.05 mg/l at a pH of 10 to 11 after the precipitation occurs. Cadmium is not precipitated in the presence of complexing ions, such as cyanide. In this case, it is necessary to pretreat the wastewater to destroy the complexing agent. For example, cyanide destruction is necessary prior to the cadmium precipitation in the presence of cyanide.

2.2 Ion Exchange

2.2.1 Principle of Ion Exchange

Ion exchangers, by a common definition, are insoluble solid materials which carry exchangeable cations or anions. These ions can be exchanged for a stoichiometrically equivalent amount of other ions of the same charge when the ion exchanger is in contact with an electrolyte solution (Helfferrich, 1962). Thus, ion exchange can be used for the removal of undesirable anions and cations from wastewater. Usually, cations are exchanged for hydrogen or sodium, and anions for hydroxyl ions.

Ion exchange resins consist of an organic or inorganic network structure with attached functional groups. Most ion exchange resins in a wastewater treatment are synthetic resins made by the polymerization of organic compounds into a porous three-dimensional structure. The degree of crosslinking between organic chains determines the internal pore structure. An ion exchanger with a higher crosslink density has a smaller

pore size. The functional ionic groups are usually introduced by making the polymeric matrix reacted with a chemical compound containing the desired group. Exchange capacity is determined by the number of functional groups per unit of resin. Cationic ion exchange resins mean that they exchange positive ions (cations); anionic mean they do negative ions (anions); and amphoteric mean they exchange both positive and negative ions. Cation exchange resins have acidic functional groups, such as sulfuric, whereas anion exchange resins contain basic functional groups, such as amine. Ion exchange resins are often classified by the nature of the functional group as strong acid, weak acid, strong base, and weak base. The strength of the acidic or basic character depends upon the degree of ionization of the functional groups, similar with the situation of soluble acids or bases. Thus, a resin with sulfonic acid groups would act as a strong acid cation exchange resin.

2.2.2 Ion Exchange for Cupric and Cadmium Ions

Ion exchange is a feasible treatment method for wastewaters containing copper and cadmium ions and some studies have been conducted using ion exchange. For example, Maliou et al. (1992) treated wastewater containing copper and lead by ion exchangers, and Sengupta and Paul (1985) did for cadmium, zinc, and copper. From the economical view, ion exchanger should treat the lower ionic concentration to avoid regeneration of ion exchanger frequently.

2.3 Adsorption

2.3.1 Principle of Adsorption

A solid surface in contact with a solution tends to accumulate a surface layer of solute molecules because of the unbalance of surface forces. These forces can be defined as: 1) chemical; 2) electrostatic; 3) physical. Chemical adsorption, or chemisorption, involves solute-sorbent interactions having the characteristics of true chemical bonds. Such sorptions are characterized by large heats of adsorption, typically 100 to 400 kJ/mol, although they may even be larger in some cases. Chemical adsorption results in the formation of a monomolecular layer of the adsorbate on the surface of adsorbent through forces of residual valence of the surface molecules.

Electrostatic adsorption resulting from coulombic attraction between oppositely charged species also involves high-energy forces and bonds, similar to electrostatic interactions between charged chemical species in solution phase. Such forces have differential heats of adsorption as large as 200 kJ/mol.

Physical adsorption results from molecular condensation in the capillaries and surface of the adsorbents. This condensation is caused by the action of van der Waals forces, comprised by a combination of London dispersion forces and classical electrostatic forces, the latter of which are generally negligible for non-polar hydrophobic compounds. Differential heats of adsorption for interaction of the van der Waals type forces are generally in the order of 5 to 10 kJ/mol for small molecules. This relatively weak bonding force is amplified in the case of hydrophobic molecules by the solvent-motivated entropy gradient that functions to drive them from solution. The combined effect is often referred to simply as hydrophobic bonding. Because the hydrophobic effect generally contributes the differential heats of adsorption of 5 to 10 kJ/mol, the

combination of hydrophobic and van der Waals sorptions may have associated heats of adsorption of 10 to 20 kJ/mol.

Generally, in the adsorption process, an equilibrium interfacial concentration will be rapidly attained on the surface of the adsorbents, followed by the slow solute diffusion into the pores of the adsorbents. The overall rate of adsorption is controlled by the rate of diffusion of the solute molecules within the capillary pores of the adsorbents. The rate varies reciprocally with the square of the particle diameter, increases with increasing concentration of solute and temperature, and decreases with increasing molecular weight of the solute. Morris and Weber (1964) found that the rate of the adsorption varied as the square root of the contact time of the adsorbent with the solute in the solution. The rate of adsorption and the uptake also increase with increasing pH for adsorption of metal ions. The adsorption capacity of adsorbents for a solute will depend on both the adsorbents and the solutes.

2.3.2 Adsorption Process

The adsorption of various compounds in aqueous systems onto or into adsorbents is a time-dependent process. But this dependence may have less influence when dealing with powder adsorbents than with granular adsorbents due to the decreasing resistance to mass transfer in particle interior. Another consideration is the identification of the rate-determining step of the adsorptive process. Generally, adsorption of metal ions from aqueous solution on porous adsorbents can be described by three consecutive steps (Weber, 1972; Smith, 1968).

The first step is transport of the adsorbate from bulk solution to the outer surface of adsorbents by molecular diffusion in the boundary layer that surrounds the particles. This is called the external or film diffusion. There is no actual film surrounding the adsorbents, but the term is used to describe the resistance to mass transfer at the surface of the particle. The mass transfer coefficient, k_f , in film theory is related to the free liquid diffusivity of the solute, D_m , and the thickness of the diffusion sublayer, y , as follows:

$$k_f = \frac{D_m}{y} \quad (2.9)$$

The concentration gradient in the liquid film around the adsorbents is the driving force in film diffusion.

The second step, termed the internal diffusion, involves the transportation of the adsorbate from the particle surface into the interior sites by diffusion within the liquid-filled pores, and the migration along the solid surface of the pore (surface diffusion) (Weber, 1972; Keinath and Weber, 1968; Weber and Rumer, 1965). Because these two transport processes act in parallel, the slower one will control the overall rate of transport. Keinath and Weber (1968) found that for a typical water or wastewater adsorption system, the rate parameter for surface diffusion was two to four orders of magnitude greater than the liquid phase pore diffusion.

The third step is adsorption of the solute on the activated sites on the interior surfaces of the pores. Since the adsorption step is very fast, it should not influence the overall kinetics (Weber, 1972; Smith, 1968). The overall rate of the adsorption process is controlled by the slowest step, which would be either film diffusion or intraparticle diffusion. However, control might also be distributed between the intraparticle and external mechanisms in some systems (Fritz, 1980; Weber, 1972).

It is noted that variation of the rate with concentration is not linear. Therefore, the concentration dependence of the adsorption rate can be used to identify the rate-controlling step. It is also recognized that the adsorption rate is controlled by film diffusion during the initial stage of the adsorption process in batch reactors and the initial breakthrough in fixed bed reactors. As the adsorbents become loaded with the adsorbate, the adsorption rate becomes controlled by intraparticle diffusion (Liu and Weber, 1981; Weber and Morris, 1963).

For processes controlled by intraparticle diffusion, the size and configuration of the adsorbate molecule should affect the overall rate of adsorption since both influence the migration of adsorbate molecules on the surface and in the pores. The larger the molecule or the more branched, the lower diffusion rate. Hence, the adsorption rate should be lower. For organic compounds, an increase in the chain length by a $-CH_2-$ group results in a reduction of the adsorption rate because the increase in the chain length apparently reduces mobility of the molecule on the surface and in the pore. Moreover, it also increases its affinity to the adsorbent surface in accordance with Traube's rule. Both effects result in a decrease of the surface diffusion inside the pores and, hence, an overall rate decrease in the observed adsorption rate. The adsorption processes in which adsorbates exhibit high affinity to adsorbents are usually controlled by the intraparticle diffusion. This is attributed to a decrease of surface diffusion of adsorbates, and thus, is less flexible to migrate on the internal surfaces of the adsorbents. Branching of the adsorbate molecule also results in a decrease of the observed adsorption rate due to the decrease in the surface diffusion rate (Weber and Morris, 1963).

2.3.3 Adsorption of Copper and Cadmium Ions

An adsorption process can be applied for removing copper and cadmium ions from wastewater. From an economic point of view, treating wastewater containing a low concentration of metal ions by adsorption is a reasonable option.

Much work about adsorption of metal ions on activated carbon has been done. For example, Netzer and Hughes (1984) reported that activated carbon could remove approximate by 98 % of copper at a pH of 5. Sorg et al. (1978) found that cadmium concentration decreased by 29-36 % when 0.05 mg/l cadmium solution was treated at a pH of 7.0 with 100 mg/l PAC-1 (Amoco PX-21) and PAC-2 (Darco HDP), respectively. Utilization of agricultural by-products for the adsorption of copper and cadmium ions will be mentioned in Chapter three.

CHAPTER THREE

LITERATURE REVIEW OF BIOSORPTION AND ADSORPTIVE MODELS

3.1 Biosorption by Agricultural By-Products

Studies on biosorption by agricultural by-products have been completed in the last several decades. Friedman and Waiss (1972) reported mercury uptakes by wool albumin, blood meal, chicken feathers, soy flour, silk, gelatin, wheat gluten, and wheat flour. They found that wool modified by N-vinyliminazole, N-vinylpyrrolidone, and 2-vinylpyridine enhanced mercury uptakes by 30-70 % compared with the non-modified wool. Odozi et al. (1985) described the preparation and properties of polymerized corncob powder (treated by sulfuric acid and phenol) and its composite (with sawdust and onion skin) ion-exchange resins for binding heavy-metal ions. The static and dynamic tests were carried out with solutions of Pb^{2+} , Ni^{2+} , Cu^{2+} , Mg^{2+} , Zn^{2+} , and Ca^{2+} ions. Their results showed that the concentration of these metal ions were greatly reduced and the exchange capacity of the cation resin for the metal ions studied was the order of 1 meq/g. Odozi and Emelike (1985) demonstrated that the resin of corncob-red onion skins could remove from 61.9 % to 84.2 % of Pb^{2+} , Ni^{2+} , Cu^{2+} , Mg^{2+} , Zn^{2+} , Ca^{2+} , and Mn^{2+} ions from various solutions. The adsorption capacity of the adsorbent for the studied ions was in the following order: $Pb^{2+} > Cd^{2+} > Ni^{2+} > Zn^{2+} > Ca^{2+} > Hg^{2+} > Mg^{2+} > Mn^{2+}$. Azab and Peterson (1989) evaluated the removal efficiencies of cadmium ions from water using biological adsorbents (human hair, bone, apricot seed shell, walnut shell, peanut shell, orange skin, irish peat, natural compost, zygorhynchus, rhizopus, *Mucor ramannianus*, penicillium caps, *Aspergillus terreus*, IRA-400 (ionex), and activated charcoal). Among

these tested materials, the ten kinds showed higher adsorption capacities than that of activated charcoal and the ion exchange resin. Singh et al. (1993) studied the adsorption of heavy metal ions by the used tealeaves powder treated with formaldehyde and sulphuric acid. The magnitudes of the adsorption capacity of the used tealeaves exhibited the following order: $Pb^{2+} > Hg^{2+} > Cd^{2+} > Ni^{2+} > Cu^{2+}$. Marshall et al. (1993) investigated the adsorptive ability of rice milling byproducts (hulls and bran) for metal ions from aqueous solution. Hulls adsorbed low level (13-27%) of Cr^{3+} , Co^{2+} , Cu^{2+} , Ni^{2+} , and Zn^{2+} at a 100 mg/l metal ion concentration. A defatted, extrusion stabilized bran was found to have a high adsorption capacity for Cr^{3+} , Cu^{2+} , and Zn^{2+} , but a much lower adsorption capacity for Co^{2+} and Ni^{2+} . Periasamy and Namasivayam (1994) showed that peanut hull carbon was an effective adsorbent for the removal and recovery of Cd^{2+} from aqueous solutions. Its adsorption capacity was superior to certain commercial activated carbons. Marshall and Champagne (1995) evaluated the adsorptive capacities of soybean hulls, cottonseed hulls, rice straw, and sugarcane bagasse for some metal ions in aqueous solutions. Their adsorptive capacities for Zn^{2+} had the following order: soybean hulls > cottonseed hulls > rice straw > sugarcane bagasse. At a subsaturated concentration of metal ion (100 mg/l), soybean and cottonseed hulls adsorbed the majority (95.6-99.7%) of Cr^{3+} , Co^{2+} , Cu^{2+} , Ni^{2+} , or Zn^{2+} . Capacities varied from 0.06 to 0.52 meq/g dry weight of adsorbents. Bosinco et al. (1996) indicated that corncob could be used effectively to remove hexavalent chromium from aqueous solutions. The process was very pH dependent, and a pH of 1 produced the best results. Al-Asheh and Duvnjak (1996) used canola meal for adsorption of copper. The uptakes of metal ions by the canola meal decreased with an increase in the concentration of the canola meal in solution, and was

enhanced with decreasing canola meal particle sizes. Lehrfeld (1996) prepared a series of cation exchange resins based on oat hulls, corncob, and sugar beet. Their reactive order was sugar pulp > corncob > oat hull. Sun and Shi (1998) investigated sunflower stalks as adsorbents for the removal of metal ions such as copper, cadmium, zinc, and chromium from wastewaters. Their experiments showed that the maximum adsorption capacities of the four heavy metals were 29.3 mg/g (Cu^{2+}), 30.73 mg/g (Zn^{2+}), 42.18 mg/g (Cd^{2+}), and 25.07 mg/g (Cr^{3+}) at the initial metal ion concentration of 1000 mg/l and the sunflower concentration of 4 g/l, respectively. The particle sizes of sunflower stalks affected the adsorption of metal ions; the finer size of particles showed better adsorption of the ions. Within 60 minutes of operation about 60-80% of these ions were removed from the solutions at the initial concentration of 100 mg/l.

In addition of the previously discussed equilibrium properties of biosorbents, process parameters of adsorption kinetics are also an important aspect for a successful adsorption process. In parallel with the investigations of adsorption properties of biosorbents, few studies on the process parameters, such as agitation speed and particle size, of metal ion biosorption have been performed. Mohammad and Akl (1991a, 1991b) evaluated the coefficients of external mass transfer and pore diffusion for the adsorption of various dyes on maize cob at various initial dye and maize cob concentrations. They predicted that external mass transfer coefficients were 0.3×10^{-9} and 0.29×10^{-9} cm/s, and surface diffusion coefficients were 0.6×10^{-8} and 0.69×10^{-8} cm²/s for Basic Blue 69 and Basic Red 22, respectively. Guibal et al. (1998) studied the effects of agitation speed and particle size for metal-anion sorption by chitosan beads. They found that particle size of chitosan bead with 0.95-2.8 mm did not influence equilibrium, and sorption kinetics was

mainly controlled by intraparticle diffusion, while an increase of the radius of chitosan flakes from less than 0.125 mm to 0.25-0.50 mm decreased the adsorption capacities from 3.4 to 1.5 mmol/g and the controlling mechanisms were both external and intraparticle diffusion. The intraparticle diffusivity range was between 10^{-13} and 10^{-10} m²/min, depending on the sorbent size and the condition.

3.2 Competitive Adsorption of Metal Ions

In industrial wastewater, there are many kinds of metal ions. They will influence uptake by adsorbents because of the competitive adsorption among them. There are two methods to investigate the competitive adsorption of metal ions. One approach is to observe the uptake of metal ions with pH change at a constant total metal ion concentration (adsorption edge curve), as Benjamin and Leckie (1981) and Cowan et al. (1991) suggested. Another approach is to observe the uptake for various total metal ion concentrations at an initial pH value (adsorption isotherm). Gadde and Laitinen (1974) used the isotherms to study heavy metal adsorption competition on hydrous manganese oxides. They found a 64% displacement of Zn²⁺ when an equal Pb²⁺ concentration of 10^{-3} M was added to the system containing Zn²⁺ concentration of 10^{-3} M at a pH of 6. The results showed no significant variations when the order of metal introduction was reversed and Pb²⁺ was added first. However, all metal ion concentrations used in these experiments exceeded their saturation limits in the adsorption of an individual metal ion. Zasoski and Burau (1988) also examined competitive adsorption using isotherms. In that study, competing metals were added in equimolar levels and in an N₂ atmosphere, avoiding precipitation. In their studies of Cd²⁺ and Zn²⁺ adsorption on hydrous

manganese oxide (δ -MnO₂), they found two types of sites: (1) high-energy sites that were saturated by metal ions; and (2) lower energy sites. The higher energy sites showed preference for Cd²⁺ over Zn²⁺, whereas the reverse was true for the low energy sites. Cadmium adsorption decreased by approximately 25% in the presence of equimolar concentrations of Zn²⁺, whereas Zn²⁺ adsorption decreased by 50% in the presence of Cd²⁺. Al-Asheh and Duvnjak (1998) investigated the adsorptions of binary metal ions (Cu²⁺ + Cd²⁺, Cu²⁺ + Ni²⁺, and Cd²⁺ + Ni²⁺) by pine bark. They concluded that the capacity of the bark for each metal in the binary systems was lower than in the single metal systems. Christophi and Axe (2000) investigated competitive adsorption of lead, copper, and cadmium on goethite. They found that the equilibrium constant for lead was greater than that of copper, which is not in agreement with their hydrated radii (Pb < Cu < Cd).

3.3 Adsorption Models

The adsorption models can be classified into two kinds: equilibrium and kinetic models. If the models have a time variable, they are called kinetic models. Otherwise, they are called equilibrium models.

3.3.1 Equilibrium Models

Adsorption phenomenon can occur on the surface of adsorbents with a single component and multi-components. The corresponding models can be termed as the single component models and the multi-component models.

1. Single-Component Models

1) Langmuir Model

The Langmuir isotherm can be derived from the equilibrium of chemical potentials in two interfacial surfaces or dynamic equilibrium between solute and solvent (Valsaraj, 2000). It is given by the following relationship:

$$q = \frac{K_l q_m c_e}{1 + K_l c_e} \quad (3.1)$$

where K_l is the Langmuir constant (l/mmol), q_m is the maximum adsorption capacity of adsorbent (mmol/g), c_e and q are the metal ion concentration in solution and the uptake by adsorbent at equilibrium, respectively. Linearizing above equation, provides:

$$\frac{1}{q} = \frac{1}{K_l q_m c_e} + \frac{1}{q_m} \quad (3.2)$$

Plotting $1/q$ versus $1/c_e$, a linear relationship can be performed, where the slope and intercept of the straight line will produce K_l and q_m , respectively. In this work, the Langmuir model was applied.

2) Freundlich Model

For a long time, the Freundlich isotherm was thought to have little theoretical value. More recently, it has been shown that it can be derived theoretically by considering the heterogeneous nature of adsorption sites (Adamson, 1997). The Freundlich isotherm is expressed as follows:

$$q = k_f c^{1/n} \quad (3.3)$$

where k_f is the Freundlich constant, and n is a constant for regression.

3) Temkin Model

The Temkin model assumes that the adsorption is characterized by a uniform distribution of binding energies, up to the maximum binding energy ΔG_{\max} , which results in the following isotherm equation (Johnson and Arnold, 1995):

$$q = q_t \ln(1 + K_t c_e) \quad (3.4)$$

where K_t (l/mol) is the equilibrium binding constant corresponding to the maximum binding energy ($K_t = \exp(-\Delta G_{\max}/RT)$), and q_t is the differential surface capacity per unit binding energy.

2 Multi-Component Equilibrium Models

Competitive isotherms, describing multi-component adsorption, are classified according to the relationship with single component isotherms.

1) Competitive Isotherms Related to the Individual Isotherm Parameters

The extension of the basic Langmuir model to competitive adsorption is based on the same hypotheses as the single-component Langmuir model, and in addition, assumes identical capacities for all components. It can be expressed as the follows (Butler and Ockrent, 1930; Markham and Benton, 1931):

$$q_{i,e} = \frac{a_i c_{i,e}}{1 + \sum_{j=1}^N b_j c_{j,e}} \quad (3.5)$$

where a_i and b_j ($i \neq j$) are derived from the corresponding individual Langmuir isotherm equation ($q_i = a_i c_{i,e} / (1 + b_i c_{i,e})$).

2) Redlich-Peterson Equation

The three-parameter isotherm of Redlich-Peterson that was empirically developed for multi-component mixtures is given as (Bellot and Condoret, 1993):

$$q_{i,e} = \frac{K_{R,i}c_{i,e}}{1 + \sum_{j=1}^N a_{R,i}c_{j,e}^{\beta_j}} \quad (3.6)$$

where β_j , $K_{R,i}$, and $a_{R,i}$ are constants for regression.

3) Competitive Isotherms Related to the Individual Isotherm Parameters and to the Correction Factors

To fit the experimental data from competitive isotherms more accurately, an additional coefficient, the interaction term η_i , was introduced in equation (3.6). The interaction term, η_i , is a characteristic for each species and depends on the concentrations of the other components. The modified competitive Langmuir isotherm is (Bellot and Condoret, 1993):

$$q_{i,e} = \frac{a_i c_{i,e} / \eta_i}{1 + \sum_{j=1}^N b_j c_{j,e} / \eta_j} \quad (3.7)$$

where a_i and b_j are given by the individual Langmuir isotherm, and the interaction terms, η_i , are estimated from competitive adsorption data.

3.3.2. Kinetic Models

The adsorption of metal ions by adsorbents involves the external diffusion through the liquid film on the surface of adsorbents, the intraparticle diffusion in the pores of adsorbents, and the chemical reaction on the surface of adsorbents. Among them, the slowest process is called the rate-controlling step that can be alone process or combined action of the two processes. Which mechanism is a rate-controlling step depends on the operating conditions, characters of metal ions, and adsorbents. Based

on the three phenomena, the corresponding three models, the external diffusion, the intraparticle diffusion, and the surface reaction models, have been derived.

1. External Diffusion Model

According to the various mass transfer theories, at least three kinds of models have been developed.

1) External Diffusion Model Based On Film Theory

The external diffusion model describes the solute concentration change in solution with time. It can be expressed as:

$$-\frac{dc}{dt} = k_f a_m (c - c_s) \quad (3.8)$$

where c and c_s are the solute concentrations (mmol/l) in the bulk solution and at the surface of adsorbent, respectively, k_f is the mass transfer coefficient between the bulk solution and the solid surface (m/s), and a_m is the specific area of the particle (m^2/m^3). The parameter a_m can be calculated by the following equation, assuming that the particles are spherical (Leusch and Volesky, 1995).

$$a_m = \frac{6m}{d_p \rho_p (1 - \varepsilon_p)} = \frac{6m}{d_p \rho_b} \quad (3.9)$$

where m , d_p , ρ_p , ρ_b and ε_p are the concentration of particles in water (g/l), the average particle size (m), the particle density (kg/m^3), the particle bulk density (kg/m^3), and the particle porosity, respectively. Integrating the equation (3.8) for the initial condition:

$$t = 0, c = c_0 \quad (3.10)$$

provides:

$$\ln \frac{c_0 - c_s}{c - c_s} = k_f a_m t \quad (3.11)$$

Since it is impossible directly to measure the solute surface concentration on biosorbents, the surface concentration can be estimated through the assumption of electrical double layer model and titration analysis. In this study, the surface concentration is taken as a constant for regression. Therefore, the surface concentration of metal ions, c_s , and the mass transfer coefficient, k_f , can be determined by non-linear regression.

2) External Diffusion Model Based on Penetration Theory

According to the penetration theory proposed by Higbie (1935), the solute concentration in solution can be expressed as (Coulson and Richardson, 1999a):

$$c = c_o + (c_s - c_o) \left[1 - \operatorname{erf} \left(\frac{y}{2\sqrt{D_m t}} \right) \right] \quad (3.12)$$

where erf is the error function, and y is the penetration depth of solute. The point value of the mass transfer coefficient k_p is:

$$k_p = \sqrt{\frac{D_m}{\pi t}} \quad (3.13)$$

3) McKay and Allen Model

McKay and Allen's model based on external mass transfer used an external mass transfer coefficient as the rate controlling coefficient to predict the concentration versus time curve for the adsorption of metal ions by adsorbents. The equation is (McKay and Allen, 1980):

$$\ln \left(\frac{c}{c_o} - \frac{1}{1+m_s K_L} \right) = \ln \left(\frac{m_s K_L}{1+m_s K_L} \right) - \frac{1+m_s K_L}{m_s K_L} k_f S_s t \quad (3.14)$$

A plot of $\ln(c/c_o - 1/(1+m_s K_L))$ versus t should be linearly correlated. The line will have an intercept of $\ln(m_s K_L/(1+m_s K_L))$ and a slope of $-(1+m_s K_L)k_f S_s/(m_s K_L)$. This correlation

gives a good agreement to support the film diffusion single-resistance assumption at low surface coverage but not at high surface coverage, indicating that an additional rate-controlling step might be involved, such as intraparticle diffusion or surface reaction.

2. Intraparticle Diffusion Model

Solute diffusion into porous material may be described by Fick's second law. Suppose a particle of a uniform radius and material is placed in a well-stirred solution of limited volume, the solute concentration in the solution is always uniform and the initial concentration is equal to zero, and initially the particle is free from solution, a combined pore and surface diffusion model with corresponding initial and boundary conditions can be expressed as the following (Tien, 1994; Grathwohl, 1998):

$$\varepsilon \frac{\partial c}{\partial t} + \rho \frac{\partial q}{\partial t} = \frac{\rho}{r^2} \frac{\partial}{\partial r} \left(D_e r^2 \frac{\partial c}{\partial r} \right) \quad (3.15)$$

$$D_e = D_p + \rho D_s \frac{\partial q}{\partial c} \quad (3.16)$$

$$D_p = D_m \frac{\varepsilon}{\tau} \quad (3.17)$$

$$c = 0, t = 0, 0 < r < a \quad (3.18)$$

$$c = c_e, t > \infty, r = a \quad (3.19)$$

$$\partial c / \partial t = 0, t > 0, r = 0 \quad (3.20)$$

where r , ε , τ , c_e , D_e , D_p , D_s , and D_m denote the radial distance (m) from the center of the particle sphere, the particle porosity, the particle tortuosity factor, the solute equilibrium concentration in solution, the effective, pore, surface and molecule (or ion) diffusivities, respectively. Usually, D_p is considered as a constant. Although D_s changes with concentration and uptake of solute, it is assumed that D_s is constant for simplification.

When the adsorption exhibits a linear isotherm, the following analytical solution of equations (3.15-3.20) has been given (Crank, 1975; Grathwohl, 1998):

$$\frac{q}{q_{\infty}} = 1 - \sum_{n=1}^{\infty} \frac{6\alpha(1+\alpha)\exp(-D_{a,ave}p_n^2/r^2)}{9+9\alpha+p_n^2\alpha^2} \quad (3.21)$$

where the p_n s are the non-zero roots of

$$\tan p_n = \frac{3p_n}{3+\alpha p_n^2} \quad (3.22)$$

$$\alpha = \frac{c_o v - q_{\infty} M}{q_{\infty} M} \quad (3.23)$$

The parameters M , v , c_o , q , and q_{∞} are the initial quantity (gram) of adsorbent in the suspension, the volume (liter) of liquid, the initial solute concentration (mmol/l) in solutions, the uptake (mmol/g) of solute at time t and equilibrium, respectively, α denotes the ratio of the mass of solute dissolved in the solution to the mass of adsorbed solute in the adsorbent under equilibrium conditions. Under a nonlinear isotherm, a numerical solution is required.

3. Reaction Kinetic Models

Similarly with the classification of general chemical kinetics, adsorption reaction kinetics models have two groups: the power series models and the exponential models.

1) The Pseudo-First Order Equation

The pseudo-first order equation is generally expressed as follows:

$$\frac{dq}{dt} = k_1(q_e - q) \quad (3.24)$$

where k_1 is the rate constant of pseudo-first adsorption. After integration and applying the initial condition: $t = 0, q = 0$, the integrated form of equation becomes:

$$\ln(q_e - q) = \ln q_e - k_1 t \quad (3.25)$$

2) The Pseudo-Second Order Equation

If the rate of adsorption exhibits a second order mechanism, the pseudo-second order chemisorptions kinetic rate equation is expressed as (Ritchie, 1977):

$$\frac{dq}{dt} = k_2 (q_e - q)^2 \quad (3.26)$$

where k_2 is the rate constant of pseudo-second order sorption (g/mmol/min). For the initial condition: $t = 0, q = 0$, the integrated form of equation (3.26) is:

$$\frac{1}{q_e - q} = \frac{1}{q_e} + kt \quad (3.27)$$

which has a linear form:

$$\frac{t}{q} = \frac{1}{kq_e^2} + \frac{t}{q_e} \quad (3.28)$$

3) The Elovich Equation

The Elovich model is a kind of the exponential equation for kinetics of adsorption. It is generally expressed as follows (Low, 1960):

$$\frac{dq}{dt} = \alpha \exp(-\beta q) \quad (3.29)$$

where α is the initial sorption rate (mmol/(g.min)), and β is the desorption constant (g/mmol).

To simplify the Elovich equation, Chien and Clayton (1980) assumed $\alpha\beta t \gg 1$ and by applying the initial condition: $q = 0$ at $t = 0$, the equation becomes:

$$q = \beta \ln(\alpha\beta) + \beta \ln t \quad (3.30)$$

Thus, the constants can be obtained from the slope and intercept of a straight line plot of q against $\ln t$. Equation (3.30) can be used to test the applicability of the Elovich equation for the kinetics of adsorption.

CHAPTER FOUR

DEVELOPMENT OF NOVEL EQUILIBRIUM AND KINETICS MODELS

4.1 A Modified Langmuir Model Including Effect of pH

The Langmuir model is widely used in adsorption. The parameters of the maximum adsorption capacity, q_m , and equilibrium constant, K_L , will change with pH in adsorption processes because of the significant effect of pH on adsorption. Esposito et al. (2002) have presented an equation to correlate q_m with pH.

$$q_m(pH) = \frac{q_0 \exp(k pH)}{1 - \{q_0 [1 - \exp(k pH)]\} / q_\infty} \quad (4.1)$$

where q_0 , q_∞ and k are constants for regression. the Langmuir model (4.1) becomes:

$$q = \frac{K_L q_m(pH) c_e}{1 + K_L c_e} \quad (4.2)$$

Unfortunately, Esposito et al. (2002) did not give the physical meaning of q_0 and q_∞ . In this study, it supposes that there are two kinds of active sites on the cell wall of the particles: the charged and no charged active sites. At pH at zero charge point (pH_{zcp}), there are only no charged active sites on the cell wall because of no coulombic effect. The following equation for correlating q_m , pH, and pH_{zcp} is suggested in this study:

$$q_m(pH) = q_{mzcp} \exp[k(pH - pH_{zcp})] \quad (4.3)$$

where q_{mzcp} and k are the constants for regression, and q_{mzcp} is the maximum no charged active sites at pH_{zcp} . Since the pH_{zcp} of adsorbents can be measured by the primary equilibrium H^+ and OH^- (Ahmed, 1965; Tewari and Campbell, 1976) or titration curves (Akratopulu et al., 1986), equation (4.3) gives a simpler formula with two parameters. Substituting equation (4.3) to the Langmuir model (4.1), it produces:

$$q = \frac{K_l q_{mzcp} c_e}{1 + K_l c_e} \exp[k(pH - pH_{zcp})] \quad (4.4)$$

If the pH_{zcp} of absorbent is not measured, equation (4.3) can be simplified as an empirical equation (4.5).

$$q_m(pH) = q_{m0} \exp(k pH) \quad (4.5)$$

where q_{m0} and k are the constants for regression. But q_{m0} does not have any physical meaning.

Furthermore, assuming that the Langmuir equilibrium constant, K_l , has the following expression:

$$K_l = K_0 \exp(n pH) \quad (4.6)$$

where K_0 and n are the constants for regression. Substituting equation (4.6) into equation (4.4), it produces:

$$q = \frac{K_0 q_{mzcp} c_e}{1 + K_0 \exp(n pH) c_e} \exp(n pH) \exp[k(pH - pH_{zcp})] \quad (4.7)$$

Equation (4.7) with four parameters can describe the uptake of solute with changes of solute concentration and pH value.

4.2 An Equilibrium Model for Competitive Adsorption

In the present experiments of biosorption of mixtures of copper and cadmium, the uptake of cadmium by the corncob particles first increases, reaches a maximum point, and then decreases, while the uptake of copper increases with increasing total metal ion concentration. In normal cases, the uptakes of two metal ions for competitive adsorption should increase as their concentrations (Christophi and Axe 2000). The present models for mixture adsorption, such as the binary Langmuir and Freundlich isotherms, cannot

describe this phenomenon because the uptakes of both competitive solutes in these models increase with the solute concentration. Generally, the uptake of metal ions in a competitive adsorption is less than that of the individual adsorption. Therefore, it is supposed that the uptake of a kind of metal ion in a competitive adsorption is equal to the difference of uptakes between two kinds of metal ions in their individual adsorptions. However, it is impossible precisely to predict mixture behavior only from individual data. Therefore, four interaction factors were added to the following equations for competitive adsorption:

$$q_1 = \frac{\delta_1 q_{m1} K_{l1} c_{e1}}{1 + \delta_1 K_{l1} c_{e1}} - \frac{\delta_2 q_{m2} K_{l2} c_{e2}}{1 + \delta_2 K_{l2} c_{e2}} \quad (4.8)$$

$$q_2 = \frac{\varepsilon_2 q_{m2} K_{l2} c_{e2}}{1 + \varepsilon_2 K_{l2} c_{e2}} - \frac{\varepsilon_1 q_{m1} K_{l1} c_{e1}}{1 + \varepsilon_1 K_{l1} c_{e1}} \quad (4.9)$$

where subscripts 1 and 2 denote the first type ion (e. g. copper) and the second type ion (e. g. cadmium), respectively. The parameters q_m and K_l are the maximum adsorption capacity and the Langmuir equilibrium constant in a single isotherm, and δ and ε are the interaction factors, which are regressed for competitive isotherms. It is noted that when δ_2 and ε_1 have small values, equations (4.8, 4.9) reduce the Langmuir model for a single component.

4.3 A Reversible Surface Reaction Model Combined with an Effectiveness Factor

Generally, any chemical reaction is reversible. When the rate of the backward reaction is very slow or cannot be observed, this reaction is considered as an irreversible reaction. An adsorption process consists of a forward reaction (adsorption) and a backward reaction (desorption). Because there is the mechanics of ion exchange on the

surface on the adsorbent, and the metal ions adsorbed can be desorbed by changing pH, both reasons indicate that the rate of backward reaction (desorption) cannot be neglected.

4.3.1 Model Development

Under powerful agitation, the external diffusion effect can be eliminated or neglected. Adsorption process will be governed by intraparticle diffusion and surface reaction. The intraparticle diffusion involves some complex diffusion processes such as surface, molecular, and pore diffusion in the pore of the particle. Their effect on mass transfer is often expressed by an effectiveness factor η , similar to catalysts in engineering for simplification. Its definition is (Smith, 1970a):

$$\eta = \frac{\text{actual rate for the whole pellet}}{\text{rate evaluated at outer surface conditions}} = \frac{r_q}{r_s} \quad (4.10)$$

Some investigations have shown that there are lots of complexation forms of metal ions on adsorbents in solutions (Hanasen et al., 1992; Robertson and Leckie, 1997). It is impossible to obtain an analytical solution for consideration of these reactions in detail in a transportation reaction model. The following reaction considers only the most basic reaction form in an adsorption process:



The surface reaction involves the reaction of unoccupied active sites of adsorbents with metal ions on the surface. Applying the mass action law to the above reversible reaction (4.11), the rate equation on the external surface of particle should be:

$$r_s = \frac{d[SOMe^+]}{dt} = k_1 \exp\left(-\frac{E_1}{RT}\right) \{Me^{2+}\}^a [SOH_t - SOMe^+]^b - k_2 \exp\left(-\frac{E_2}{RT}\right) [SOMe^+]^c \{H^+\}^d \quad (4.12)$$

where [] and { } denote the surface concentration (mmol/g) and the solution concentration (mmol/l) of ions, respectively, SOH is the unoccupied surface active sites at equilibrium (mmol/g), SOMe⁺ represents the occupied surface active sites by metal ions at equilibrium (mmol/g), SOH_t is the total surface active sites (mmol/g). Me²⁺ and H⁺ are the metal ion and the proton concentration, k₁ and k₂ are the frequency (or preexponential) factors, E₁ and E₂ are the activation energies for forward and backward reactions, and the coefficients a, b, c, and d are the regression constants. Since the surface reaction (4.11) can be considered as an elementary reaction, the coefficients a, b, c, and d are assumed equal to one.

$$\frac{d[SOMe^+]}{dt} = k_{ads} \{Me\}^{2+} [SOH_t - SOMe^+] - k_{des} [SOMe^+] \{H^+\} \quad (4.13)$$

where k_{ads} and k_{des} are equal to k₁exp(-E₁/RT) (l/(mmol.min)) and k₂exp(-E₂/RT) (l/(mmol.min)). For convenience, using the following symbols in stead of those in equation (4.13), q = [SOMe⁺], c = [Me], c_H = [H⁺], q_m = [SOH_t], and q = [SOMe⁺], it produces:

$$\frac{dq}{dt} = k_{ads} c(q_m - q) - k_{des} q c_H \quad (4.14)$$

At a constant or average pH during the adsorption process, equation (4.14) becomes:

$$\frac{dq}{dt} = k_{ads} c(q_m - q) - k_{des} q \quad (4.15)$$

where $k_{desH} = k_{des}[H^+]$ (min^{-1}). Substituting the equation (4.10) into equation (4.15), it produces:

$$\frac{dq}{dt} = \eta [k_{ads}c(q_m - q) - k_{desH}q] \quad (4.16)$$

4.3.2 The Solution of Model

According to conservation of mass in the reactor, the solute concentration is:

$$c = c_o - \frac{qM}{v} \quad (4.17)$$

where c_o , M and v are the initial concentration of metal ions in suspension, the mass quantity of corn cob particles (g), and the water volume (l) in the beaker, respectively.

Substituting equation (4.17) into equation (4.16), it produces:

$$\frac{dq}{dt} = \eta \left[k_{ads} \left(c_o - \frac{Mq}{v} \right) (q_m - q) - k_{desH}q \right] \quad (4.18)$$

When equation (4.18) is integrated with the initial condition $t = 0$, $q = 0$, it produces:

$$q = \frac{\frac{4A}{C} \left[\exp \left(t\eta C \sqrt{\left(\frac{B}{C} \right)^2 - \frac{4A}{C}} \right) - 1 \right]}{2 \left\{ \frac{B}{C} + \sqrt{\left(\frac{B}{C} \right)^2 - \frac{4A}{C}} - \left(\frac{B}{C} - \sqrt{\left(\frac{B}{C} \right)^2 - \frac{4A}{C}} \right) \exp \left(t\eta C \sqrt{\left(\frac{B}{C} \right)^2 - \frac{4A}{C}} \right) \right\}} \quad (4.19)$$

where

$$A = k_{ads}q_m c_o \quad (4.20)$$

$$B = - \left(\frac{k_{ads}q_m M}{v} + k_{ads}c_o + k_{desH} \right) \quad (4.21)$$

$$C = \frac{k_{ads}M}{v} \quad (4.22)$$

when $\eta = 1$, equation (4.19) represents the uptake for surface reaction control.

$$q = \frac{\frac{4A}{C} \left[\exp \left(tC \sqrt{\left(\frac{B}{C}\right)^2 - \frac{4A}{C}} \right) - 1 \right]}{2 \left\{ \frac{B}{C} + \sqrt{\left(\frac{B}{C}\right)^2 - \frac{4A}{C}} - \left(\frac{B}{C} - \sqrt{\left(\frac{B}{C}\right)^2 - \frac{4A}{C}} \right) \exp \left(tC \sqrt{\left(\frac{B}{C}\right)^2 - \frac{4A}{C}} \right) \right\}} \quad (4.23)$$

Furthermore, if the external diffusion has been eliminated, the intrinsic rate constants k_{ads} and k_{desH} can be obtained from equation (4.23).

4.3.3 The Determination Strategy of Model Parameters and Design of Experiments

The four (k_{ads} , k_{desH} , q_m , and η) parameters in equation (4.19) can be determined by regression using the least square method. But the regression often cannot provide only one set of parameters if there are more than two parameters in models unless the narrow ranges of these parameters as the initial trial points are known. To avoid this uncertainty, the experiments can be designed as follows: 1) The maximum adsorption capacity q_m can be obtained from Langmuir isotherm at the same pH value. 2) Using very fine size particles (0.21 mm for this study) in the adsorption experiment, assuming the elimination of intraparticle diffusion for this particle ($\eta = 1$), and under powerful agitation (200 rpm for this study), the intrinsic rate constants k_{ads} and k_{desH} in equation (4.23) can be determined. 3). Using the different size particles greater than 0.21 mm in other adsorption experiments, the effectiveness factor η in equation (4.19) can be estimated when the intrinsic rate constants k_{ads} and k_{desH} have been determined in step 2).

There are no more than two parameters in each step (one example for determination of parameters in the model (4.19) is seen in Appendix).

CHAPTER FIVE

EXPERIMENTAL

5.1 Materials and Methods

5.1.1 Materials

As indicated in Chapter three, some investigations about biosorption of metal ions by corncob particles have been reported. But a wide study including both equilibrium and kinetics of biosorption of copper and cadmium ions by corncob particles has not yet been conducted.

Biosorbent: Vaughan et al (2001) reported that the corncob consisted of cellulose 41, hemicellulose 44, lignin 10, protein 2.0, starch 1.0, lipid 1.0, and ash 1.0 % (Fig. 5.1).

The corncob used in this study was provided by Flynn Produce Ltd. Mississauga, ON, Canada. The crude corncob was dried in an oven at 70°C for 48 hours. The dried corncob was cut into particles in a granulator (Laboratory Mill, model 4, Arthur H. Thomas Company). Then these particles were washed by deionized water with agitation for 20 minutes. After stilling for 10 minutes, the supernatant water containing some light particles was removed. The washing operation was repeated three times. The residual solids were dried in an oven at 100°C for 48 hours. These particles are called as the mixed size particles. Then a part of the mixed size particles were further sieved to obtain four size fractions: less than 0.42 mm, between 0.42 mm and 0.71 mm, between 0.71 mm and 1.10 mm, and between 1.10 mm and 1.58 mm, respectively. For the uses in calculations, the average particle sizes were taken as the middle values each fraction.

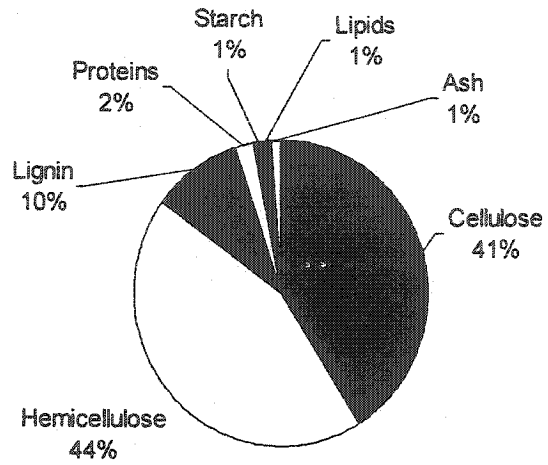


Fig. 5.1: Corncob particles composition (Vaughan et al., 2001)

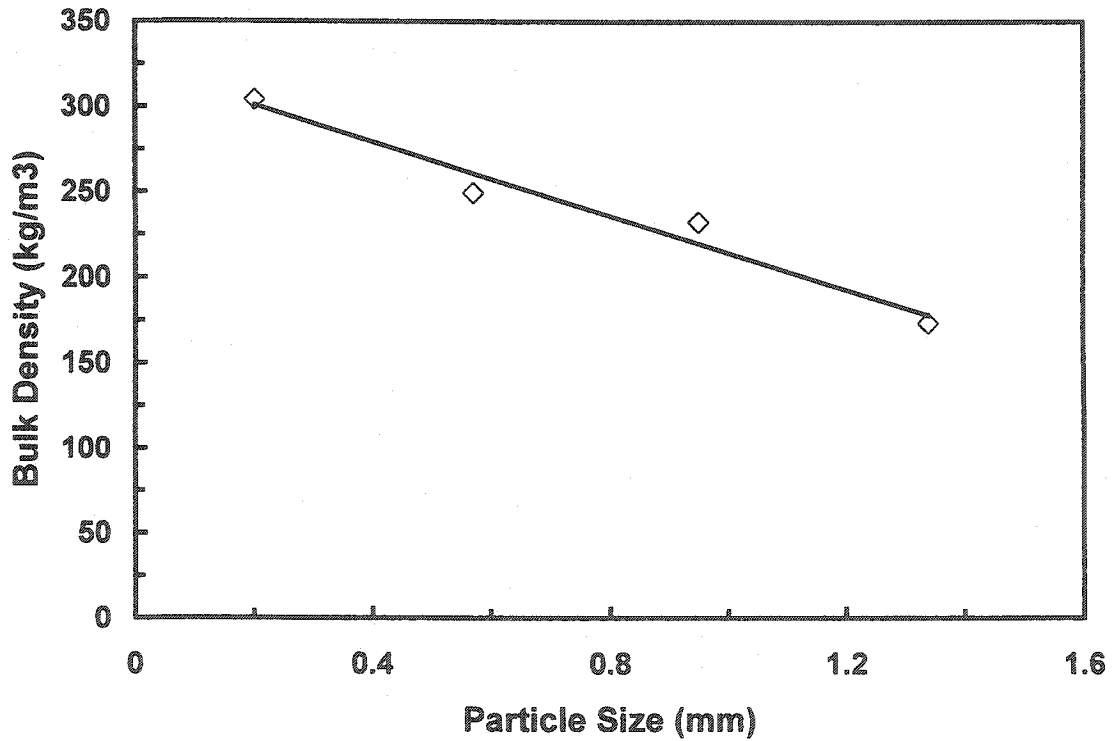


Fig. 5.2: The relationship between bulk densities and size of corncob particles. Symbols are experimental data, and solid lines are predicted data using Eq. (5.1).

They are 0.21, 0.57, 0.95, and 1.34 mm, respectively. The bulk densities of these fractions were determined by the volumetric method. The particles were filled in a 10 ml cylinder under shaking. The results are shown in Fig. 5.2. The relationship between the densities of the corncob particles and the sizes can be expressed as a linear equation (Eq. (5.1)):

$$D_n = 322.05 - 117.9d_p \quad (5.1)$$

where D_n is the density of the corncob particles (kg/m^3), and d_p is the size of the corncob particles (mm).

Some corncob particles were treated with 1 M NaOH solution to remove some components in the corncob to check their effect for adsorption. Ten grams of corncob particles were added in the 100 ml solution of 1 M NaOH. The suspension was heated to the boiling point, and kept at a boiling temperature for 20 minutes with stirring. After cooling, the suspension was filtered through filter paper (No. 42, Whatman), and then washed with deionized water. This operation was repeated three times. Finally, the filter cake was dried at 100°C for 48 hours. After drying, about 2.0 g of dry matter was obtained. Hence, about 80 % of the components from the corncob particles were extracted.

Chemicals: Cupric and cadmium stock solutions of 5000 and 1000 mg/l were prepared from cupric nitrate ($\text{Cu}(\text{NO}_3)_2 \cdot 2\text{H}_2\text{O}$, certified A. C. S., Fisher Scientific) and cadmium nitrate ($\text{Cd}(\text{NO}_3)_2 \cdot 4\text{H}_2\text{O}$, certified A. C. S., Fisher Scientific). The nitrate as an anion was selected since it hardly forms the complexes with metal ions.

Buffers: Two buffers were used in their suitable pH range. They are: 1) MES (2-[N-Morpholino]ethanesulfonic acid, $\text{C}_6\text{H}_{13}\text{NO}_4\text{S}$, Sigma Chemical Co.), which had been

proven that it weakly binds with cupric ions (Good et al, 1966), for copper in the range of pH 4.0-5.5; and 2) HEPES (N-[2-Hydroxyethyl]piperazine-N'-[2-ethanesulfonic acid], $C_8H_{18}N_2O_4F$, Sigma Chemical Co.) for cadmium in the range of pH 6.0-8.3.

5.1.2 Analytical Methods

1. Cupric and Cadmium Ion Measurement

The cupric and cadmium ion concentrations in the solution were measured by an Atomic Absorption Spectrophotometer (Varian Techtron Pty. Limited, AA1475 Series) at a wavelength of 324.8 nm for copper and 228.8 nm for cadmium. The spectrophotometer was calibrated by a series of standard solutions, which were prepared from 1000 mg/l copper and cadmium reference solutions (Fisher Scientific), for each run.

2. pH Measurement

The pH of the suspension was measured by a Fisher pH meter (AR50, Fisher Scientific) with a combined electrode (accuTup+, Cat. 13-620-185, Fisher Scientific) and an automatic temperature compensation probe. The calibrations for the pH meter were performed with the pH buffer solutions (pH 4.00, 7.00, and 11.00, Fisher Scientific).

5.2 Experimental Technique

5.2.1 Equilibrium of Adsorption (Adsorption Isotherm)

Experiments were performed in a series of 125 ml Pyrex flasks immersed in a thermostat, which was maintained at the required constant temperature. First, a 1000 ml flask containing 400 ml deionized water and the required buffer quantity (if applicable) was kept in the thermostat until the required temperature of the buffer solution was

attained. The required buffer quantity was determined by the prescription of Perrin and Dempsey (1974). A 2M NaOH solution was used to adjust the solution pH to the required value. Then the solution was distributed to 8 flasks of 125 ml containing 0.500 g of corncob particles each to form the suspension. Next, the cupric or cadmium nitrate stock solution of 1000 mg/l was added to the each flask by pipettes according to the initial metal ion concentration requirement. The final volume in each flask was 50 ml. The flasks were kept in a shaker (Blue M) at a constant temperature for at least 12 hours. Finally, a 3 ml sample was taken from each flask by a syringe, and filtered through a 0.45 μm membrane (Milipore Co.).

If the buffer was not used, the experimental procedure was simplified. After adding the required cupric or cadmium ions into flasks containing water, the initial pH was adjusted to the required value by 0.1 M NaOH and 0.1 M HNO₃ (Fisher Scientific). Then the suspensions in the flasks were shaken and the samples were taken at various intervals. The most of the experimental points (including the kinetic experiments) were conducted two times. The departures between the duplicated points were less than 7 %. Using the error bar, these departures are shown in the figures of Chapter six

The initial metal ion concentrations for a single component usually ranged from 20 mg/l to 100 mg/l, but in some cases the maximum concentration was 140 mg/l. For the binary components, two ratios of copper and cadmium (mg/mg) 1.00 and 0.565 (the molecular ratios were 1.769 and 1.00) were used. The total metal ion concentrations (copper plus cadmium) range was from 40 mg/l to 200 mg/l.

As discussed in Chapter 2.1, at higher pH values, metal ions form hydroxides and they precipitate. Equation (2.8) can roughly estimate the maximum pH value when

precipitation does not occur. The solubility products of cupric and cadmium hydroxides are 1.6×10^{-19} and 2.3×10^{-14} , respectively (Holleman, 2001a). Using equation (2.8), it can be calculated that the values of pH 6.00 for copper and 8.71 for cadmium are the maximum values at which the precipitation does not occur at equilibrium concentration of 100 mg/l for copper and cadmium in solutions, respectively. It should be noted that this criterion is vague for the following reasons. The first reason is that a solubility product as a criterion is only suitable for a homogeneous phase. Once the solubility product is exceeded, a solid phase (precipitate) appears. However, this adsorption process did not employ a homogeneous system. It had an additional solid substance, the corncob particles, in these experiments. The second reason is that the metal ion concentration in equation (2.8) means the equilibrium concentration (at the end of the contact time) rather than the initial concentration. In general, the equilibrium concentration is lower than the initial concentration.

To check the appearance of the precipitate at a higher pH, an equilibrium experiment using the method in Chapter 5.2.1 was conducted at a pH of 5.9 for copper. When the experiments were completed, two samples were taken from the solution. One sample was passed through a membrane. The metal ion concentrations in the filtrate and another sample were measured to check the appearance of the precipitate from the concentration difference of the two samples. The other similar experiments were also conducted at a pH of 8.3 for cadmium. The tests showed that there was no appearance of metal hydroxide precipitates at the initial pH of 5.9 for copper and 8.3 for cadmium because the metal ion concentrations of the two samples had little differences (Fig. 5.3

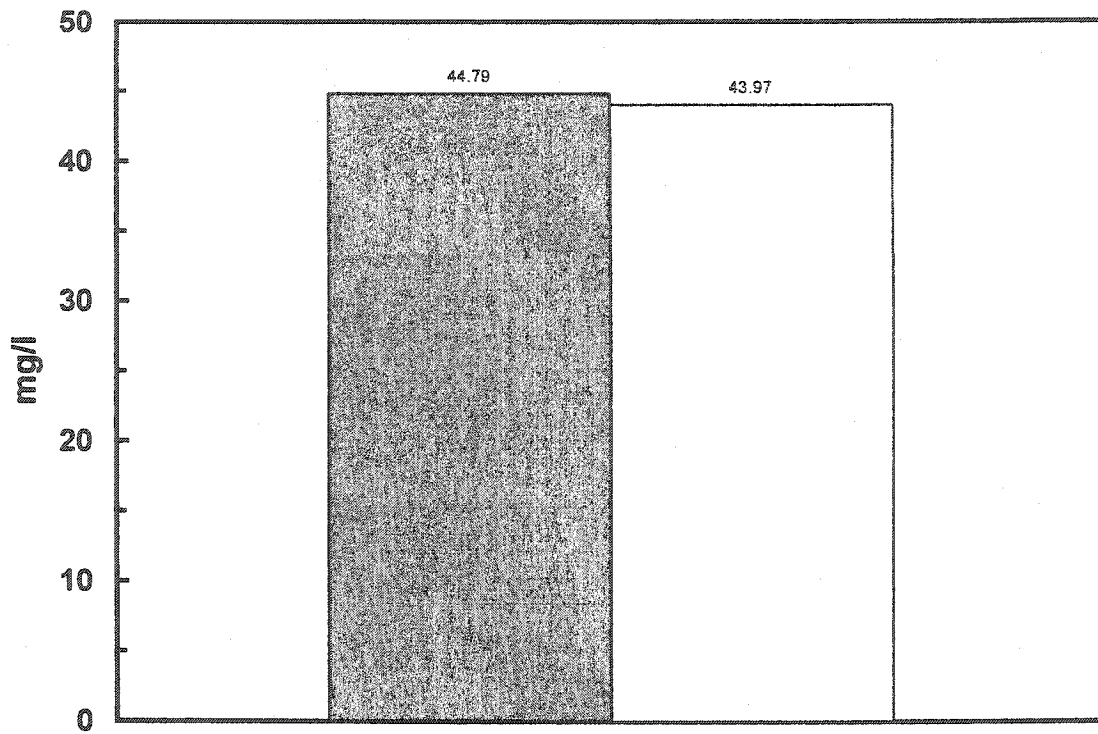


Fig. 5.3: Copper concentration comparison before and after membrane filtration. % before filtration, \exists after filtration.

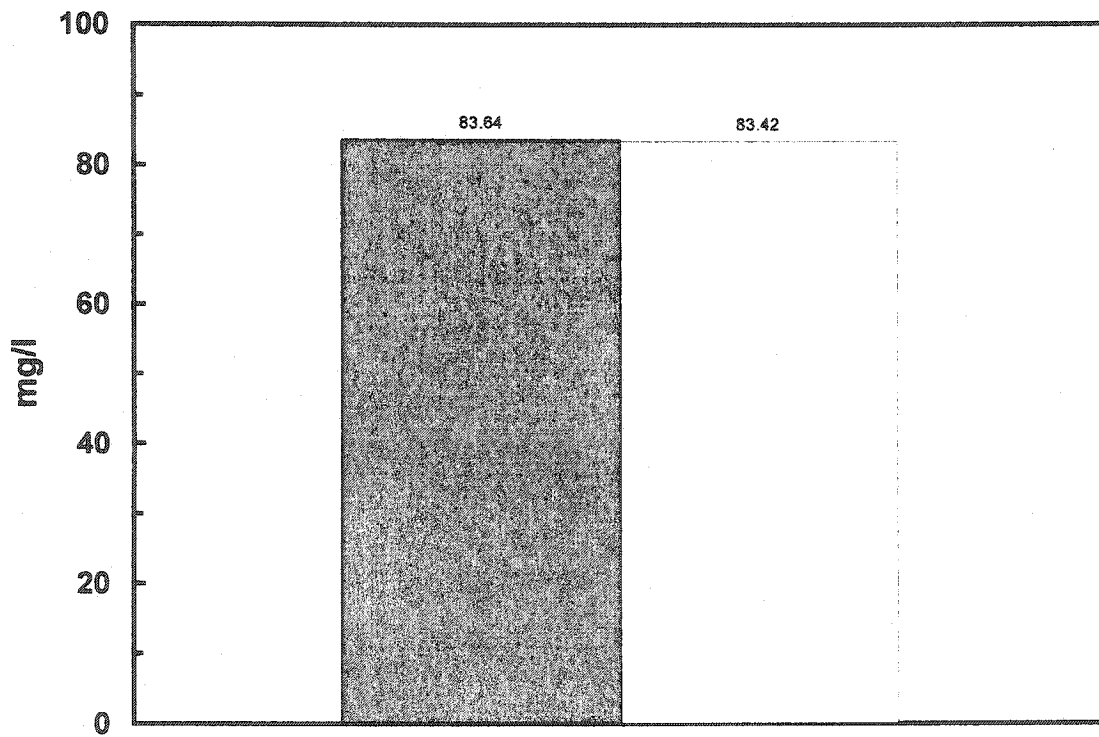


Fig. 5.4: Cadmium concentration comparison before and after membrane filtration. % before filtration, \exists after filtration.

and 5.4). Their related errors were 1.14 % and 0.91 % for copper and cadmium concentrations in the solution, respectively.

5.2.2 Kinetics of Adsorption

Experiments were performed at 23°C in a 500 ml Pyrex beaker that had an inside diameter 0.1 m. The beaker was equipped with a mechanical agitator with an adjustable agitation speed. The agitator had an impeller with a diameter of 0.051 m. The distance of the impeller from the bottom of the beaker was 0.014 m. When starting the experiments, the required mass of corncob particles was added into the beaker containing 495 ml of deionized water. Then the agitator was run for 5 minutes at the required speed in order to soak the corncob particles with water. The required quantities of 0.1 M NaOH and metal ion from 5000 mg/l cupric (or cadmium) nitrate stock solution were added to the suspension by pipettes. The pH values in the suspension were measured immediately and recorded as the initial pH. The height of the liquid in the beaker was about 0.054 m. Samples were taken from the beaker at the required time (usually, 1, 2, 3, 5, 10, 20, 40, 70, and 110 minutes) by a syringe, and filtered through a 0.45 µm membrane (Milipore Co.).

5.2.3 Measurement of pH at Zero Charge Point of Corncob

The primary equilibrium method of H⁺ and OH⁻ was adopted to measure the pH at zero charge point (pH_{zcp}) of the corncob particles in this study (Ahmed, 1966; Tewari and Campbell, 1976). Fifty milliliters of 0.1 M sodium nitrate solution as a background electrolyte was added in a 125 ml flask. Carbon dioxide in the solution was purged with

nitrogen. The pH value of the solution was adjusted to the required initial value with 0.1 M HNO₃. Then 0.500 g of the corncob particles was added in the solution. The pH would increase or decrease, depending on the initial pH of the solution. After about 5 minutes, the pH value was stable, and it was considered as the final pH. This operation was repeated several times until the final pH in the suspension was equal or approximately equal to the initial pH. This value represents the pH_{zcp} of the corncob particles. All the operations were carried out under nitrogen atmosphere. The result showed that pH_{zcp} was 4.97 for the mixture of various sizes of the corncob particles.

CHAPTER SIX

RESULTS AND DISCUSSIONS

6.1 Effect of pH on Adsorption Isotherms

Since a biosorption process is analogous to an ion exchange process, the pH of the aqueous solution has a significant effect on metal uptake. The adsorption isotherms of cupric ion using two fractions of corncob particle sizes (the mixed and 0.21 mm size) in water at an initial pH of 4.0, 5.0, 5.5, and 6.0 and with the buffer (MES) at a pH of 4.0, 4.5, 5.0 and 5.5 are shown in Figs.6.1 - 6.3. The same experiments were performed for cadmium at various pH values in water and with the two different buffers (HEPES and MES), and the results are displayed in Figs. 6.4 - 6.7. All the seven figures indicate that the uptakes of copper and cadmium quickly increase with an increase of the initial pH. For example, when the initial pH is increased from 4.0 to 5.5 at a solute equilibrium concentration of 0.60 mmol/l in the solution, the uptakes increase from 0.024 mmol/g to 0.068 mmol/g (Fig. 6.1), i. e., the ratio of the latter and the former is 2.83. The uptakes of copper in the presence of the buffer at a pH of 4.0 and 5.5 are 0.035 mmol/g and 0.10 mmol/g (Fig. 6.3), and the ratio of the latter and the former is 2.85. Figs. 6.4 - 6.6 show the same trend for the adsorption of cadmium. For example, the uptake of cadmium increases from 0.022 mmol/g at a pH of 4.0 to 0.058 mmol/g at a pH of 8.3 at a solute equilibrium concentration of 0.20 mmol/l (Fig. 6.4). This indicates that the pH is an important factor in the adsorption of heavy metal ions.

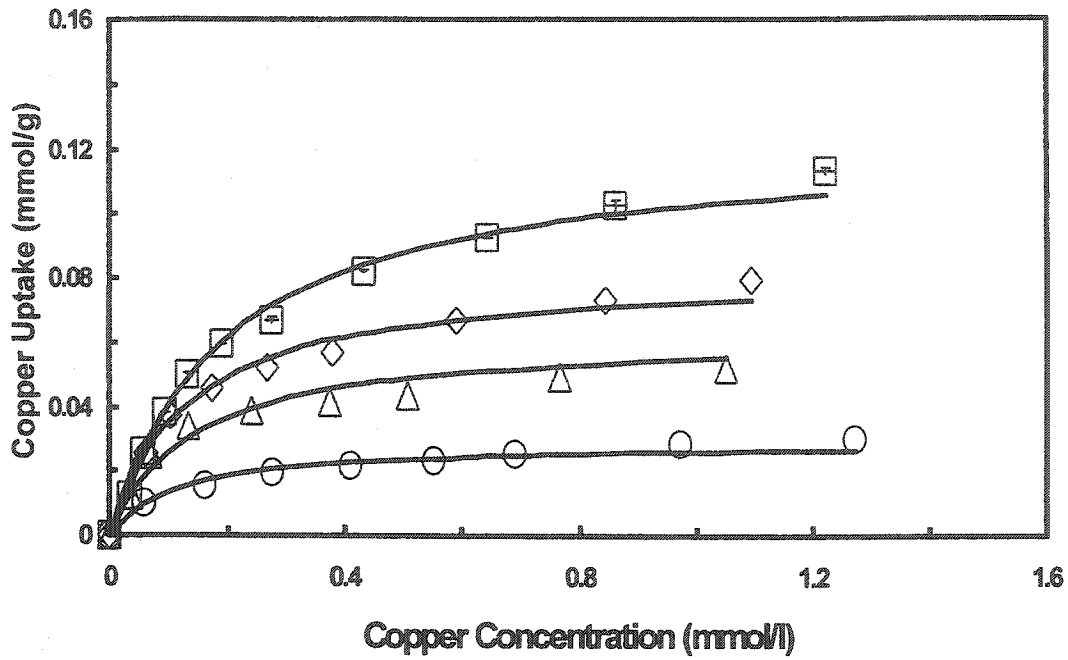


Fig. 6.1: Effect of pH on adsorption isotherms of copper in water solution (mixed size particles, corn cob concn. 10 g/l), \circ pH 4.0, \triangle pH 5.0, \diamond pH 5.5, \square pH 6.0. Symbols are experimental data, and solid lines are predicted data using Eq. (3.1).

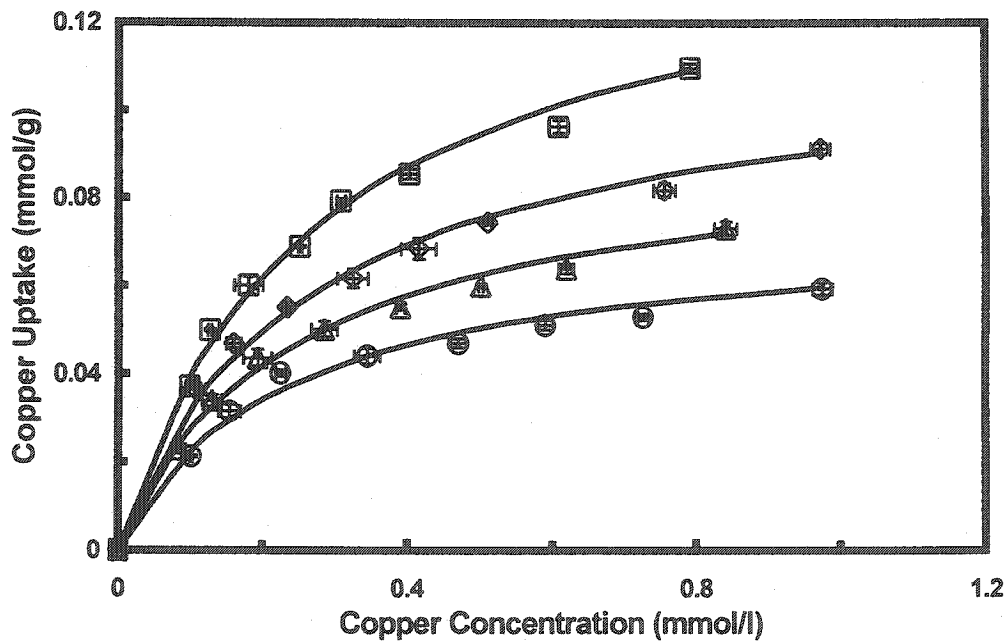


Fig. 6.2: Effect of pH on adsorption isotherms of copper in water solution (0.2 mm size particles, corn cob concn. 10 g/l), \circ pH 4.5, \triangle pH 5.0, \diamond pH 5.5, \square pH 6.0. Symbols are experimental data, and solid lines are predicted data using Eq. (3.1).

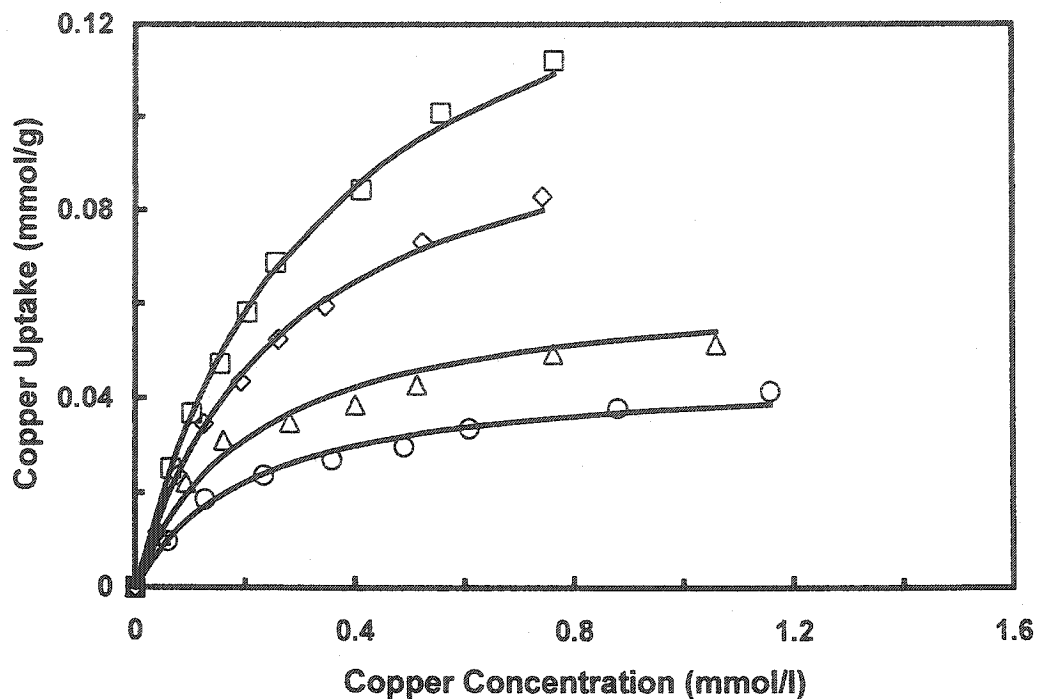


Fig. 6.3: Effect of pH on adsorption isotherms of copper with MES (mixed size particles, corncob concn. 10 g/l). \circ Symbols are experimental data, and solid lines are predicted data using Eq. (3.1).

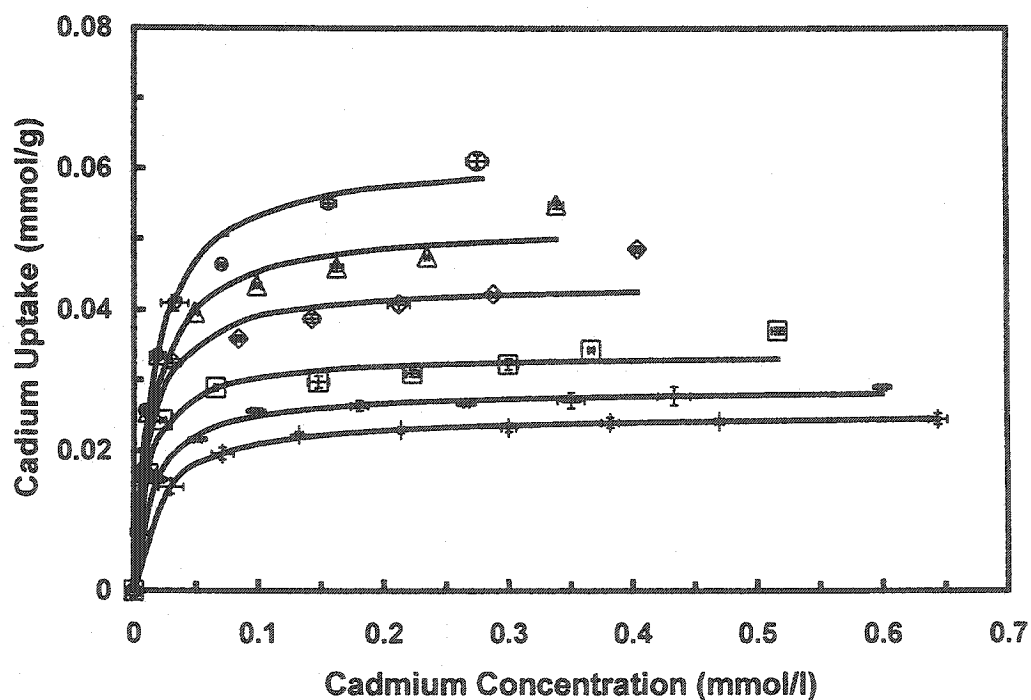


Fig. 6.4: Effect of pH on adsorption isotherms of cadmium in water solution (mixed size particles, corncob concn. 10 g/l). + pH 4.0, - pH 5.0, \square pH 6.0, \diamond pH 7.0, \triangle pH 7.6, \circ pH 8.3. Symbols are experimental data, and solid lines are predicted data using Eq. (3.1).

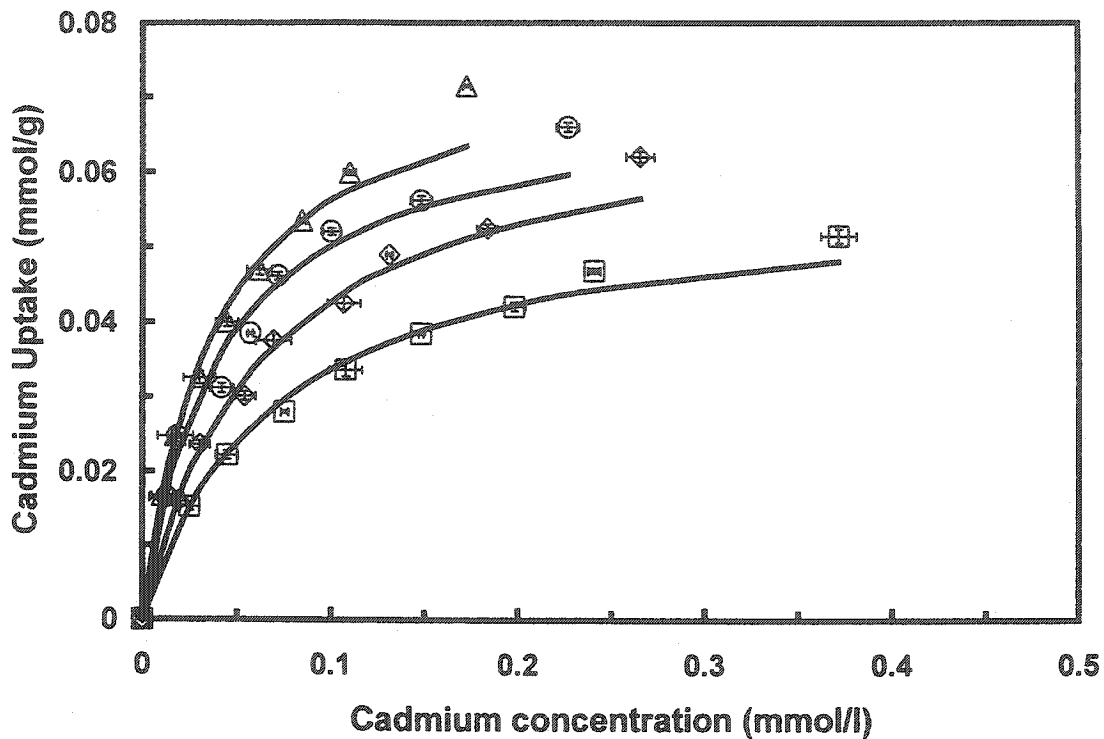


Fig. 6.5: Effect of pH on adsorption isotherms of cadmium in water solution (0.2 mm size particles, corn cob concn. 10 g/l). \square pH 6.0, \diamond pH 7.0, \circ pH 7.6, \triangle pH 8.3. Symbols are experimental data, and solid lines are predicted data using Eq. (3.1).

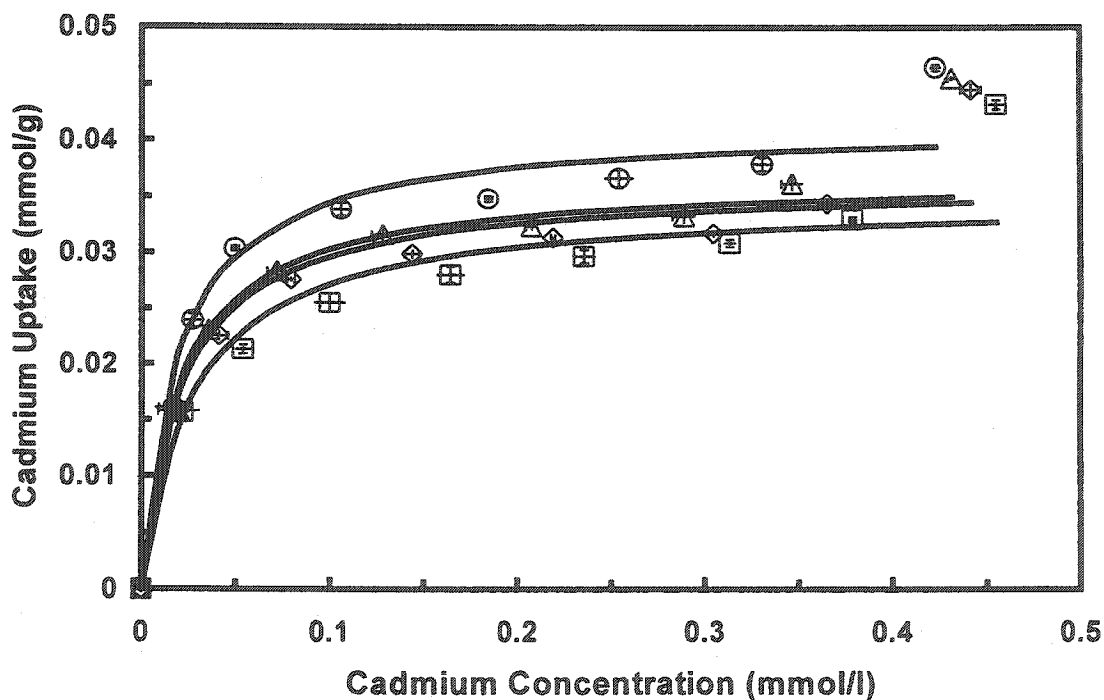


Fig. 6.6: Effect of pH on adsorption isotherms of cadmium with HEPES (mixed size particles, corn cob concn. 10 g/l). \square pH 6.0, \diamond pH 7.0, \triangle pH 7.6, \circ pH 8.3. Symbols are experimental data, and solid lines are predicted data using Eq. (3.1).

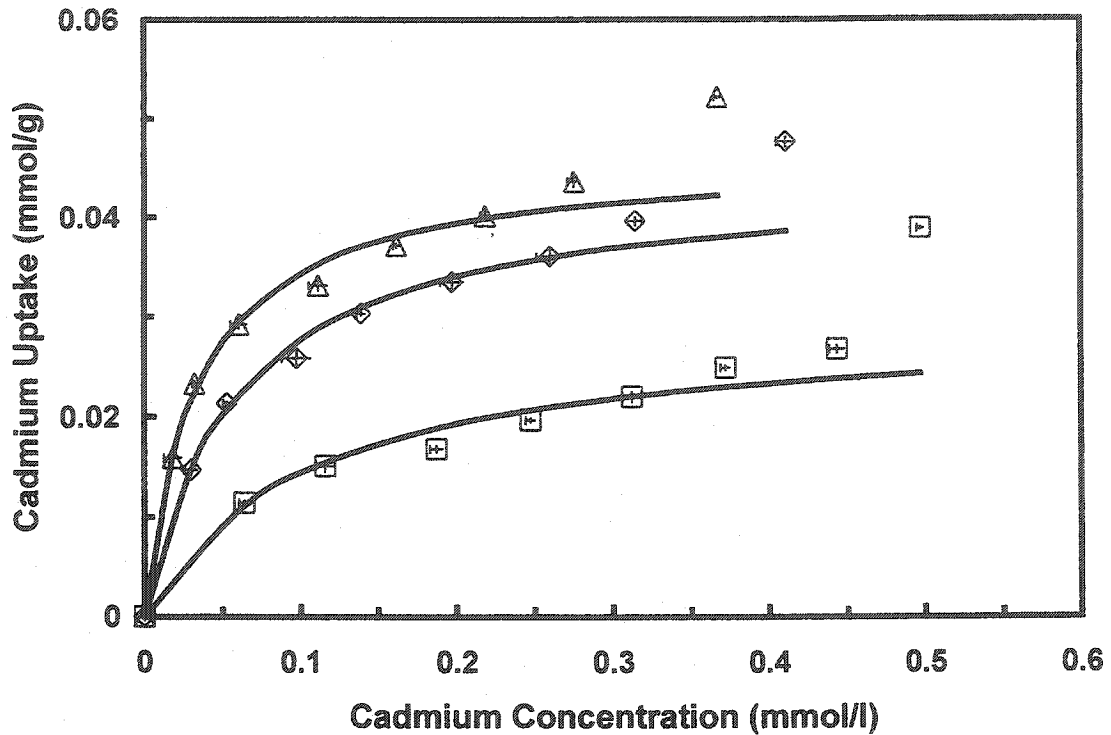


Fig. 6.7: Effect of pH on adsorption isotherms of cadmium with MES (mixed size particles, corncob concn. 10 g/l). □ pH 4.0, ◇ pH 5.0, △ pH 6.0. Symbols are experimental data, and solid lines are predicted data using Eq. (3.1).

Since a change of the initial pH in the solution influences both the active sites on cell wall and the metal solution chemistry, three explanations have been presented for this phenomenon. The first explanation is the difference between the pH in the solution and the pH at the zero charge point (pH_{zcp}) (or pH at isoelectric point) of biosorbents. The bonding formed between metal ions and active sites on the cell wall can be ascribed to chemical and coulombic factors. The latter can be estimated by the difference between the pH_{zcp} and the pH in the solution (Nernst's law) (Fokkink et al., 1989).

$$\Psi_0 = 0.059(pH_{zcp} - pH) \quad (6.1)$$

where Ψ_0 is the surface potential of the cell wall. The surface of the cell wall with a negative potential favors the adsorption of the positively charged metal ions. When the

solution pH value increases from the pH_{zcp} , the absolute value (negative potential) of the surface potential increases, the coulombic contribution to the adsorption increases, and then the adsorption capacity increases. The second explanation is the presence of competitive adsorption between protons and metal ions. At a low pH, there are many protons in the solution. The metal ions will compete with the protons for binding with the active sites on the cell surface. This competition will significantly decrease at a high pH when the concentration of protons greatly decreases. The third explanation is the ligands on the cell wall. At a lower pH, the cell wall has more positive ligands than at a higher pH. The entire cell wall favors associating with protons because the metal ions suffer stronger repulsive forces from the positive ligands on the cell wall than protons (Zhou and Kiff, 1991). As the pH increases, more ligands become negative, and they easily attract the positively charged metal ions.

On the other hand, the uptakes of copper in the presence of the buffer (MES) (Fig. 6.3), which does not form complexes with cupric ions (Good et al., 1966), are greater than those without a buffer (Fig. 6.1) at the same initial pH and solute equilibrium concentration in the solution. The reason for this is that the uptakes in the presence of the buffer (Fig. 6.3) are at a constant pH, while the uptakes with water (Fig. 6.1) occur at lower pH values than their initial pH values. However, the uptakes of cadmium with the HEPES buffer (Fig. 6.6) are lower than those without the buffer (Fig. 6.4). The cause may be that HEPES binds with cadmium ions or occupies the active sites on the cell wall, which decreases the adsorption of cadmium ions by the active sites.

The linearized Langmuir model (equation (3.2)) was used to determine the two parameters (K_l and q_m) of the model for the experimental data given in Figs. 6.1-6.7

Table 6.1: Parameters: q_m and K_l of the Langmuir model (Eq. (3.1)) for copper at various pH values

Initial pH	4.0	5.0	5.5	6.0
Mixed size in water				
q_m (mmol/g)	0.0291	0.0623	0.0900	0.123
K_l (l/mmol)	8.70	7.17	5.65	2.88
0.21mm size in water				
q_m (mmol/g)	0.0741	0.0934	0.1034	0.147
K_l (l/mmol)	4.27	4.06	3.80	3.63
pH (with MES)	4.0	4.5	5.0	5.5
q_m (mmol/g)	0.0458	0.0653	0.106	0.140
K_l (l/mmol)	4.706	4.581	3.90	3.80

Table 6.2: Parameters: q_m and K_l of the Langmuir model (Eq. (3.1)) for cadmium at various pH values

Initial pH (without buffer)	4.0	5.0	6.0	7.0	7.6	8.3
Mixed size in water						
q_m (mmol/g)	0.0252	0.0287	0.0337	0.0439	0.0522	0.0620
K_l (l/mmol)	48.3	64.9	88.62	78.25	65.99	61.96
0.21mm size in water						
q_m (mmol/g)			0.0572	0.0700	0.0702	0.0772
K_l (l/mmol)			14.25	15.70	24.91	26.54
pH (with HEPES)			6.0	7.0	7.6	8.3
q_m (mmol/g)			0.0348	0.0362	0.0367	0.0413
K_l (l/mmol)			35.36	45.14	47.22	50.37
pH (with MES)	4.0	5.0	6.0			
q_m (mmol/g)	0.0294	0.0443	0.0462			
K_l (l/mmol)	9.47	16.5	28.9			

(Tables 6.1 and 6.2). The maximum adsorption capacities q_m increase with an increase of pH for the isotherms in the water solution and with the buffer both for copper and cadmium, while the Langmuir equilibrium constants decrease for copper (Table 6.1), and increase for cadmium with 0.21 mm particle size (Table 6.2), and with the two buffers (Table 6.2). For cadmium in the water, the Langmuir equilibrium constants increase in the initial pH ranging from 5.0 to 6.0 (Table 6.2). After the initial pH of 6.0, the Langmuir equilibrium constants decrease until the initial pH reaches 8.3. Guibal et al. (1995) reported that q_m and K_l increased with the pH when they studied uranium sorption on chitosan. However, they also reported that the q_m was almost a constant and that K_l decreased with an increase of the pH for uranium sorption on glutamate glucan.

It is also noted that there are some obvious departures from the Langmuir isotherm for the experimental points of the maximum cadmium concentrations (Figs. 6.4-6.7, and 6.13). One of the explanations is that at a higher metal ion concentration, the chemical adsorption occurred to form the multi-layer adsorption, which contravened the one of the assumptions of the Langmuir model: a monolayer physical adsorption. Another explanation is that at a higher metal ion concentration, the precipitation took place in the solution. These precipitates settled down in the bottom of the flasks or were separated by the membrane if the samples contained the precipitates.

Equations (4.3) and (4.6) were used to correlate the maximum adsorption capacity and the equilibrium constant with the pH. The regression parameters, q_{mzcp} , k , K_0 , and n , of in equations (4.3) and (4.6) are shown in Tables 6.3 and 6.4. These parameters were used in equation (4.7) and the simulated curves are shown in Figs. 6.8 and 6.9.

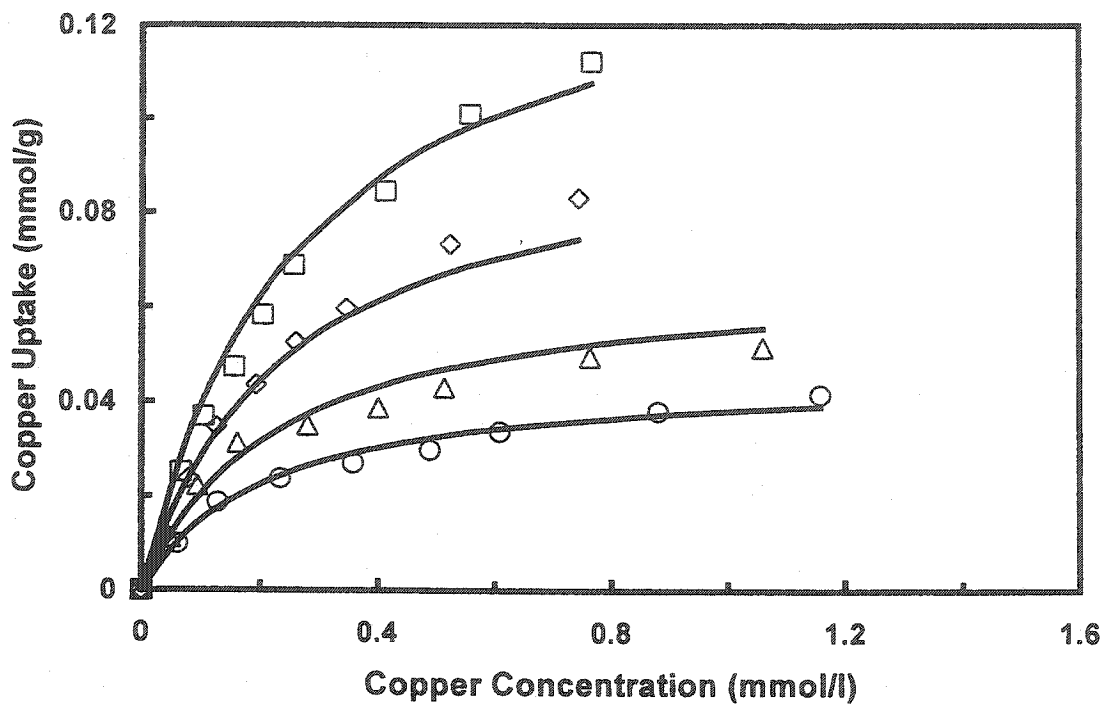


Fig. 6.8: Effect of pH on isotherms of copper with MES (mixed size, (conditions as Fig. 6.3) ○ pH 4.0, △ pH 4.5, ◇ pH 5.0, □ pH 5.5. Symbols are experimental data, and solid lines are predicted data using Eq. (4.7).

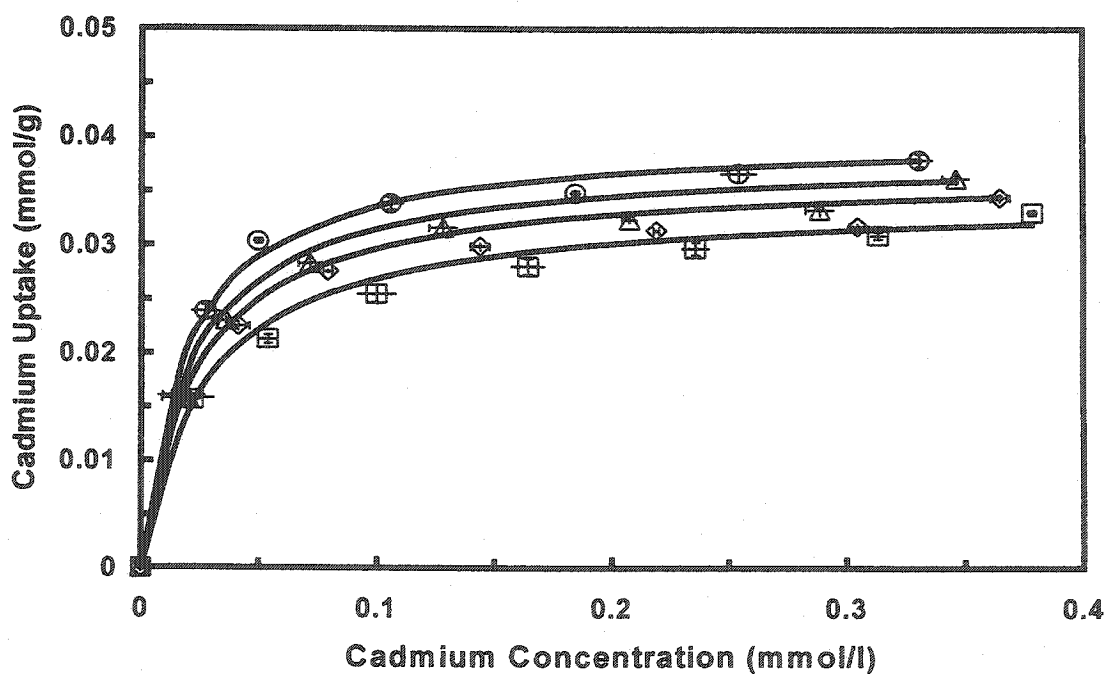


Fig. 6.9: Effect of pH on isotherms of cadmium with HEPES (mixed size, (conditions as Fig. 6.6) □ pH 6.0, ◇ pH 7.0, △ pH 7.6, ○ pH 8.3. Symbols are experimental data, and solid lines are predicted data using Eq. (4.7).

Table 6.3: Parameters: q_{mzcp} , k , K_0 , and n of Eqs. (4.3, 4.6) for copper

Conditions	Mixed size	Mixed size, MES
q_{mzcp}	0.0598	0.0966
k	0.727	0.767
K_0	75.19	9.061
n	-0.505	-0.1605

Table 6.4: Parameters: q_{mzcp} , k , K_0 , and n of Eqs. (4.3, 4.6) for cadmium

Conditions	Mixed size	Mixed size, HEPES	Mixed size, MES
q_{mzcp}	0.0256	0.0319	0.0389
k	0.267	0.0685	0.226
K_0	238.4	14.68	1.016
n	-0.1639	0.1524	0.558

6.2 Effect of pH on Adsorption Isotherm of Copper and Cadmium in Mixture

To study the competitive adsorption between copper and cadmium ions, a series of mixture isotherms at the various initial pH values were determined (Figs. 6.10 - 6.13). Two molecular ratios of 1.77 of copper and cadmium and 1.00 were used. The uptake of copper in the mixture of copper and cadmium increases (Figs. 6.10 and 6.12), whereas the uptake of cadmium first increases and then decreases with increasing total metal ion concentration (inversed U-shaped isotherm) (Figs. 6.11 and 6.13). This phenomenon in the diluted solution is not in agreement with a number of reported data in which the uptakes of both competitive metal ions will increase with the increase of their concentrations (Christophi and Axe, 2000). Although this phenomenon is not found in the adsorption of the dilute solution (i. e., there are three components in a solution, water and two adsorbed solutes. In this system, the concentrations of both adsorbed solutes are

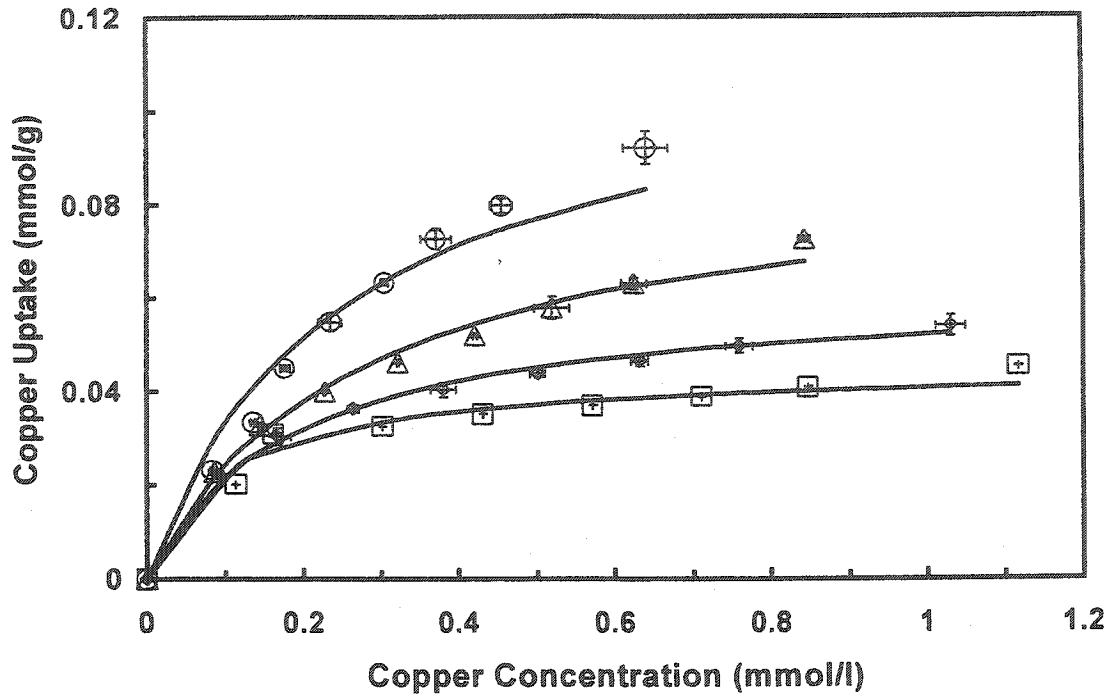


Fig. 6.10: Effect of pH on adsorption isotherms of copper in mixture (mixed size particles, corncob concn. 10 g/l, mol. ratio 1.77). \square pH 4.5, \diamond pH 5.0, \triangle pH 5.5, \circ pH 5.9. Symbols are experimental data, and solid lines are predicted data using Eq. (4.8).

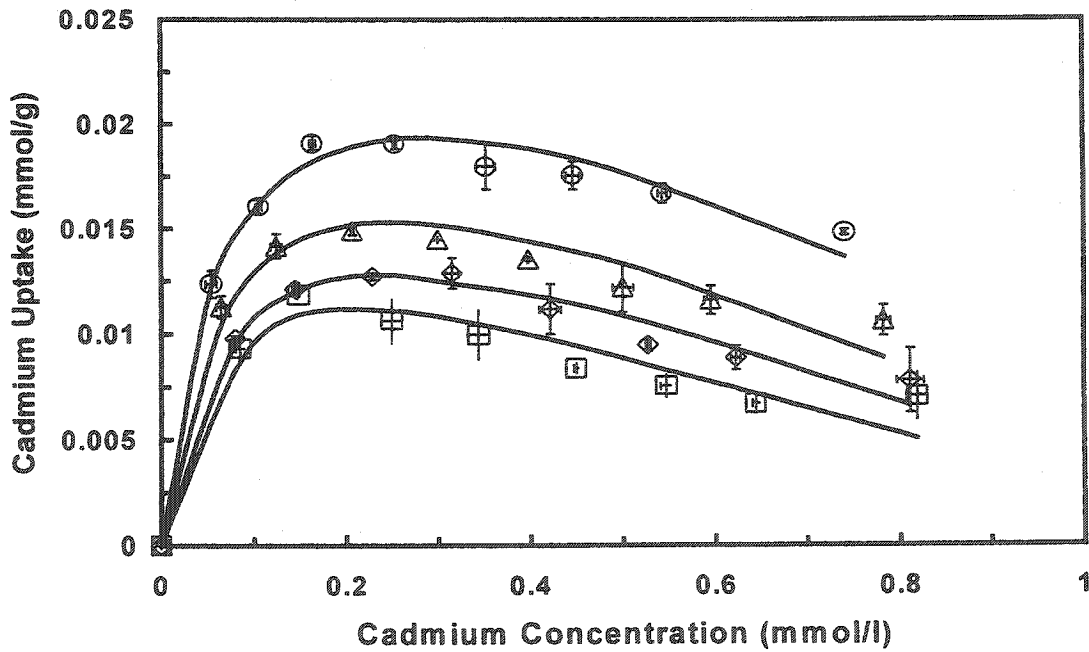


Fig. 6.11: Effect of pH on adsorption isotherms of cadmium in mixture (mixed size particles, corncob concn. 10 g/l, mol. ratio 1.77). \square pH 4.5, \diamond pH 5.0, \triangle pH 5.5, \circ pH 5.9. Symbols are experimental data, and solid lines are predicted data using Eq. (4.9).

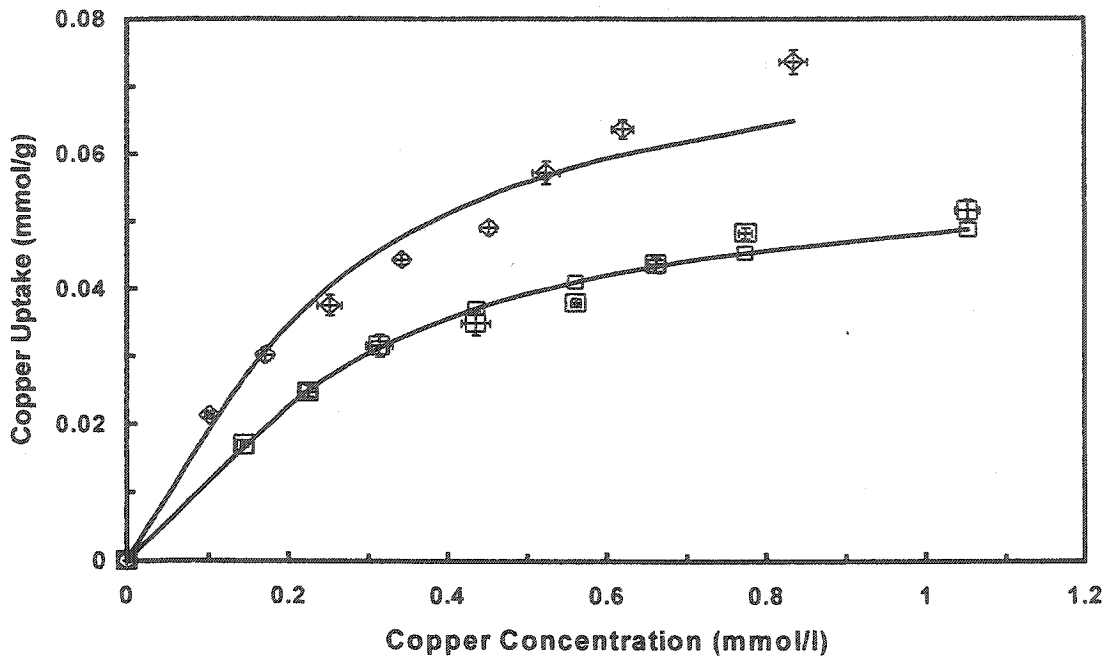


Fig. 6.12: Effect of pH on adsorption isotherms of copper in mixture (mixed size particles, corncob concn. 10 g/l, mol. ratio 1.00). \square pH 5.5, \diamond pH 5.9. Symbols are experimental data, and solid lines are predicted data using Eq. (4.8).

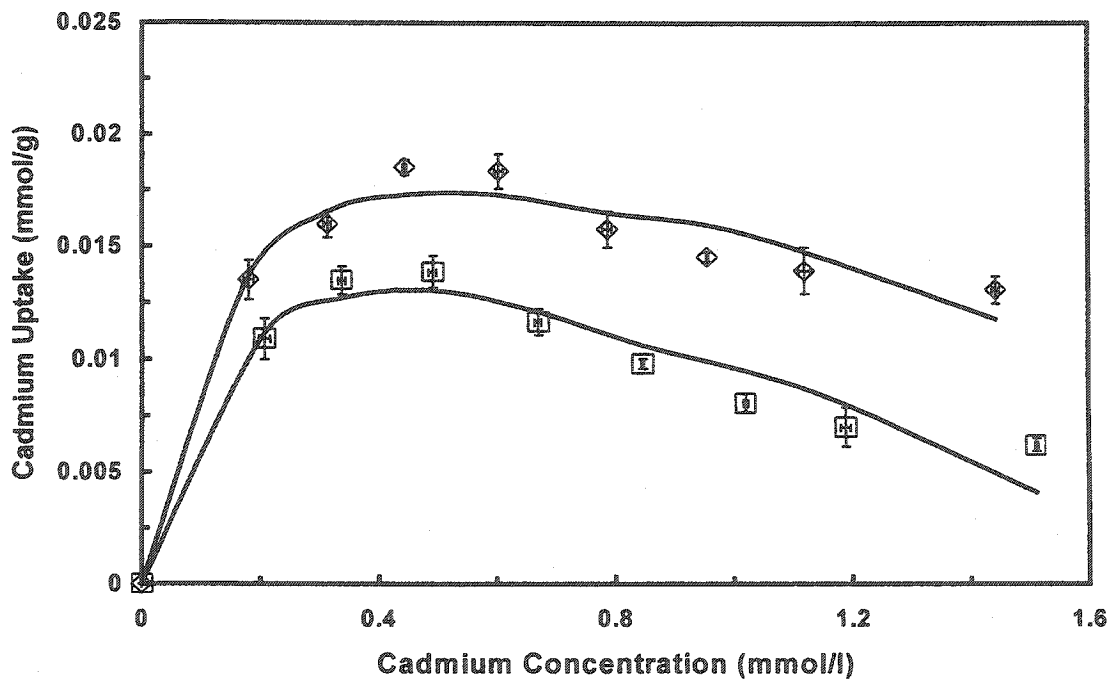


Fig. 6.13: Effect of pH on adsorption isotherms of cadmium in mixture (mixed size particles, corncob concn. 10 g/l, mol. ratio 1.00). \square pH 5.5, \diamond pH 5.9. Symbols are experimental data, and solid lines are predicted data using Eq. (4.9).

very low compared with that of a water solvent), some observations of inversed U-shaped isotherms (Schwuger and Smolka, 1977; Ash et al., 1973; Kipling, 1951) have been reported for binary component adsorption, which is called the isotherm of composition change (i. e., there are only two components, the solute and the solvent in the solution, - no water. Both components are adsorbed on an adsorbent simultaneously. In this binary system, the two components have comparable concentrations (for example, 40 % to 60 %)). Moreover, Schwuger and Smolka (1977) found that the uptakes of the anionic surfactants from the mixture were even greater than those for individual surfactant adsorption when they studied the adsorption of anionic and nonionic surfactants on the activated carbon. This phenomenon was not observed when the tests were carried out in this study. The uptake of copper from the mixture (Fig. 6.10) is somewhat lower than that from the individual solution (Fig. 6.1) at the same initial pH and equilibrium concentration in the solution, whereas the uptake of cadmium from the mixture (Fig. 6.11) is much lower than that from the individual solution (Fig. 6.4). Compared to the two cases of molecular ratio of copper and cadmium of 1.77 (Figs. 6.10 and 6.11) and 1.00 (Figs. 6.12 and 6.13) for the competitive adsorption, the latter has the lower uptakes than the former both for copper and cadmium. For example, at the initial pH of 5.5 and equilibrium concentration of 0.40 mmol/l, the uptakes of copper are 0.052 mmol/g for the molecular ratio of 1.77 (Fig. 6.10) and 0.034 mmol/g for the ratio of 1.00 (Fig. 6.12), while the corresponding uptakes for cadmium are 0.0135 mol/g (Fig. 6.11) and 0.0125 mmol/g (Fig. 6.13). It is obvious that the molecular ratio in the mixture has a greater effect on the uptake of copper than that of cadmium. It is also expected that if the

adsorption process is conducted at a molecular ratio greater than 1.77, which has more copper ions in the solution, more cupric ions will be adsorbed.

Tobin et al. (1984) reported that the molar uptake of metal ions by the biomass of *R. arrhizus* was higher for metal ions with a larger ionic radius than ions with a smaller ionic radius. This observation is not in agreement with the results from the present work. Cupric ion has a smaller radius (0.72 Å) than cadmium radius (0.97 Å) (Table 6.5), and the uptakes of the former are several times larger than the uptakes of the latter. One of the possible causes is the difference of molecular weight between copper and cadmium. The former is 63.54, while the latter is 112.4. The heavier molecules have a slower motion speed on the surface and in the pores, which decreases the adsorption rate, and then affects the adsorption equilibrium. The second explanation may be that the corn cob particles possess a majority of small pores in their interior, which made the cupric ions with a smaller radius were easier adsorbed than cadmium ions with a larger radius. The third explanation may be that copper has one unpaired electron (Table 6.5), while all the electrons of cadmium are paired. Consequently, the unpaired electron of copper may be easily attracted by the electric field originating from adsorbents (Chong and Volesky, 1996)

The curves in Figs. 6.8 - 6.11 and the values in Table 6.6 were obtained by fitting equations (4.8, 4.9) using the experimental data from the mixtures of copper and cadmium. The very small values of the interaction factor δ_2 for molecular ratio 1.77 indicate that copper exhibits a greater affinity than cadmium in their mixture; while the uptake of cadmium is affected considerably by the competitive cupric ions. This also

Table 6.5: Metal ion data

Characteristics	Cu ²⁺	Cd ²⁺
Atomic weight ⁽¹⁾	63.54	112.4
Ionic radius (nm) ⁽⁵⁾	0.072	0.097
Electronegativity ⁽²⁾	1.9	1.69
Polarizability (ground state) (10 ⁻²⁴ cm ³) ⁽³⁾	6.1	7.2
Electron configuration ⁽⁴⁾	[Ar]3d ¹⁰ 4s ¹	[Kr]4d ¹⁰ 5s ²

(1), (2), (3) David (1998 a, b, c)

(4) Holleman (2001 b)

(5) Holtzclaw et al (1984)

Table 6.6: Interaction factors: δ_1 , δ_2 , ε_1 , and ε_2 of adsorption isotherms (Eqs. (4.8, 4.9)) in mixture of copper and cadmium at various pH values

Initial pH (mol. ratio 1.77)	4.5	5.0	5.5	5.9
Cu				
δ_1	1.20	0.735	0.645	1.16
δ_2	6.20x10 ⁻¹⁰	1.32x10 ⁻⁵	2.94x10 ⁻⁸	2.97x10 ⁻¹⁶
Cd				
ε_1	0.0604	0.0488	0.0511	0.0743
ε_2	0.0953	0.0975	0.121	0.165
Initial pH (mol. ratio 1.00)			5.5	5.9
Cu				
δ_1			1.06	1.69
δ_2			0.298	0.166
Cd				
ε_1			0.0541	0.0609
ε_2			0.0520	0.0594

implies that the cadmium biosorption by the corncob particles is reversible. With increasing total metal ion concentration, some cadmium ions adsorbed are replaced by cupric ions, which results in the decrease of the uptake of cadmium. However, this competitive ability of copper depends on the molecular ratio of copper and cadmium. When decreasing the molecular ratio from 1.77 to 1.00, the corresponding values of the interaction factors δ_2 increase several orders of magnitude. For example, δ_2 are 2.94×10^{-8} at a pH of 5.5 and the molecular ratio of 1.77 and 0.298 at a pH of 5.5 and the ratio of 1.00, respectively. This suggests that the competitive ability of copper greatly decreases with decreasing the molecular ratio.

6.3 Effect of Temperature on Adsorption Isotherms

It is well known that a change of temperature can cause a shift of chemical equilibrium (uptake for adsorption) for either exothermic or endothermic reactions. To study the effect of temperature on biosorption, the isotherms of cupric ion by the corncob particles in the presence of the buffer (MES) at a pH of 5.5 and temperatures 25°C, 35°C, 45°C, 55°C, and 65°C, and cadmium ions using HEPES buffer at a pH of 7.6 and temperatures 15°C, 25°C, 45°C, 55°C, and 65°C are shown in Figs. 6.14 and 6.15, respectively. The results in these figures show that the uptakes of copper and cadmium increase with temperature which confirms the other researcher's observations (Sag and Kutsal, 2000; Aksu and Akprinar, 1991; Kuyucak and Volesky, 1988). For example, Sag and Kutsal (2000) observed that the uptakes of Pb^{2+} , Cr^{6+} , Fe^{3+} , and Cu^{2+} on *R. arrhizus* and *Z. ramigera* increased in the temperature range of 15°C to 35°C.

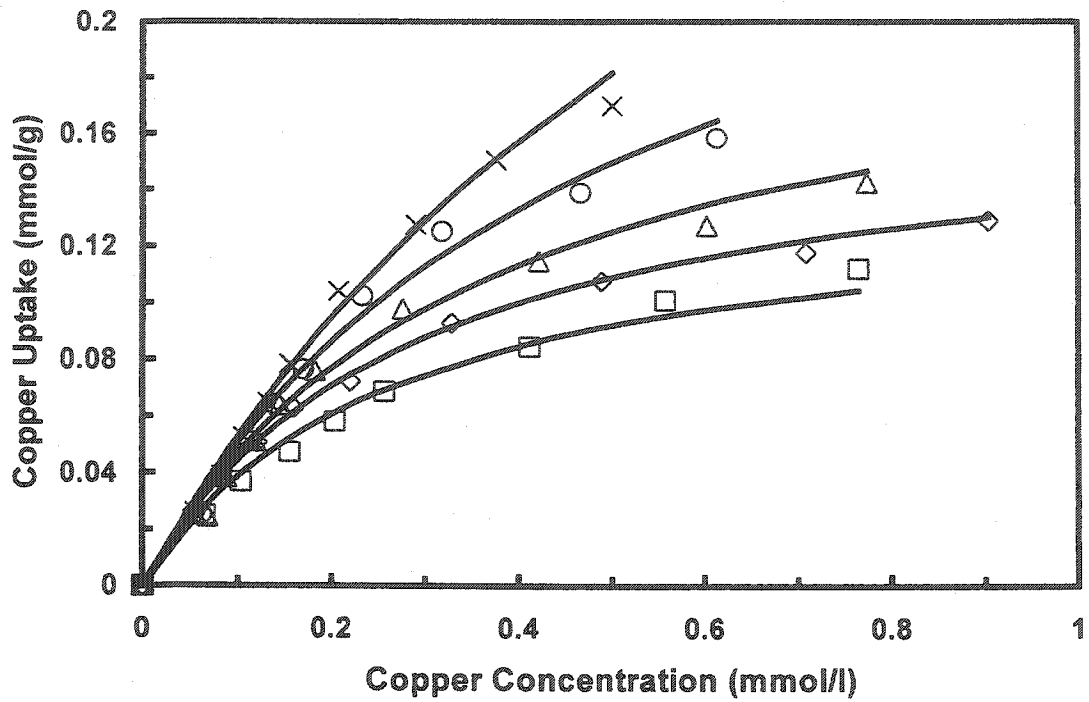


Fig. 6.14: Temperature effect on adsorption isotherms of copper with MES (mixed size particles, pH 5.5, corncob concn. 10 g/l). \square 25°C, \diamond 35°C, \triangle 45°C, \circ 55°C, \times 65°C. Symbols are experimental data, and solid lines are predicted data using Eq. (3.1).

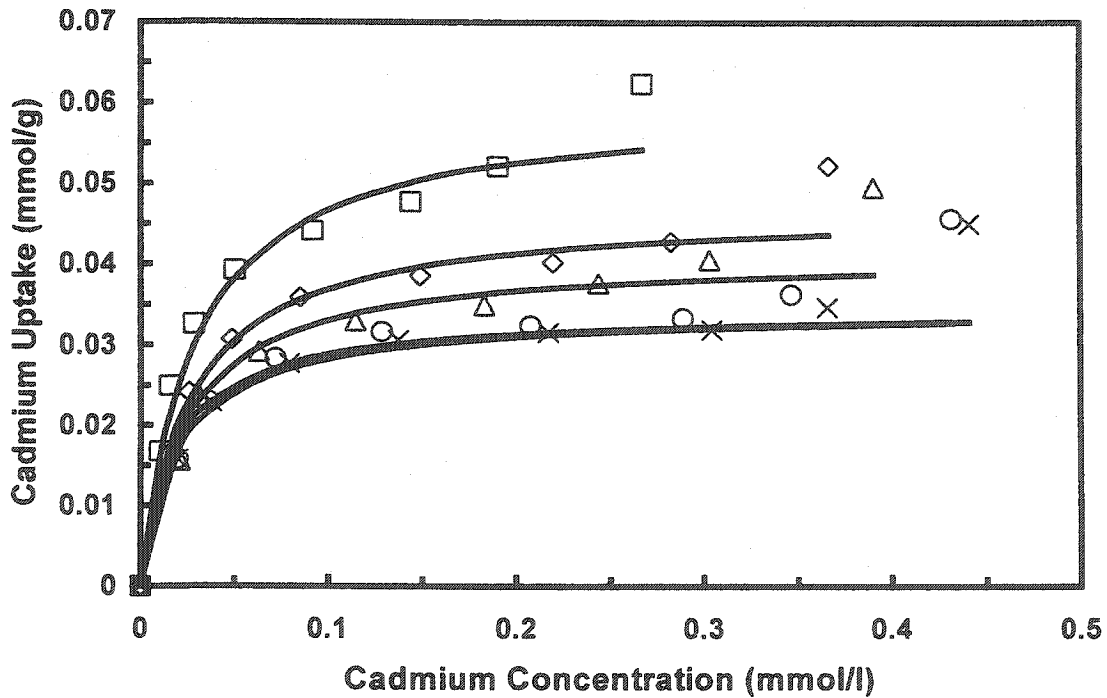


Fig. 6.15: Temperature effect on adsorption isotherms of cadmium with HEPES (mixed size particles, pH 7.6, corncob concn. 10 g/l). \times 15°C, \circ 25°C, \triangle 45°C, \diamond 55°C, \square 65°C. Symbols are experimental data, and solid lines are predicted data using Eq. (3.1).

The Langmuir model (3.1) was used to fit the experimental data in Figs. 6.14 and 6.15. The Langmuir parameters, the Langmuir equilibrium constants and the maximum adsorption capacities, are listed in Tables 6.7 and 6.8. There are two aspects of the effect of temperature on the two Langmuir parameters. First, the maximum adsorption capacities q_m of cupric and cadmium ions increase with temperature. For example, q_m increases from 0.14 mmol/g at 25°C to 0.464 mmol/g at 65°C for copper, and 0.0367 mmol/g to 0.060 mmol/g for cadmium. This trend for the maximum adsorption capacities is in agreement with the observations of other investigators (Johnson, 1990; Tewari and Lee, 1975). For example, Johnson observed that the maximum adsorption capacity of goethite for cadmium approximately doubled as the temperature was increased from 10°C to 70°C. Second, the Langmuir equilibrium constant K_l decreases with increasing temperature. This suggests that the adsorption of cupric and cadmium ions on the corncob

Table 6.7: Parameters: q_m and K_l of Langmuir model (Eq. (3.1)) for copper with MES at pH 5.5 and various temperatures

Temperature(°C)	25	35	45	55	65
q_m (mmol/g)	0.140	0.171	0.214	0.294	0.464
K_l (l/mmol)	3.80	3.50	2.80	2.07	1.28

Table 6.8: Parameters: q_m and K_l of Langmuir model (Eq. (3.1)) for cadmium with HEPES at pH 7.6 and various temperatures

Temperature(°C)	15	25	45	55	65
q_m (mmol/g)	0.0342	0.0367	0.041	0.0467	0.060
K_l (l/mmol)	53.6	47.2	41.3	37.5	35.0

particles is exothermic according to the chemical equilibrium principle. Compared to the parameters of the Langmuir model for copper with those for cadmium, the maximum adsorption capacity of the corncob particles is more sensitive to copper than cadmium for an increase of temperature. For example, the ratio of the maximum adsorption capacity for copper at 65°C and 25°C is 3.31, whereas for cadmium, the ratio is 1.64.

The enthalpy change, ΔH , of adsorption can be calculated from the Van't Hoff equation (Smith, 1979b):

$$\frac{d \ln K_e}{dT} = \frac{\Delta H}{RT^2} \quad (6.2)$$

where K_e is the equilibrium constant, T is the absolute temperature, and R is the general gas constant (8.314 J/(mol.K)). Assuming that the heat of adsorption is independent of temperature, equation (6.2) can be integrated, and the following expression is obtained:

$$\ln K_e = \frac{-\Delta H}{RT} + D \quad (6.3)$$

where D is the integral constant.

From the relationship between the free energy and the equilibrium constant,

$$\Delta G = -RT \ln K_e \quad (6.4)$$

and from the definition of free energy,

$$\Delta G = \Delta H - T\Delta S \quad (6.5)$$

the following equation is obtained:

$$\ln K_e = \frac{-\Delta H}{RT} + \frac{\Delta S}{R} \quad (6.6)$$

Equation (6.6) shows that the logarithm of the equilibrium constant is an inverse function of temperature. Therefore, a plot of $\ln K_e$ versus $1/T$ should yield a straight line. From its slope, the enthalpy change (heat) of adsorption can be calculated.

It is noted that the value of the equilibrium constant depends on the adopted reaction equation. For example, the Langmuir equilibrium constant K_l represents the following adsorption reaction:



Since there is a mechanism of ion exchange between the active sites on the cell surface and the solutes in the adsorption process, the following reaction may be more appropriate:



The relationship of the equilibrium constants for the reactions (6.7) and (4.11) is given by the following equation:

$$K_e = [H^+]K_l \quad (6.8)$$

Moreover, the equilibrium constant in the Van't Hoff equation (6.6) should be dimensionless. But the Langmuir equilibrium constant K_l has a unit $l/mmol$ in a dilute solution. To apply K_l with the inversed concentration unit of molarity (mol/l) rather than molecular friction to equation (6.6), an infinite dilute solution must be chosen as a standard state solution. At this standard state, K_l is dimensionless. Therefore, the result calculated from equation (6.6) is based on this standard state. An advantage for adopting the equilibrium constant K_e is that K_e itself is dimensionless. The calculated results using K_e are not related to the standard state, i. e., neither related to a pure solute nor an infinite dilute solution.

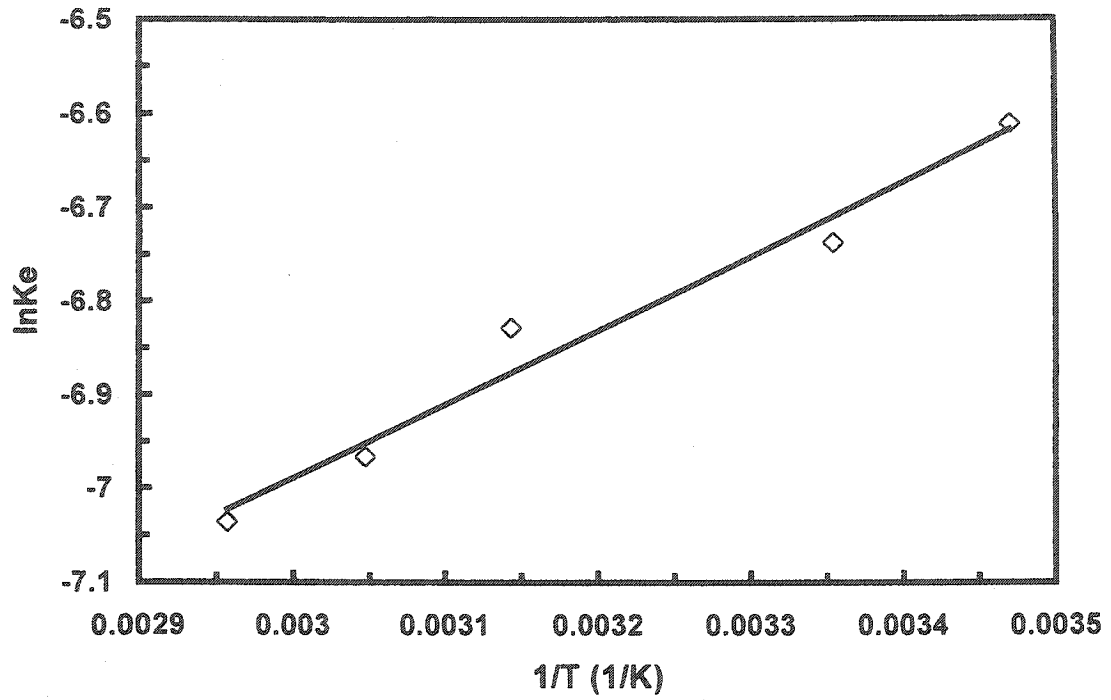


Fig. 6.16: Effect of temperature on equilibrium constant K_e in copper adsorption by corn cob particles \diamond exper. Points. Solid line refers to Eq. (6.6).

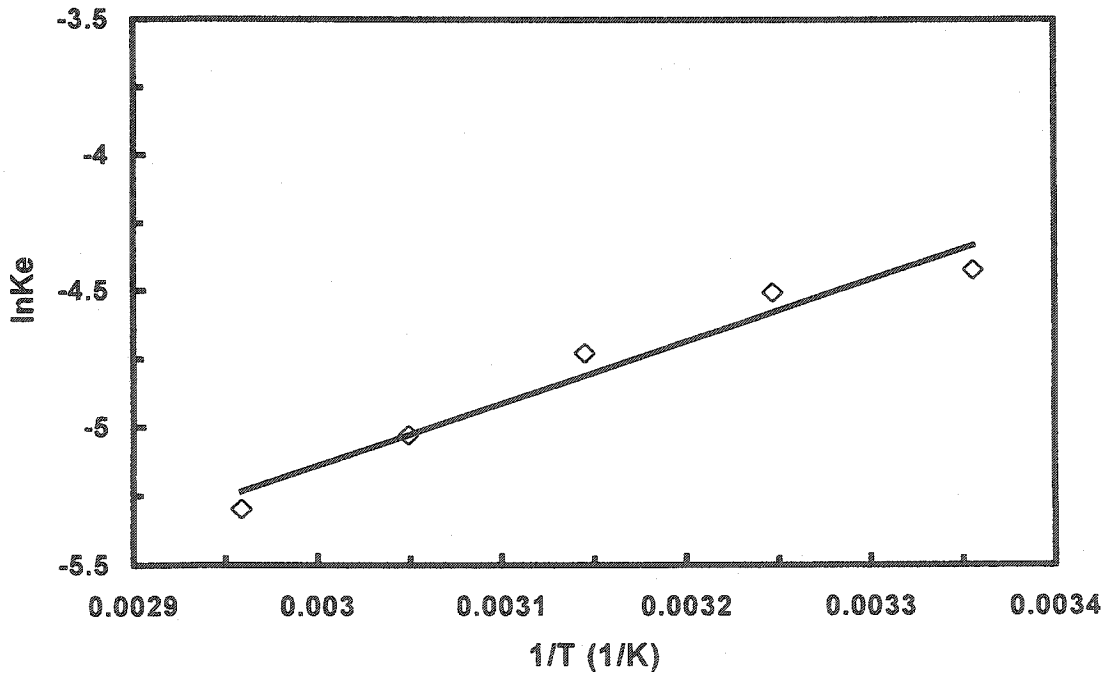


Fig. 6.17 Effect of temperature on equilibrium constant K_e in cadmium adsorption by corn cob particles \diamond exper. Points. Solid line refers to Eq. (6.6).

Figs. 6.16 and 6.17 show the two plots of natural logarithms of the equilibrium constants versus the inverses of absolute temperatures, whose slopes and intercepts indicate the enthalpy changes (-19.0 kJ/mol for copper and -6.38 kJ/mol for cadmium) of adsorption and the entropy changes (-99.6 J/(mol.K) for copper and -77.6 J/(mol.K) for cadmium), respectively. The negative values of the enthalpy changes show that the adsorption processes of cupric and cadmium ions on the corncob particles are exothermic. Sun and Shi (1998) reported that the enthalpy changes of cupric ion adsorption on sunflower stalks were -6.143 (particle size < 60 mesh) and -40.57 (particle size 25-45 mesh) kJ/mol. Generally speaking, gas adsorption processes are exothermic due to the liberation of heat for state change of the gas (Corapcioglu and Huang, 1987). For the metal ion adsorption in solutions, either exothermic or endothermic processes are possible because of the implication of the ion exchange mechanism. According to the ion exchange mechanism, the protons on the surface of adsorbents are replaced by the metal ions in the solutions. Therefore, the entire adsorption processes (reaction (4.11)) of the metal ions on the adsorbents may be represented by the following two reactions: the desorption of protons from the active sites (equations (6.9) and (6.10)):



and the adsorption of the metal ions on the active site of the surface of the adsorbents (equation (6.7)). The desorption of protons from the surface is an endothermic reaction (Fokkink, et. al., 1989). Therefore, if the absolute value of the enthalpy change (Eq. (6.7)) is greater than the enthalpy change of the desorption of protons, the adsorption process would be exothermic; otherwise, the process would be endothermic.

From the intercepts of the straight lines in Figs. 6.16 and 6.17, the entropy changes of adsorption were calculated. They are -99.6 J/(mol.K) for copper and -77.6 J/(mol.K) for cadmium on the corncob particles, respectively. Entropy has been defined as the degree of chaos of a system. During the adsorption process, the adsorbate ions become associated with the surface of the adsorbent resulting in the loss of their degree of freedom; while the released protons from the active sites on the surface enhance their degree of freedom under the mechanism of ionic exchange. According to statistical thermodynamics, the entropy change is a function of the number of ways Ω . In general, the number of ways of arranging identical N particles of configuration $\{n_1, n_2, \dots\}$, i.e., n_1 in one group, n_2 in another group, n_3 in another group, and so on, is

$$\Omega = N!/(n_1!n_2!n_3!\dots n_j!\dots) \quad (6.11)$$

where $n_i!$ denotes $n_i(n_i - 1)(n_i - 2)\dots 1$ (Haynie, 2001). Therefore, the numbers of ways are not only dependent on the number of the identical particles in a system, but also on the particle configuration. Since the reaction (4.11) has assumed that a proton will be replaced by a metal ion, and cupric and cadmium ions have more configurations than that of protons, the negative values of entropy change may be reasonable.

6.4 Effect of Agitation Speed on Kinetics of Adsorption

As indicated in Chapter one, adsorption kinetics is influenced by some factors of mass transfer, for example, agitation speed. Five agitation speeds (50, 70, 100, 200, and 300 rpm) were selected to study their effects on external diffusion. Figs. 6.18 and 6.19 represent the changes of copper and cadmium concentrations in the solution in the presence of the corncob particles. At the same contact time, the cupric and cadmium ions

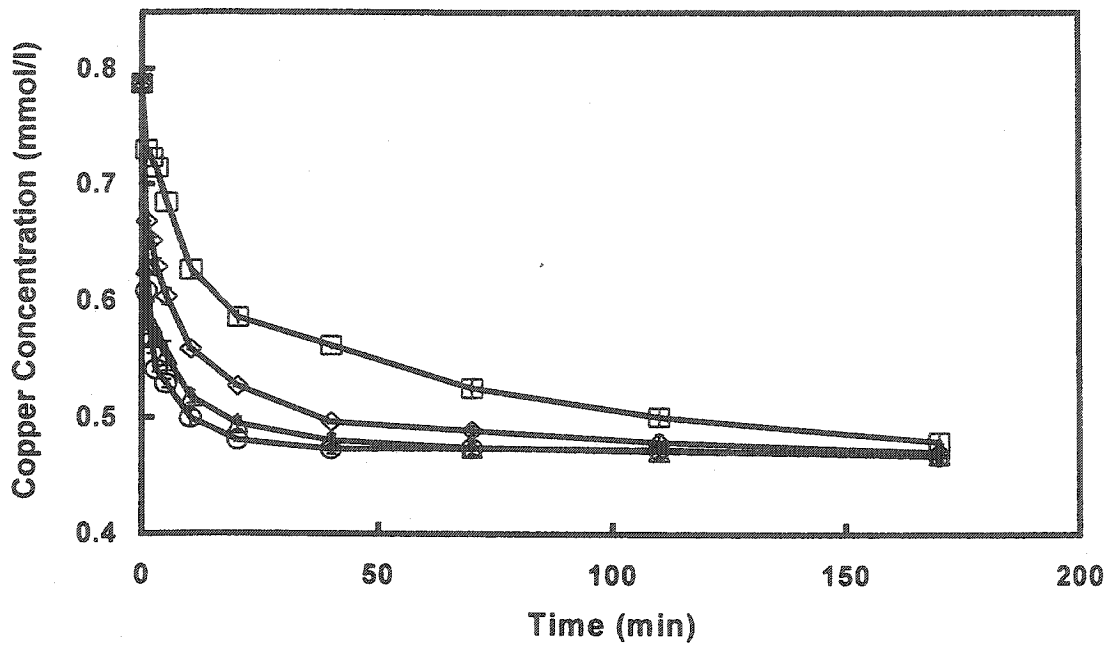


Fig. 6.18: Effect of agitation speed on copper concentration in solution (initial pH 4.8, Cu concentration 50 mg/l, 0.95 mm size particles, corncob concn. 10 g/l). □ 50 rpm, ◇ 70 rpm, △ 100 rpm, ○ 200 rpm.

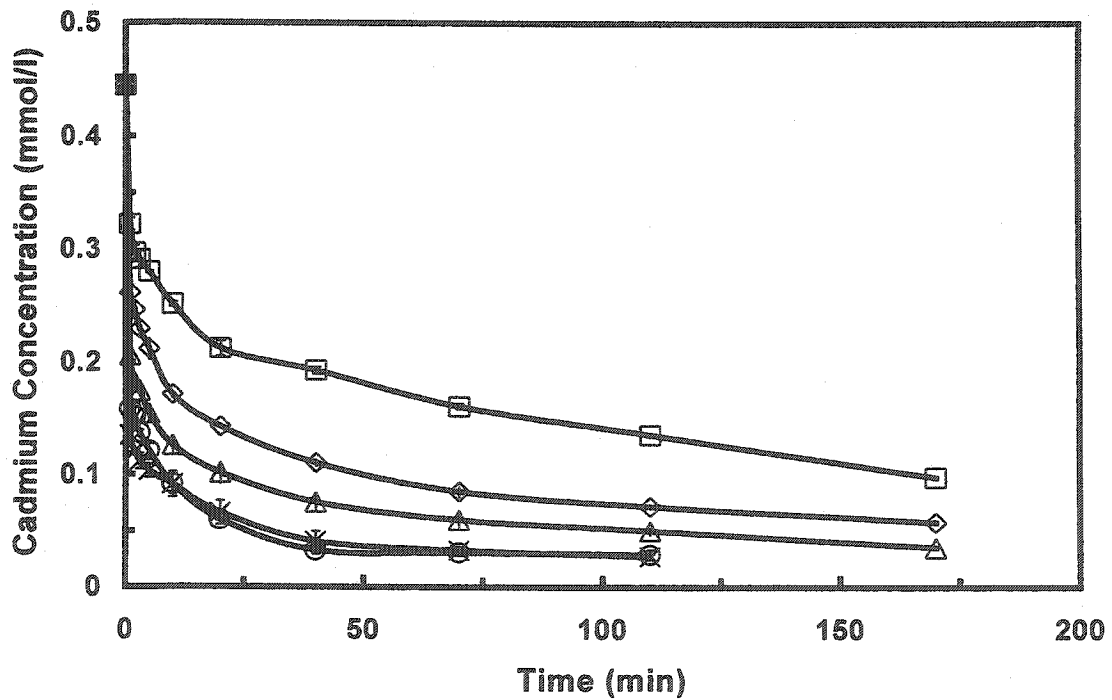


Fig. 6.19: Effect of agitation speed on cadmium concentration in solution (initial pH 7.6, Cd concentration 50 mg/l, 0.57 mm size particles, corncob concn. 10 g/l). □ 50 rpm, ◇ 70 rpm, ○ 100 rpm, △ 200 rpm, × 300 rpm.

in the solutions have lower concentrations when using a higher agitation speed (Figs. 6.18 and 6.19). For example, at the contact time of 40 min, the copper concentrations are 0.56 mmol/l at 50 rpm and 0.48 mmol/l at 200 rpm (Fig. 6.18), and the cadmium concentrations are 0.20 mmol/l and 0.030 mmol/l (Fig. 6.19), respectively. Moreover, the four curves in Fig. 6.18 and the five curves in Fig. 6.19 gradually approach their final equilibrium concentrations (0.48 mmol/l for copper and 0.30 mmol/l for cadmium) at the end of experiments, respectively. It can be explained for this phenomenon that with increasing agitation speed, the degree of turbulence in the solution increases, and the thickness of the liquid boundary layer surrounding the particles becomes thinner. Under these conditions, the external diffusion coefficient increases. Finally, the boundary layer becomes very thin and closes to the laminar sub-layer. Consequently, the external diffusion resistance (coefficient) will be constant or can be neglected.

Equation (3.11) was used to fit the experimental data in Figs. 6.18 and 6.19. The specific areas of the corncob particle in equation (3.11) were estimated by equation (3.9) and are summarized in Table 6.9 where the concentration (m) of the corncob particles in water is equal to 10 g/l.

Table 6.9: The relationship between specific area and size of corncob particles ($m = 10$ g/l)

Particle size (mm)	0.2	0.57	0.95	1.34
Bulk density (kg/m^3)	304	249	232	173
Specific area (m^2/m^3)	987	423	272	258

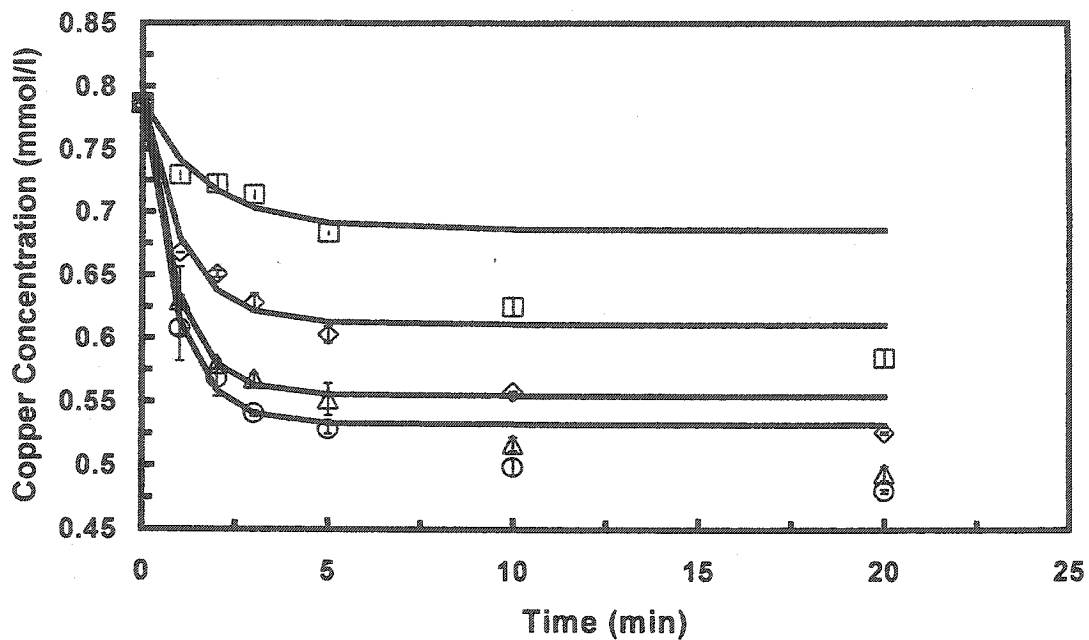


Fig. 6.20: Effect of agitation speed on copper concentration in solution (conditions as Fig. 6.18). \square 50 rpm, \diamond 70 rpm, \triangle 100 rpm, \circ 200 rpm. Symbols are experimental data, and solid lines are predicted data using Eq. (3.11).

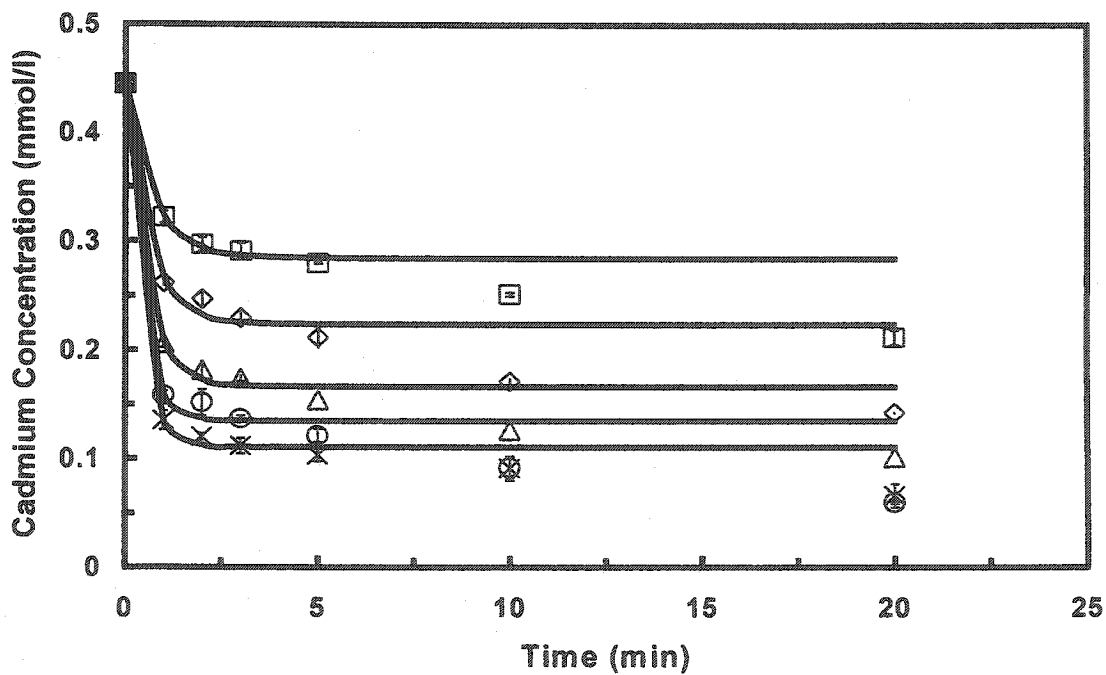


Fig. 6.21: Effect of agitation speed on cadmium concentration in solution (conditions as Fig. 6.19). \square 50 rpm, \diamond 70 rpm, \circ 100 rpm, \triangle 200 rpm, \times 300 rpm. Symbols are experimental data, and solid lines are predicted data using Eq. (3.11).

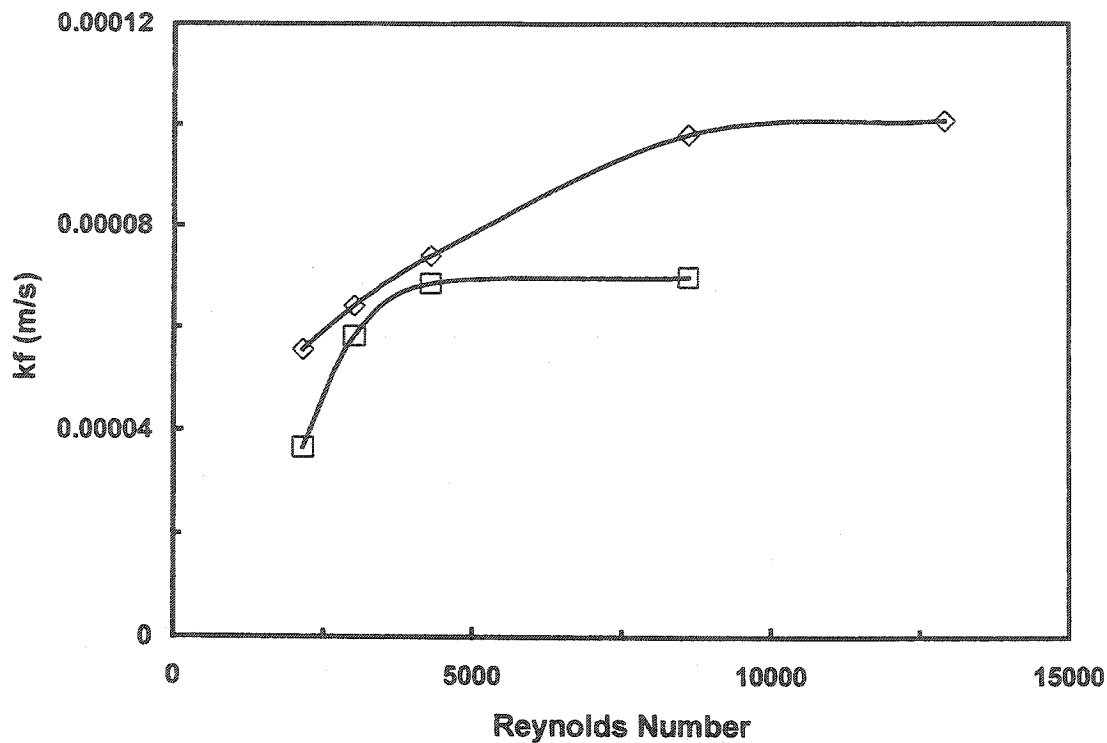


Fig. 6.22: The relationship between external diffusion coefficient and Reynolds number. □ Cu, ◇ Cd.

It was found that equation (3.11) cannot be used for the whole time range, and it can be applied only for the initial 5 minutes of the adsorption process. The simulated curves for 20 minutes are shown in Figs. 6.20 and 6.21. This may suggest that the rate-controlling mechanism changes during the adsorption process. In the beginning of the adsorption process, the external diffusion controls the adsorption process since the metal concentration in the solution is high. The driving force for mass transfer in the pores of the particles is great, and the surface reaction is fast. At a later time, the metal ion concentration in the solution becomes lower, and the intraparticle diffusion in the pores of the particles becomes a main resistance. The external diffusion coefficients obtained by equation (3.11) are shown in Fig. 6.22. They are plotted versus the modified Reynolds number that is defined as (Coulson and Richardson, 1999 b):

$$\text{Re} = \frac{nD_i^2 \rho_l}{\mu_l} \quad (6.12)$$

where n , D_i , ρ_l , and μ_l are the agitation speed (round per second), the diameter of impeller (m), the density of water (kg/m^3), and the viscosity of water (Pa.s). The external diffusion coefficient of k_f increases from 3.65×10^{-5} m/s and 5.56×10^{-5} m/s at Re number of 2155 to 6.99×10^{-5} m/s and 10.0×10^{-5} m/s at Re number of 8618 for copper and cadmium, respectively. The results show that the external diffusion coefficients for both ions tend to attain the maximum value with an increase in the Re number. This observation is opposite of that reported by Leusch and Volesky (1995). They obtained an approximately straight line for the relationship between k_f and Re number when they studied Cd^{2+} adsorption on *Sargassum fluitans*. They also reported that the values of the external diffusion coefficients were between 0.6×10^{-5} m/s and 3.8×10^{-5} m/s at Re number 6000 and 10000, respectively. Mohammad and Akl (1991a) evaluated that the external mass transfer coefficients were 0.3×10^{-5} m/s and 0.29×10^{-5} m/s for dyes Basic Blue 69 and Basic Red 22 on maize cob, respectively. Their smaller external mass transfer coefficients may result from the weaker electrostatic interaction between the active sites on the cell surface of the corncob particles and the dyes than the metal ions. Guibal et al. (1998) observed that the external diffusion coefficient changes in 150 and 260 rpm were not appreciable (1.68×10^{-5} m/s to 1.48×10^{-5} m/s) in metal-anion adsorption by chitosan beads. The present work gives a larger change of the external diffusion coefficients in a wider agitation speed range. In addition, the volumetric external diffusion coefficients k_v ($k_v = k_f a_m$) in this study are 0.00993 s^{-1} to 0.019 s^{-1} for copper, and 0.0235 s^{-1} to 0.0427 s^{-1} for cadmium. These values are two orders of magnitude greater than those (0.00012 s^{-1} - 0.00033 s^{-1}) reported by Al-Asheh and Duvnjak (1996). The reason may be that in their

experiments the shaker was used, which produced less eddy degree than the agitator used in this study.

6.5 Effect of Particle Size on Kinetics of Adsorption

Particle size is another factor influencing adsorption kinetics because it determines the transport distance of metal ions in the interior of the particles. The effects of four fractions of the corncob particles with the average sizes of 0.21, 0.57, 0.95, and 1.34 mm on the adsorption kinetics of copper and cadmium were investigated, and the results are shown in Figs. 6.23 - 6.26. With an increase of the particle size of the adsorbent, the uptakes of copper and cadmium ions per mass unit of the corncob particles decrease. For example, at the contact time of 40 minutes, the uptakes of copper are 0.040 mmol/g for the corncob particle size 0.21 mm and 0.027 mmol/g for 1.34 mm (Fig. 6.24), and the uptakes of cadmium are 0.039 mmol/g and 0.033 mmol/g (Fig. 6.26), respectively. This is in agreement with the kinetic principle: the smaller particles have a larger contacted area with the adsorbates per unit of mass of the adsorbent, resulting in a faster adsorption. However, Fig. 6.24 indicates that with the increasing contact time, the final uptakes of copper in the four curves do not approach to the same value at the equilibrium concentrations. This suggests that the particle size may affect the final equilibrium state of cupric ions in the solution. A similar observation has been reported by Jha et al. (1988). They noted that cadmium adsorption capacity increased with decreasing chitosan adsorbent size. However, it seems that the uptake of cadmium has little dependence on the particle size in this adsorption kinetics study (Fig. 6.26). The

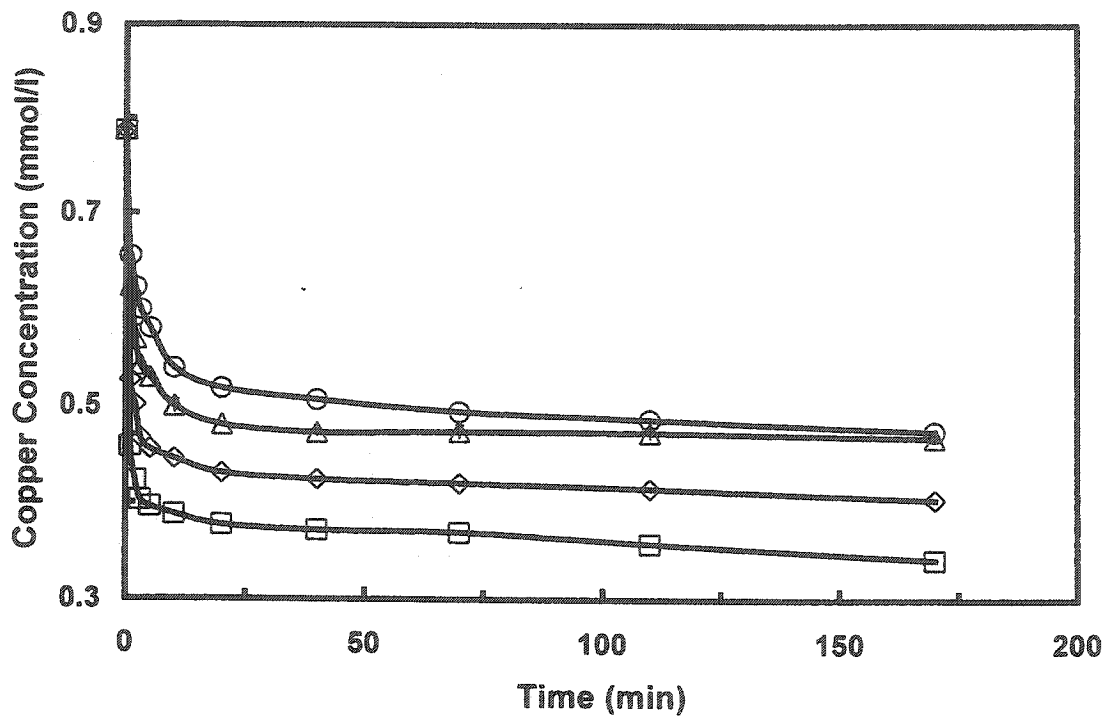


Fig. 6.23: Effect of corn cob particle size on copper concentration in solution (initial pH 4.8, initial concentration 50 mg/l, agitation speed 200 rpm, corn cob concn. 10 g/l). □ <math><0.42\text{ mm}</math>, ◇ between 0.42 mm and 0.71 mm, △ between 0.71 mm and 1.10 mm, ○ between 1.10 mm and 1.58 mm.

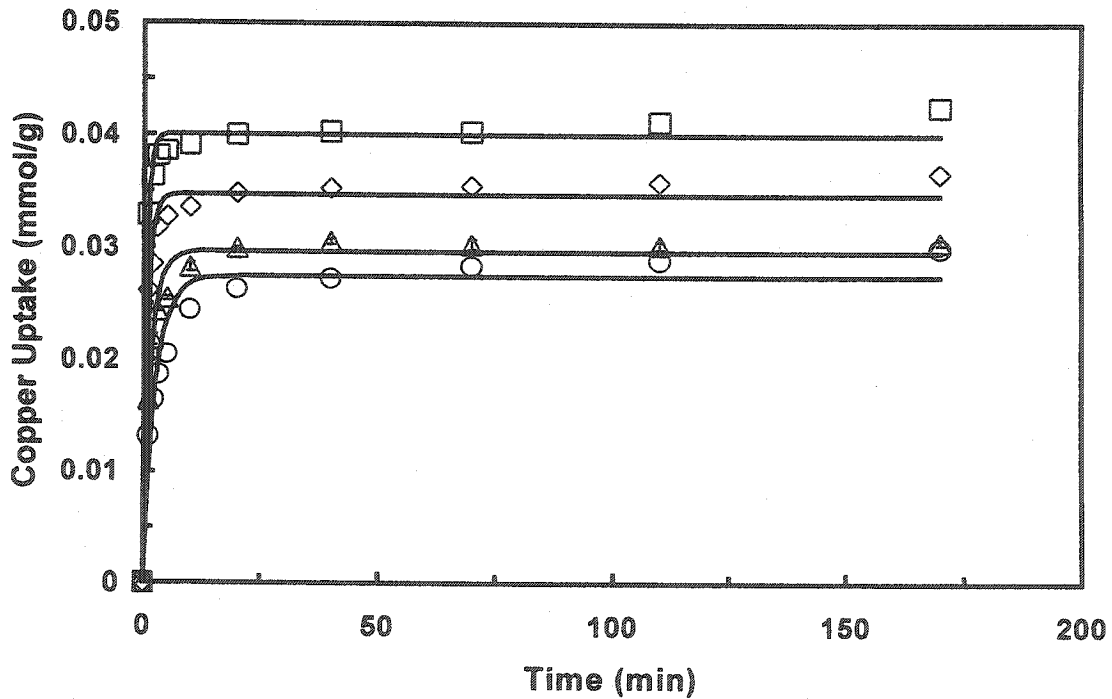


Fig. 6.24: Effect of corn cob particle size on uptake of copper (conditions as Fig. 6.23). □ <math><0.42\text{ mm}</math>, ◇ between 0.42 mm and 0.71 mm, △ between 0.71 mm and 1.10 mm, ○ between 1.10 mm and 1.58 mm. Symbols are experimental data, and solid lines are predicted data using Eq. (4.19).

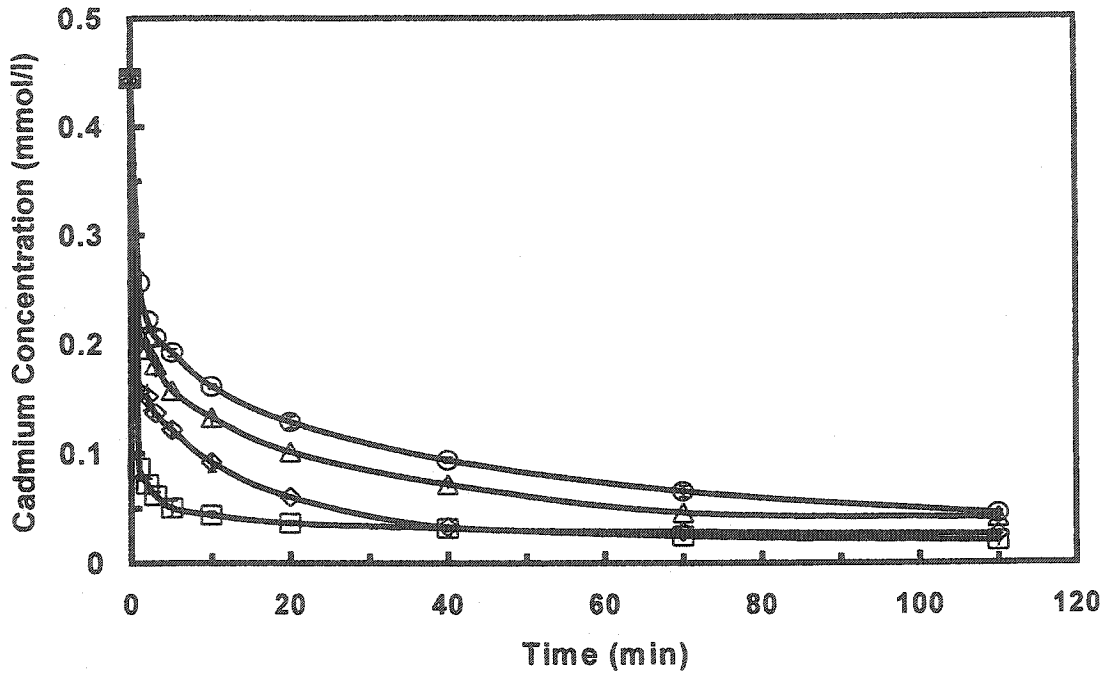


Fig. 6.25: Effect of corn cob particle size on cadmium concentration in solution (initial pH 7.6, initial concentration 50 mg/l, agitation speed 200 rpm, corn cob concn. 10 g/l). □ <0.42 mm, ◇ between 0.42 mm and 0.71 mm, △ between 0.71 mm and 1.10 mm, ○ between 1.10 mm and 1.58 mm.

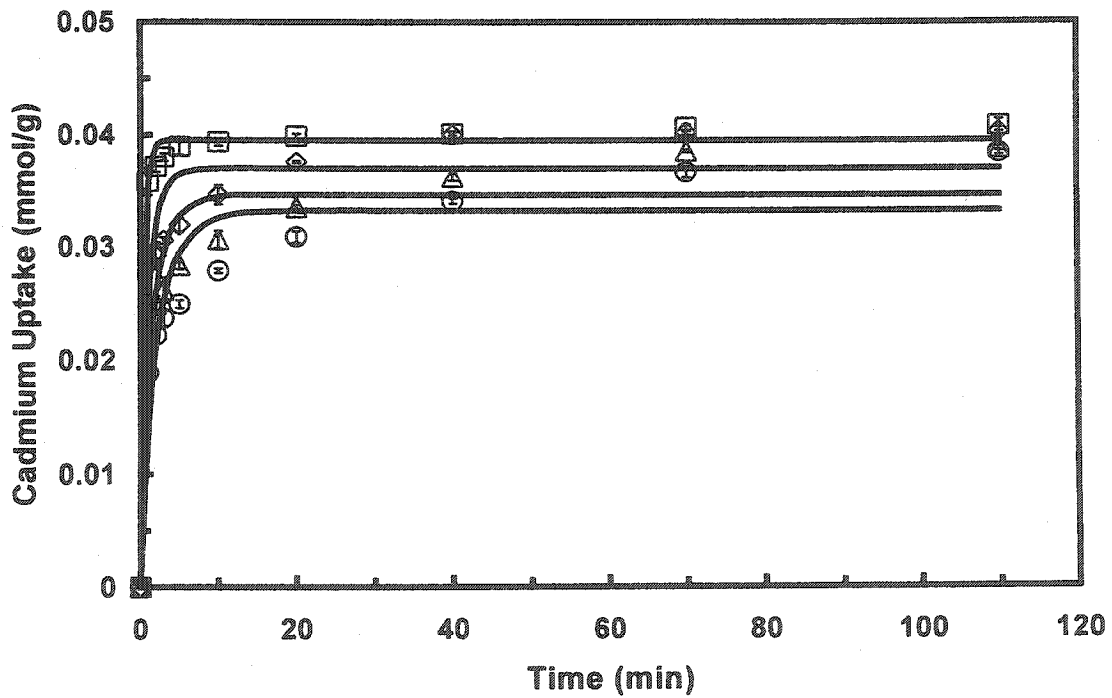


Fig. 6.26: Effect of corn cob particle size on uptake of cadmium (conditions as Fig. 6.25). □ <0.42 mm, ◇ between 0.42 mm and 0.71 mm, △ between 0.71 mm and 1.10 mm, ○ between 1.10 mm and 1.58 mm. Symbols are experimental data, and solid lines are predicted data using Eq. (4.19).

reason may be that corncob particles have the high removal efficiencies for cadmium ions (i. e., the lower cadmium ion concentrations in the solution) at a pH of 7.6. This means that the pH is a more important factor than the corncob particle size for the uptake of cadmium. It is noted that at the end of contact time, the concentrations of cadmium in the solution are close for the various particle sizes (Fig. 6.25). This may produce difficulties to distinguish the effect of the particle size from that of the higher pH. Guibal et al. (1998), and Ebihara and Takeuchi (1991) also observed that the uptakes were independent of particle size when they studied metal-anion adsorption by chitosan beads and the zinc-binding capacity of refined corn hull, respectively. One of the reasons for this difference may be related to the surface area of the pores in the particles. When the particles have a greater surface area of the pores compared to the external surface area of the particles, the uptake may be independent of the particle size because the increasing percentage of the surface area resulting from decreasing the particle size is small. Otherwise, the adsorption capacity of the adsorbent is dependent on the particle size.

Equation (4.19) was used to fit the experimental data in Figs. 6.24 and 6.26. The maximum adsorption capacity q_m was determined by the Langmuir isotherm model at the same pH value (Tables 6.1 and 6.2). In chemical reaction engineering, it is often assumed that there is no intraparticle diffusion resistance (i. e., the effectiveness factor $\eta = 1$) for the catalyst powder nor for the catalyst with the minimum size in order to investigate the effect of the catalyst size (Smith, 1970c). It is supposed that the intraparticle diffusion was eliminated in the experiments with the minimum particle size of 0.20 mm ($\eta = 1$). The intrinsic forward and backward reaction constants k_{ads} (1.082 and 2.88 l/(mmol.min) for copper and cadmium, respectively) and k_{desH} (0.472 and 0.184 min⁻¹ for copper and

cadmium, respectively) were determined by nonlinear regression from two curves with the particle size of 0.21 mm (Figs. 6.24 and 6.26). For the other three curves, the above values for k_{ads} and k_{desH} were considered as the constants. The adjusted parameters in the surface reaction model (4.19) for nonlinear regression were the effectiveness factor and the maximum adsorption capacity since both parameters are a function of the particle size and pH. The results are shown in Tables 6.10 and 6.11.

Table 6.10: Parameters: η and q_m in Eq. (4.19) for copper at various corncob particle sizes ($k_{ads} = 1.082 \text{ l}/(\text{mmol}\cdot\text{min})$, $k_{desH} = 0.472 \text{ min}^{-1}$)

Particle size (mm)	0.21	0.57	0.95	1.34
η	1.0	0.762	0.461	0.285
q_m (mmol/g)	0.085	0.0688	0.0553	0.0507

Table 6.11: Parameters: η and q_m in Eq. (4.19) for cadmium at various corncob particle sizes ($k_{ads} = 2.88 \text{ l}/(\text{mmol}\cdot\text{min})$, $k_{desH} = 0.184 \text{ min}^{-1}$)

Particle size (mm)	0.21	0.57	0.95	1.34
η	1.0	0.555	0.413	0.309
q_m (mmol/g)	0.0902	0.0684	0.0570	0.0520

The effectiveness factors and the maximum adsorption capacities decrease from 1 and 0.085 mmol/g at the particle of size of 0.21 mm to 0.285 and 0.0507 mmol/g at 1.34 mm for copper, respectively. For cadmium, the corresponding values are from 1 and 0.0902 mmol/g to 0.319 and 0.0520 mmol/g. With increasing the particle size, the diffusion distance of metal ions in the pores of the particles, and the internal mass transfer resistance increase, the effectiveness factor will finally decrease. In addition, it appears

that the change of particle size not only influences the effectiveness factor, but also the maximum adsorption capacity. In principle, the effectiveness factor as a kinetic parameter cannot change the chemical equilibrium, only influence the reaction rate. As a matter of fact, the four curves (Fig. 6.24) do not reach the same uptake at an approaching equilibrium point with changing the particle size. This strongly suggests that the maximum adsorption capacity of the corncob particles for copper changes with the particle size resulting in the uptake change.

6.6 Effect of Initial pH on Kinetics of Adsorption

The initial pH values not only influence the adsorption equilibrium, but also influence the kinetics because more protons can easily react with the active sites on the surface of the cell wall when the initial pH increases. Figs. 6.27 - 6.30 show the changes of the cupric ion concentration in the water solution and the uptakes on the corncob particles at various initial pH values with time. The concentrations of the corncob particles in the water solution were 10 and 20 g/l, respectively. Similarly, Figs. 6.31 and 6.32 give the cadmium adsorption kinetics on the corncob particles with the concentration of 10 g/l. At an initial higher pH value, the proton concentration in the solution is low, and this decreases its competitive adsorption with the metal ions, and enhances the uptake of the metal ions by the corncob particles. For example, at the contact time of 40 minutes, the uptakes of copper are 0.023 mmol/g at an initial pH of 4.4 and 0.056 mmol/g at an initial pH of 5.9 (Fig. 6.28), and the uptakes of cadmium are 0.028 mmol/g at an initial pH of 5.8 and 0.04 mmol/g at an initial of pH 7.6 (Fig. 6.32), respectively. However, the experiments showed that the adsorptions of cupric and

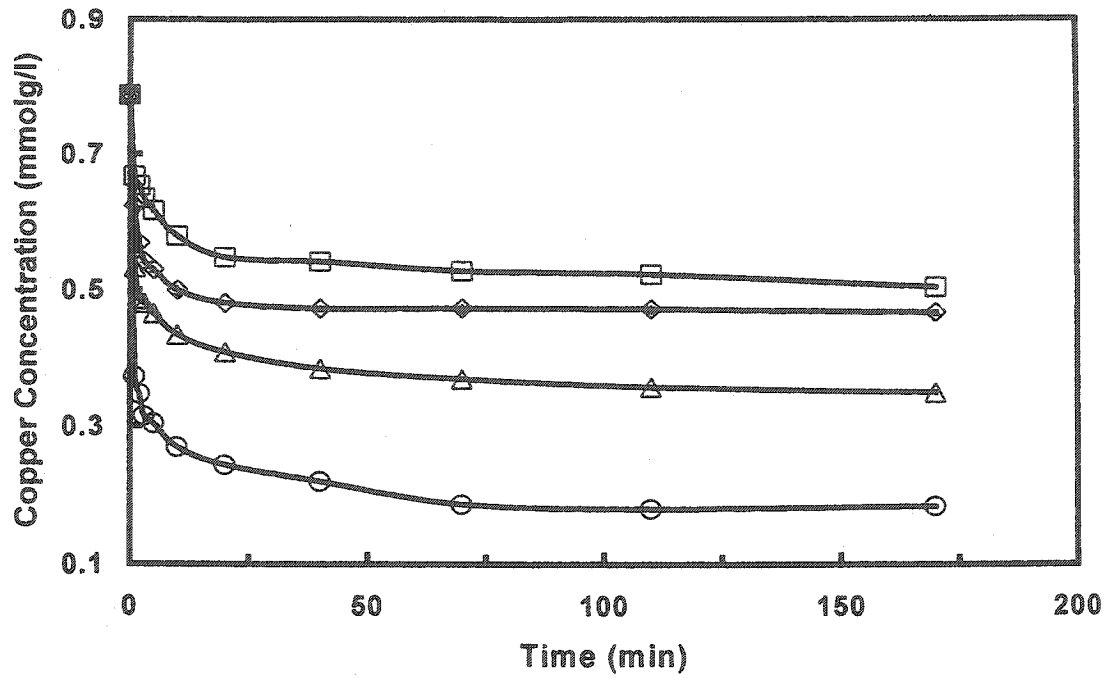


Fig. 6.27: Effect of pH on copper concentration in solution (initial concentration 50 mg/l, 0.95 mm size particles, agitation speed 200 rpm, corn cob concn. 10 g/l). □ pH 4.4, ◇ pH 4.8, △ pH 5.6, ○ pH 5.9.

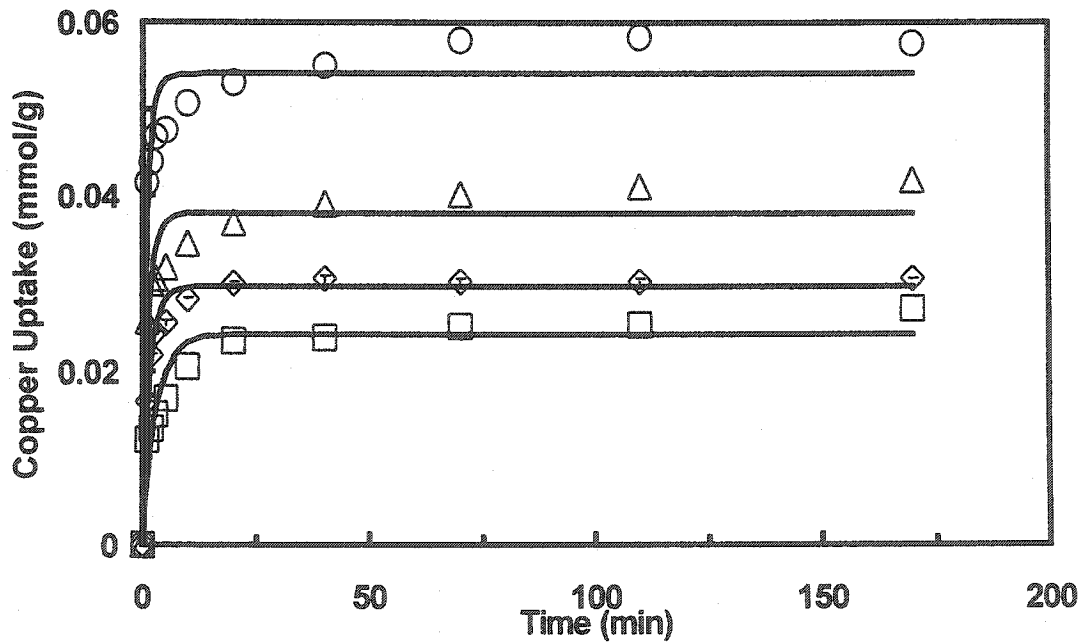


Fig. 6.28: Effect of pH on uptake of copper (conditions as Fig. 6.27). □ pH 4.4, ◇ pH 4.8, △ pH 5.6, ○ pH 5.9. Symbols are experimental data, and solid lines are predicted data using Eq. (4.19).

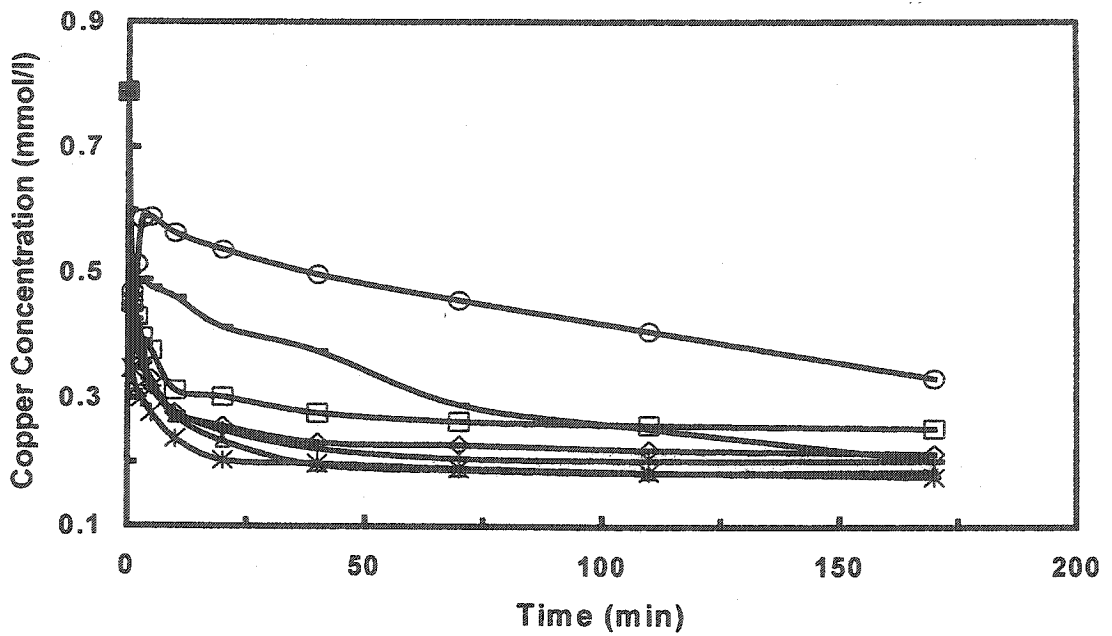


Fig. 6.29: Effect of pH on copper concentration in solution (initial concentration 50 mg/l, 0.95 mm size particles, agitation speed 200 rpm, corn cob concn. 20 g/l). □ pH 4.8, ◇ pH 5.1, + pH 6.1, △ pH 6.2, × pH 6.6, - pH 7.2, ○ pH 9.3.

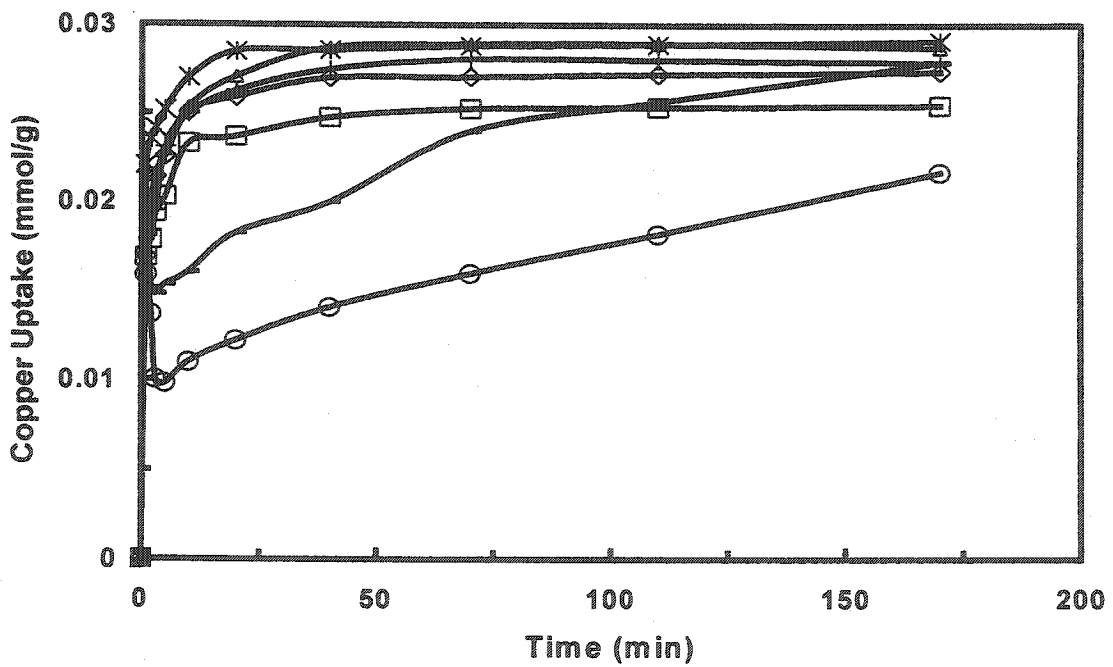


Fig. 6.30: Effect of pH on uptake of copper (conditions as Fig. 6.29). □ pH 4.8, ◇ pH 5.1, + pH 6.1, △ pH 6.2, × pH 6.6, - pH 7.2, ○ pH 9.3.

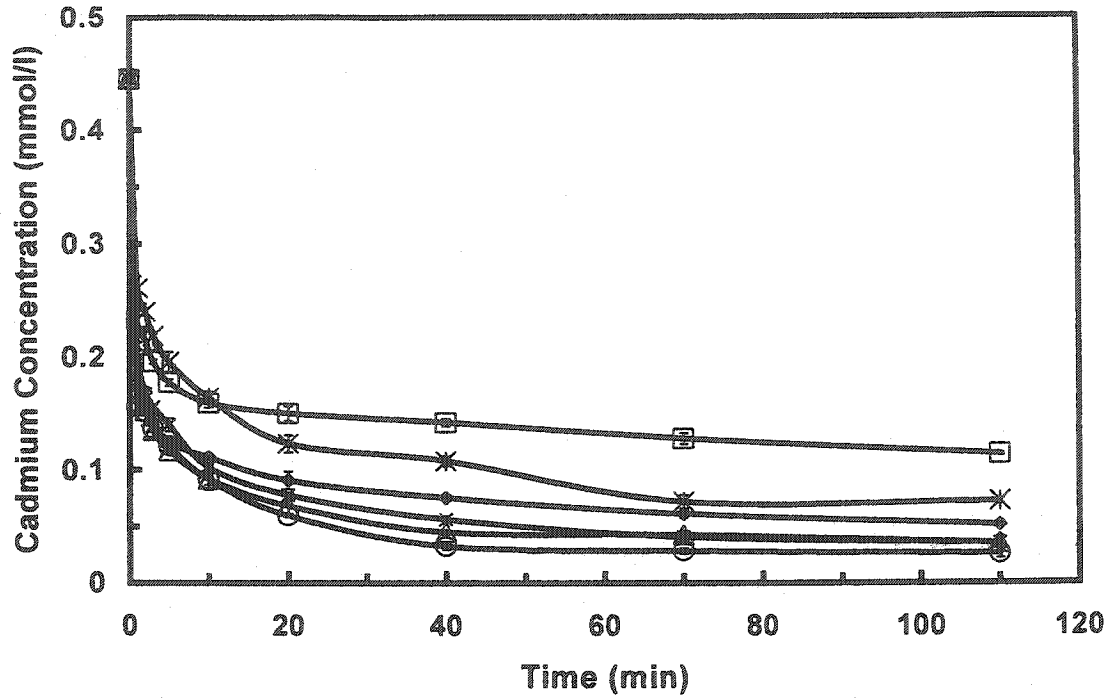


Fig. 6.31: Effect of pH on cadmium concentration in solution (initial concentration 50 mg/l, 0.57 mm size particles, agitation speed 200 rpm, corncob concn. 10 g/l). □ pH 5.8, ◇ pH 6.7, △ pH 7.3, ○ pH 7.6, x pH 8.3.

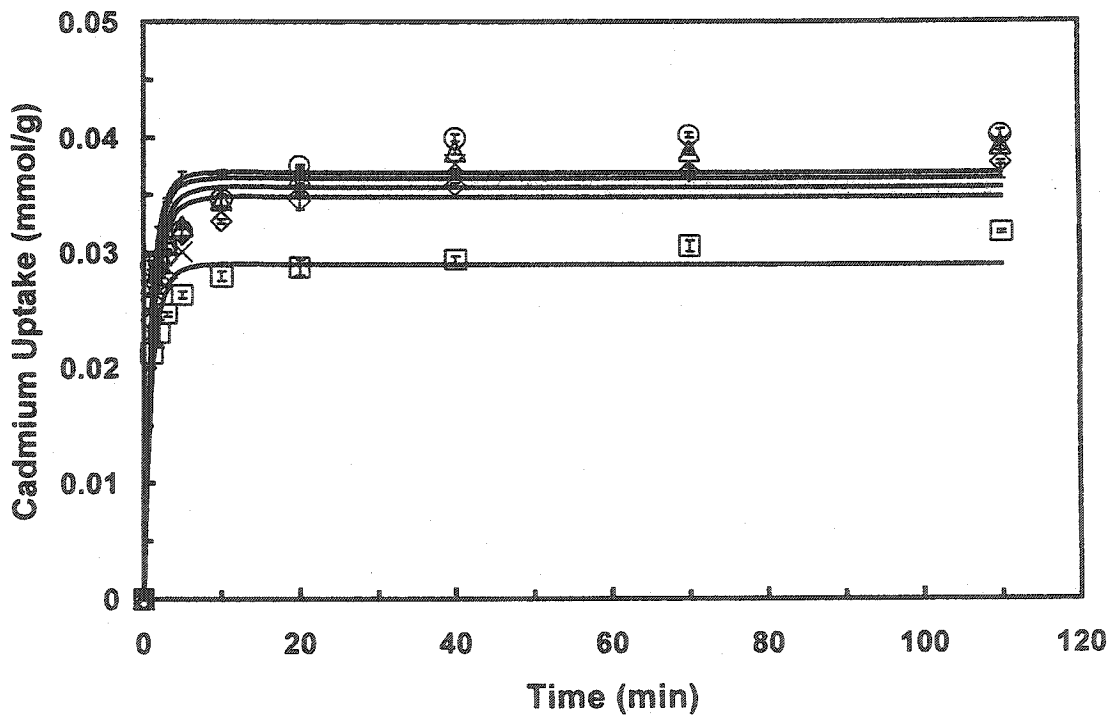


Fig. 6.32: Effect of pH on uptake of cadmium (conditions as Fig. 6.31). □ pH 5.8, ◇ pH 6.7, △ pH 7.3, ○ pH 7.6, x pH 8.3. Symbols are experimental data, and solid lines are predicted data using Eq. (4.19).

cadmium ions decrease at the pH values higher than 6.6 for copper (Fig. 6.30) and 8.3 for cadmium (Fig. 6.32). For example, at the contact time of 40 minutes, the uptakes of copper are 0.028 mmol/g at an initial pH of 6.6 and 0.018 mmol/g at an initial pH of 7.2 (Fig. 6.30), and the uptakes of cadmium are 0.040 mmol/g at an initial pH of 7.6 and 0.037 mmol/g at an initial pH of 8.3 (Fig. 6.32), respectively. This may be caused by the loss of some components, which are mainly responsible for the adsorption of the metal ions, from the corncob particles.

The curves in Figs. 6.28 and 6.32 are obtained by applying equation (4.19). As previously discussed in Chapter 6.4, the maximum adsorption capacity of the adsorbent and the effectiveness factor are two adjustable parameters in that model because both of them depend on the pH. The rate constants k_{ads} and k_{desH} (1.082 l/(mmol.min) and 2.88 l/(mmol.min), and 0.472 min⁻¹ and 0.128 min⁻¹ for copper and cadmium, respectively) were determined in Chapter 6.5. These values can be applied other operating conditions, such

Table 6.12: Parameters: η and q_m in Eq. (4.19) for copper at various pHs ($k_{ads} = 1.082$ l/(mmol.min), $k_{desH} = 0.472$ min⁻¹)

pH	4.4	4.8	5.6	5.9
η	0.246	0.310	0.530	0.548
q_m (mmol/g)	0.0435	0.0558	0.0783	0.147

Table 6.13: Parameters: η and q_m in Eq. (4.19) for cadmium at various pHs ($k_{ads} = 2.88$ l/(mmol.min), $k_{desH} = 0.184$ min⁻¹)

pH	5.8	6.7	7.3	7.6	8.3
η	0.530	0.542	0.550	0.555	0.524
q_m (mmol/g)	0.0409	0.0580	0.0655	0.0684	0.0616

as various pH values, because they are the intrinsic rate constants, which do not change with the operating conditions. The fitted maximum adsorption capacity, q_m , and the effectiveness factor, η , are listed in Tables 6.12 and 6.13.

The changes of the maximum adsorption capacities with the pH in the kinetic experiments are similar with their changes in the isotherm tests. The effectiveness factor increases with the pH. Since the effectiveness factor reflects the ratio of the reaction rate in the pore to the rate on the surface of the particles, the OH^- ion increase at a higher initial pH will enhance the adsorption capacity of the adsorbent, and then accelerate the reaction rate in the pore. However, at a pH of 8.3, both the maximum adsorption capacity and the effectiveness factor for adsorption of cadmium are lower than those at a pH of 7.6 (Table 6.13). The reason is that at a too high pH value, some components in the corncob particles were dissolved and lost into the water solution.

6.7 Effect of Biomass Concentration on Kinetics of Adsorption

Biomass concentration is another factor that influences the adsorption kinetics. It is expected that a higher biomass concentration in a reactor will result in a faster adsorption rate. Figs. 6.33 and 6.34 show the cupric ion concentrations in the solution and the uptakes by the corncob particles at four biomass concentrations (2.5, 5.0, 7.5, and 10 g corncob/liter water) with time. Figs. 6.35 and 6.36 show the similar results for cadmium. Fig. 6.37 indicates the effect of biomass concentrations on the solute concentration at a lower initial cadmium concentration (5 mg/l). At the same contact time, a lower concentration of the metal ions in the solution can be reached by a higher biomass concentration. For example, at the contact time of 40 minutes, the concentrations

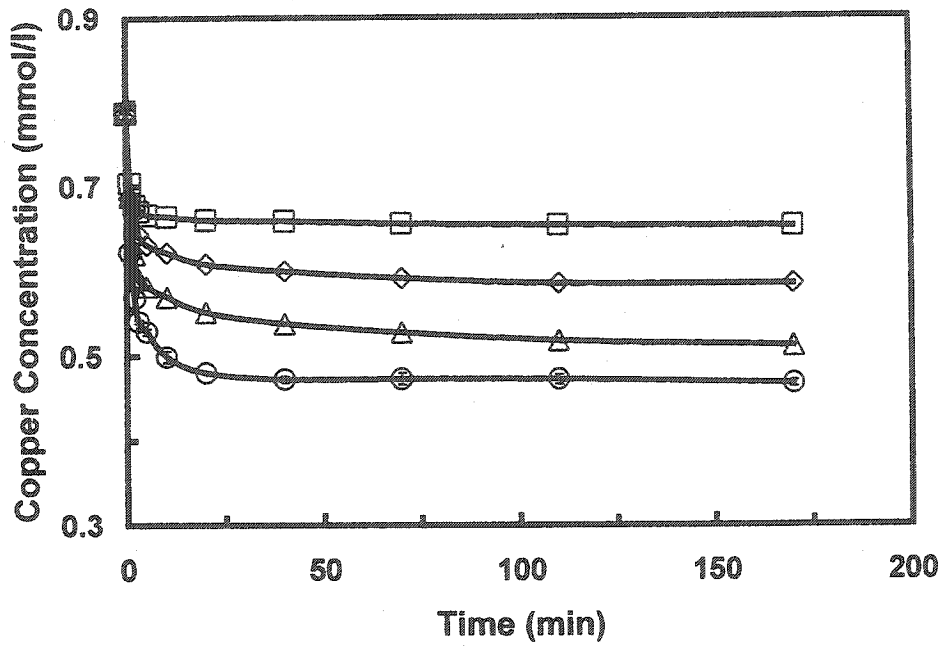


Fig. 6.33: Effect of corn cob concentration on copper concentration in solution (initial concentration of copper 50 mg/l, 0.95 mm size particles, initial pH 4.8, agitation speed 200 rpm). □ 2.5 g/l, ◇ 5 g/l, △ 7.5 g/l, ○ 10 g/l.

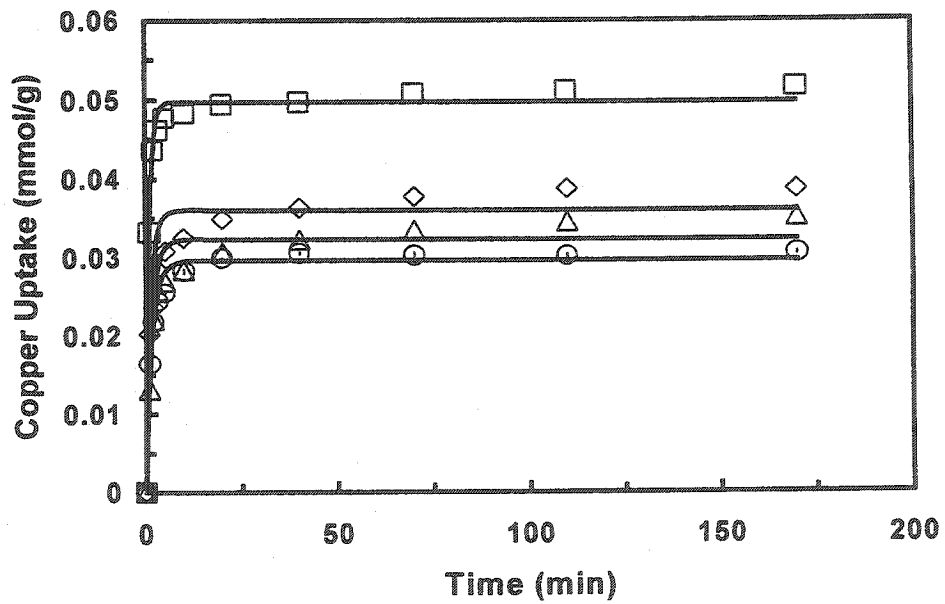


Fig. 6.34: Effect of corn cob concentration on copper of uptake (conditions as Fig. 6.33). □ 2.5 g/l, ◇ 5 g/l, △ 7.5 g/l, ○ 10 g/l. Symbols are experimental data, and solid lines are predicted data using Eq. (4.19).

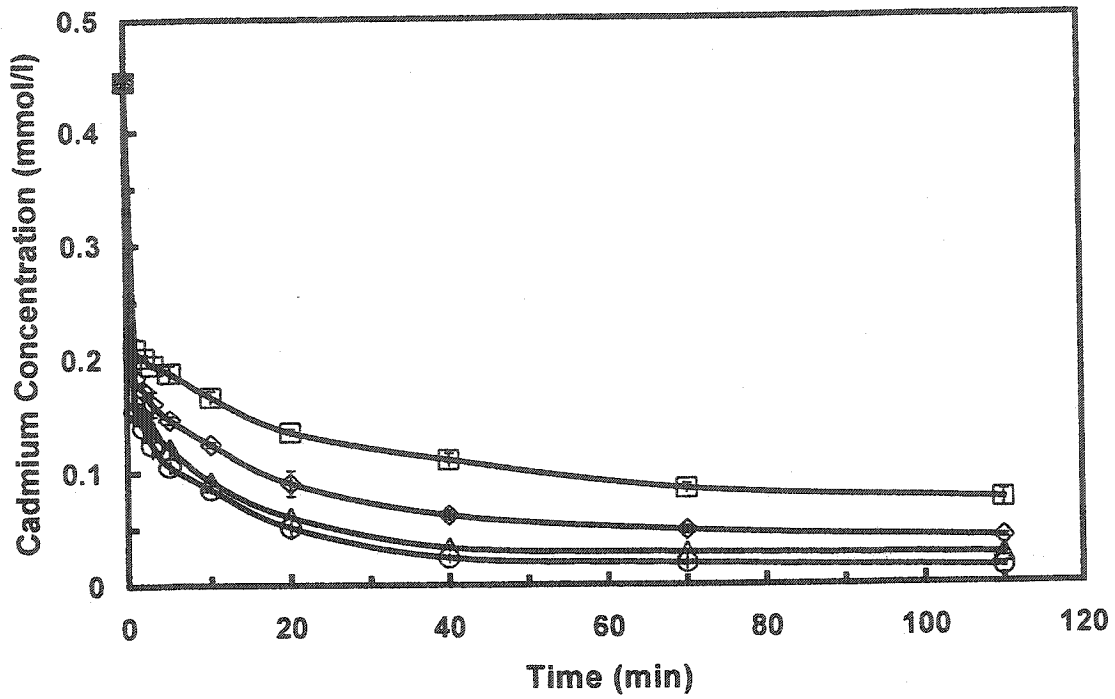


Fig. 6.35: Effect of corn cob concentration on cadmium concentration in solution (initial concentration of cadmium 50 mg/l, 0.57 mm size particles, initial pH 7.6, agitation speed 200 rpm). \square 5 g/l, \diamond 8 g/l, \triangle 10 g/l, \circ 20 g/l.

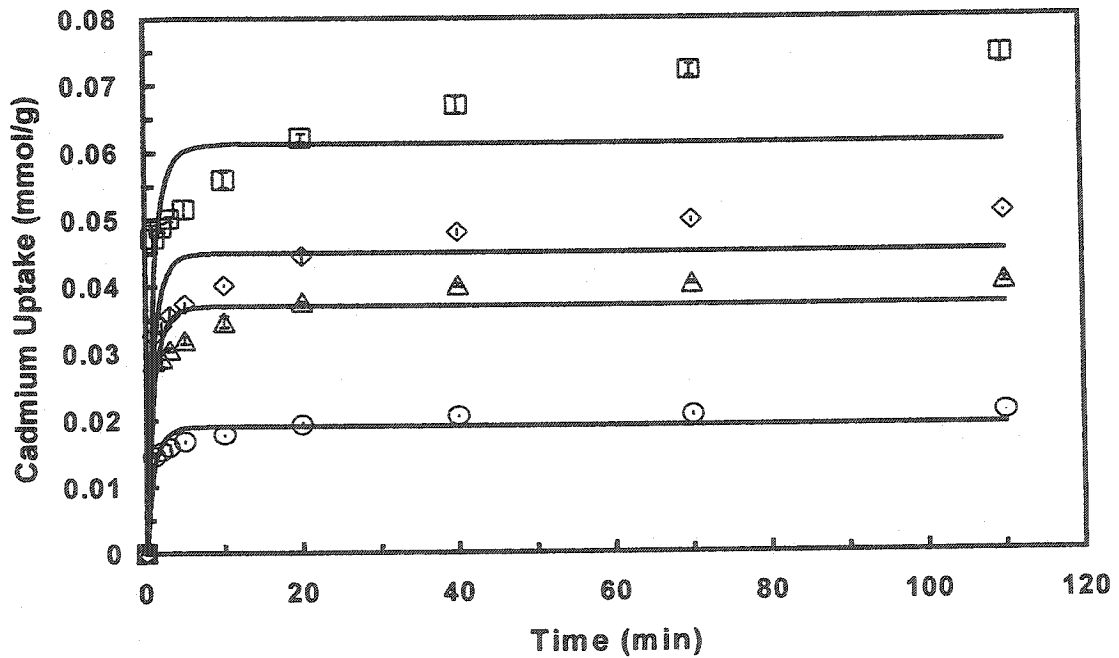


Fig. 6.36: Effect of corn cob concentration on uptake of cadmium (conditions as Fig. 6.35). \square 5 g/l, \diamond 8 g/l, \triangle 10 g/l, \circ 20 g/l. Symbols are experimental data, and solid lines are predicted data using Eq. (4.19).

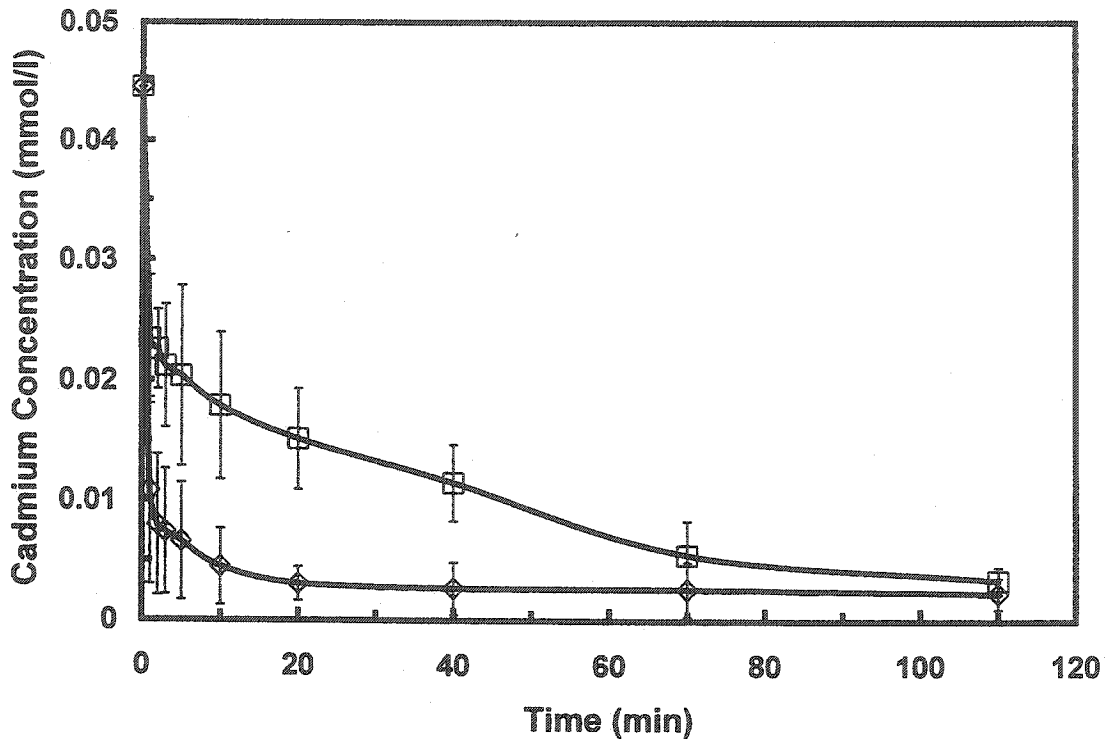


Fig. 6.37: Effect of corn cob concentration on cadmium concentration in solution (initial concentration of cadmium 5 mg/l, 0.57 mm size particles, initial pH 7.6, agitation speed 200 rpm). □ 5 g/l, ◇ 10 g/l.

of copper are 0.67 mmol/l for a biomass concentration of 2.5 g/l and 0.48 mmol/l for 10 g/l (Fig. 6.33), and the concentrations of cadmium are 0.13 mmol/l for a biomass concentration 5 g/l and 0.030 mmol/l for 20 g/l (Fig. 6.35), respectively. Furthermore, when the biomass concentration is higher, the biomass can remove more metal ions from the solution, and has a higher removal efficiency, but the uptake per mass unit of the adsorbent is lower. For example, the removal efficiency increases from 16 % at a concentration of corn cob particle of 2.5 g/l to 74 % at a concentration of 10 g/l (Fig. 6.33), while the corresponding uptake decreases from 0.050 mmol/g to 0.029 mmol/g for copper (Fig. 6.34). At a constant concentration of metal ions, an increase of biomass concentration means a decrease of reaction possibility for every active site of the cells.

Consequently, the uptake of the solute decreases. From the view of the cells, the electrostatic interactions between cells may be a significant factor on the effect of biomass concentration for the uptake of adsorption (Itoh et al. 1975). When the biomass concentration increases, the distance between cells becomes small, and their repulsive action becomes stronger, which result in a decrease of uptake.

Equation (4.19) was used to fit the adsorption kinetics shown in the four curves in Figs. 6.34 and 6.36. The simulated curves for copper in Fig. 6.34 are close to the experimental points. However, the simulated curves for cadmium with the lower biomass concentrations, for example, 5 g/l, in Fig. 6.36 have greater departures from the experimental points. These departures can be reduced by an adjustment of the rate constants (i.e., the increase of number of adjustable parameters). Both the effectiveness factors and the maximum adsorption capacities fitted from equation (4.19) decrease with increasing the concentration of the corncob particles (Tables 6.14 and 6.15). This suggests that an increase in biomass concentration will result in a decrease of effectiveness of biomass. Moreover, it could be concluded that regeneration of the adsorbent in an adsorption process should be carried out more frequently with an increase in biomass concentration.

Table 6.14: Parameters: η and q_m in Eq. (4.19) for copper at various corncob concentrations ($k_{ads} = 1.082 \text{ l}/(\text{mmol}\cdot\text{min})$, $k_{desH} = 0.472 \text{ min}^{-1}$)

Corncob concn. (g/l)	2.5	5.0	7.5	10
η	0.784	0.420	0.358	0.310
q_m (mmol/g)	0.0824	0.0619	0.0581	0.0558

Table 6.15: Parameters: η and q_m in Eq. (4.19) for cadmium at various corn cob concentrations ($k_{ads} = 2.88 \text{ l}/(\text{mmol}\cdot\text{min})$, $k_{desH} = 0.184 \text{ min}^{-1}$)

Corn cob concn. (g/l)	5	8	10	20
η	0.693	0.610	0.555	0.514
q_m (mmol/g)	0.0892	0.0784	0.0684	0.0376

6.8 Effect of Initial Metal Ion Concentration on Kinetics of Adsorption

The initial metal ion concentration in solutions is an important factor. With an increase of the metal ion concentration, the difference in the concentrations between the bulk solution and the surface of the corn cob particles becomes larger, the driving force for mass transfer increases, and the adsorption rate increases. Figs. 6.38 - 6.41 show the effect of the initial cupric ion concentrations in the solution on the adsorption kinetics and the uptakes of these ions by the corn cob particles at a pH of 4.8 and 5.9. The same tests were carried out with cadmium ions, and the results are displayed in Figs. 6.42 and 6.43. The results show that the removal efficiency (= (initial concentration - equilibrium concentration)/initial concentration) is lower when the concentration of metal ions is higher. However, the uptake of ions by the adsorbent increases with increasing the initial metal ion concentration. For example, the equilibrium concentrations of copper in the solution are 0.080 mmol/l at the end of the contact time for an initial copper concentration of 10 mg/l, and 0.52 mmol/l for an initial copper concentration of 50 mg/l. (Fig. 6.38). The corresponding removal efficiencies for these conditions are 0.492 and 0.339; while the metal ion uptakes by the corn cob particles are 0.0080 mmol/g and 0.0295 mmol/g (Fig. 6.39). It is concluded that at a higher initial metal ion concentration, the biosorptions of copper and cadmium ions by the corn cob particles have the lower

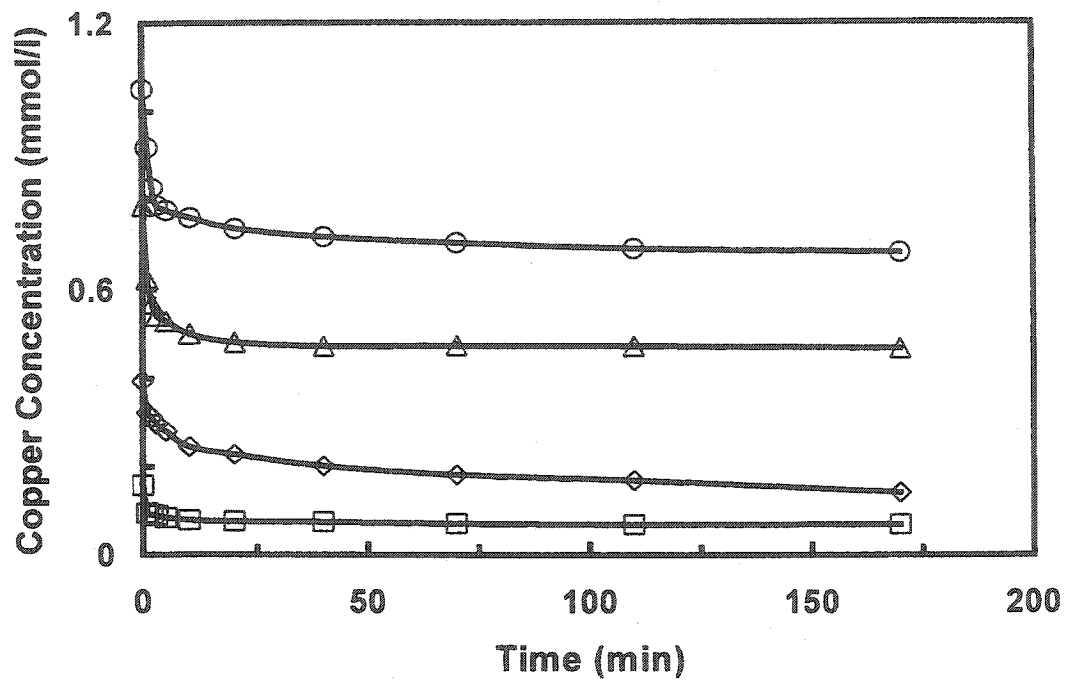


Fig. 6.38: Effect of initial concentration on copper concentration in solution (0.95 mm size particles, initial pH 4.8, agitation speed 200 rpm, corncob concn. 10 g/l). □ 10 mg/l, ◇ 25 mg/l, △ 50 mg/l, ○ 70 mg/l.

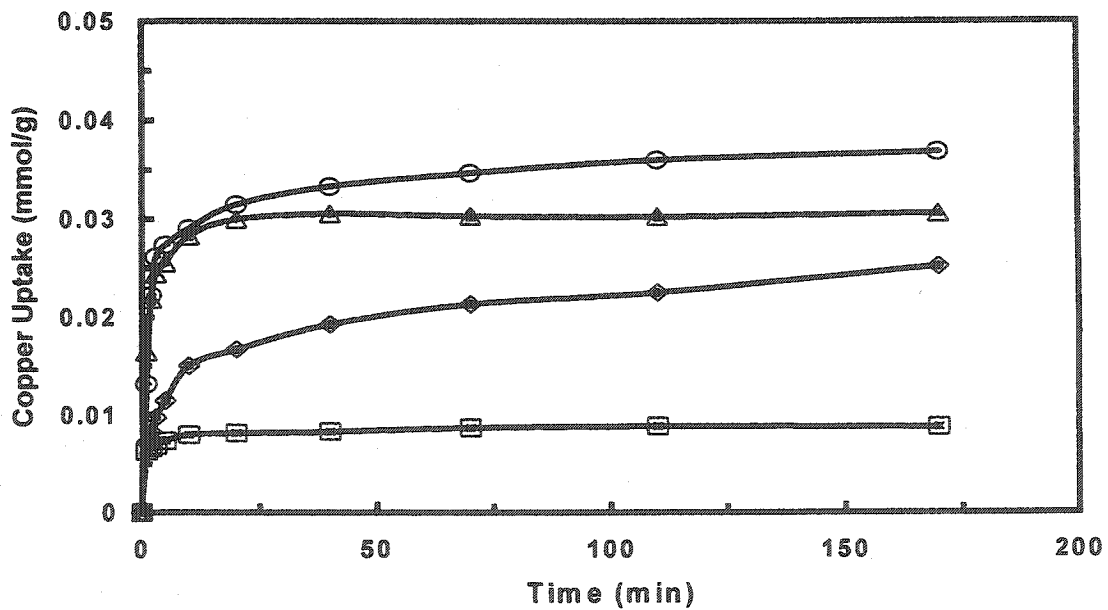


Fig. 6.39: Effect of initial concentration on uptake of copper (conditions as Fig. 6.38). □ 10 mg/l, ◇ 25 mg/l, △ 50 mg/l, ○ 70 mg/l.

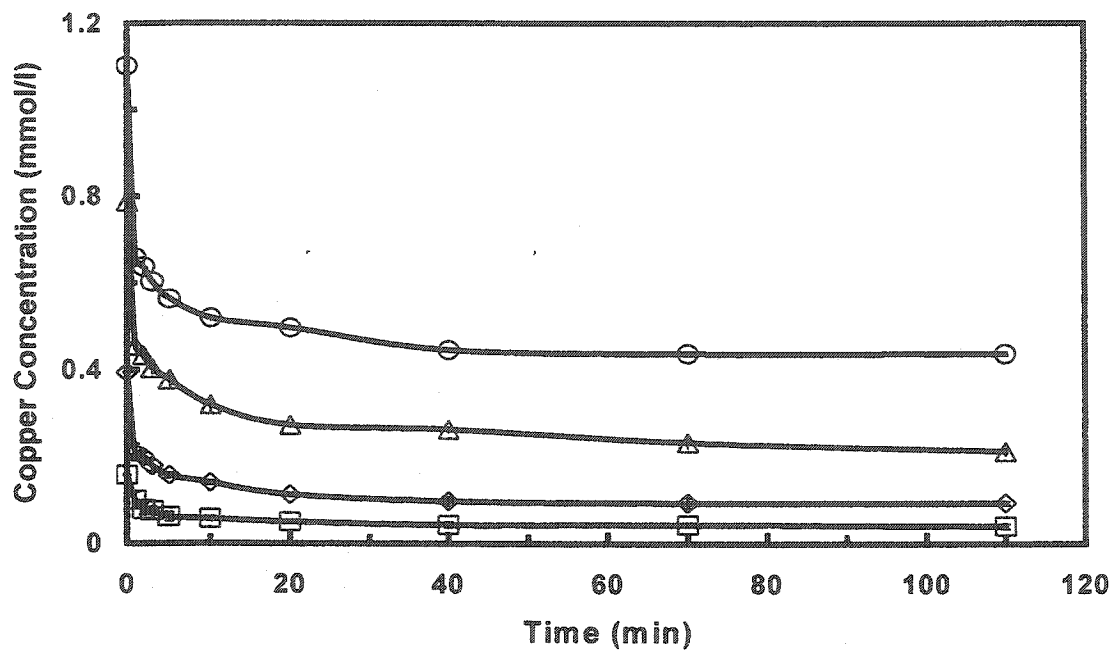


Fig. 6.40: Effect of initial concentration on copper concentration in solution (0.95 mm size particles, initial pH 5.9, agitation speed 200 rpm, corn cob concn. 10 g/l). □ 10 mg/l, ◇ 25 mg/l, △ 50 mg/l, ○ 70 mg/l.

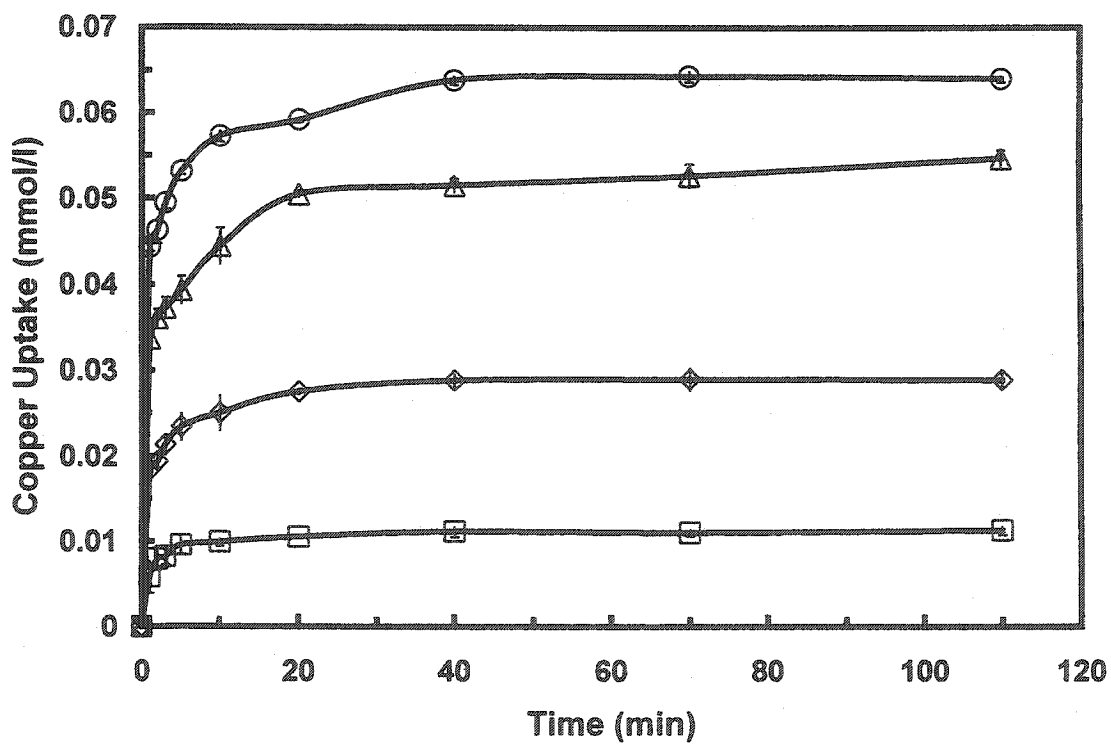


Fig. 6.41: Effect of initial concentration on uptake of copper (conditions as Fig. 6.40). □ 10 mg/l, ◇ 25 mg/l, △ 50 mg/l, ○ 70 mg/l.

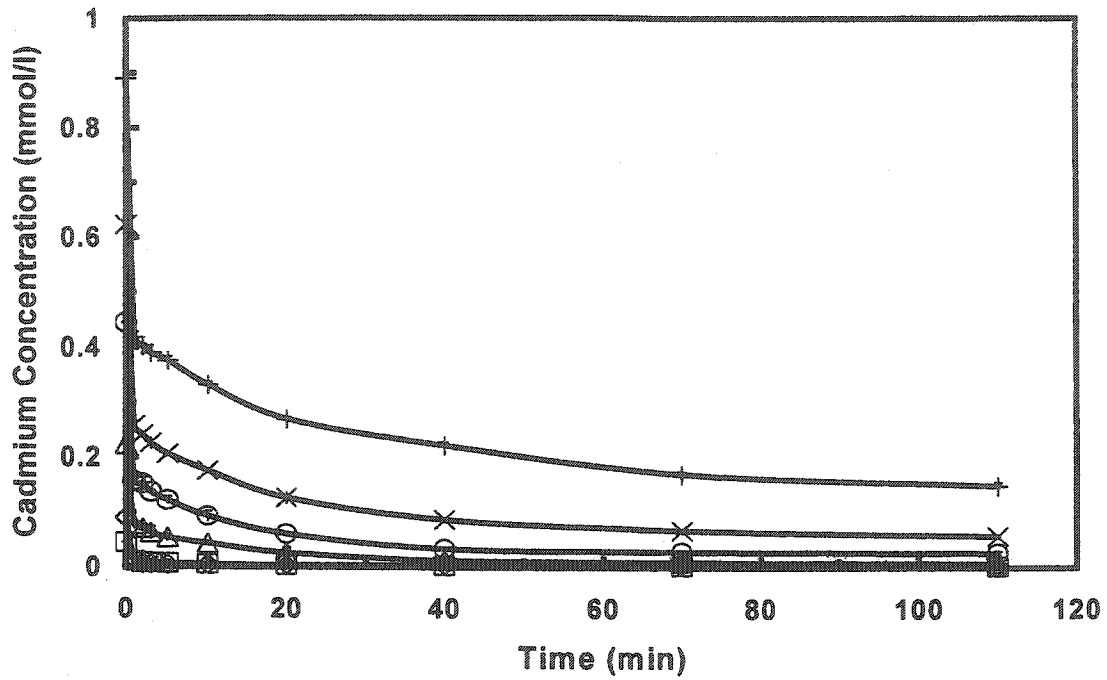


Fig. 6.42: Effect of initial concentration on cadmium concentration in solution (0.57 mm size particles, initial pH7.6, agitation speed 200 rpm, corncob concen. 10 g/l). □ 5 mg/l, ◇ 10 mg/l, △ 25 mg/l, ○ 50 mg/l, × 70 mg/l, + 100 mg/l.

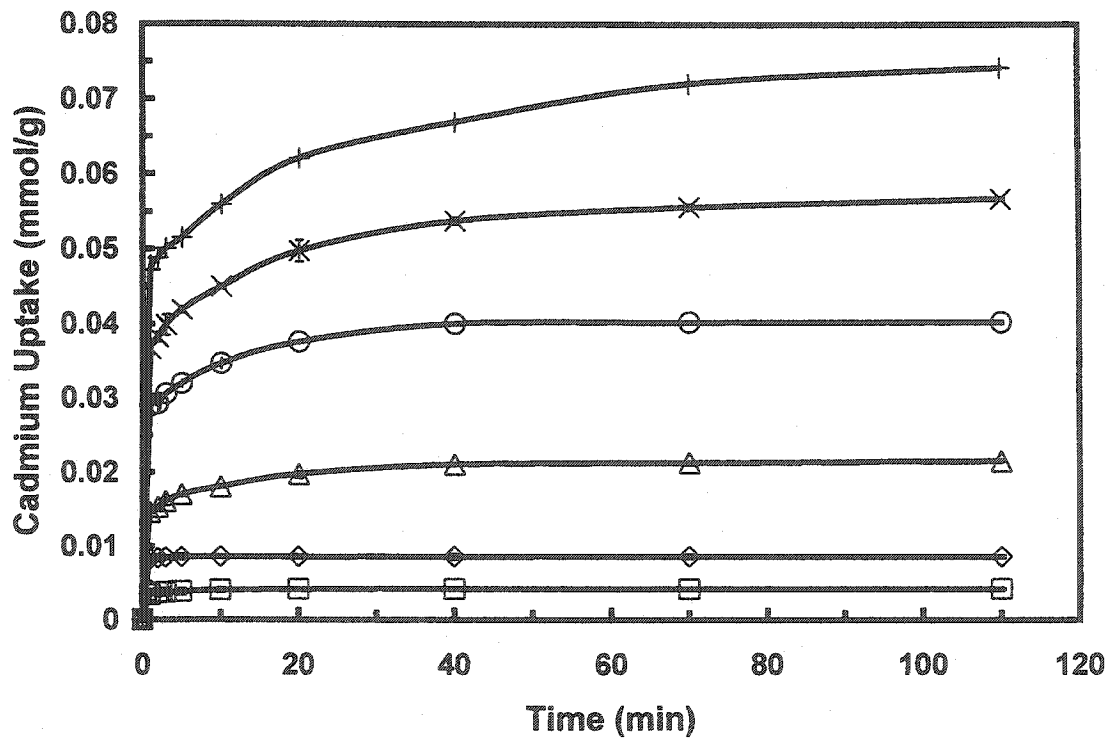


Fig. 6.43: Effect of initial concentration on uptake of cadmium (conditions as Fig. 6.42). □ 5 mg/l, ◇ 10 mg/l, △ 25 mg/l, ○ 50 mg/l, × 70 mg/l, + 100 mg/l.

removal efficiencies, and the higher uptakes. Since the adsorption capacity is constant for a certain quantity of the corncob particles, a higher ion concentration will result in a decrease of removal efficiency. On the other hand, a higher ion concentration contributes to a higher uptake because of a higher mass transfer driving force.

6.9 Effect of Pretreatment of Corncob Particles with Sodium Hydroxide

As indicated in Chapter 6.6, the uptake of metal ions by the corncob particles decreases at the too high initial pH values. To confirm this phenomenon, some corncob particles were treated by 1 M sodium hydroxide. The result of base treatment shows that about 80 % of the components in the corncob particles have been removed (Chapter 5.1.1). The isotherms for copper using the corncob particles treated with sodium hydroxide and without the treatment are showed in Fig. 6.44. The isotherms show that the uptake is much lower when the base-treated corncob particles were used. For example, at an equilibrium concentration of 0.50 mmol/l in the solution, the uptakes are 0.034 mmol/g for the pretreated corncob particles and 0.082 mmol/g for the untreated corncob particles. As indicated in Chapter 5.1.1, 85 % of the contents of the corncob particles are cellulose and hemicellulose. The cellulose will be degraded into various organic acids under the conditions of fairly concentrated alkali, such as 1 M NaOH, above 80°C (Biermann, 1996). The much lower uptake for the pretreated corncob particles, which were treated by 1 M NaOH at 100°C (Chapter 5.1.1), indicates that the cellulose and hemicellulose in the corncob particles have been changed into various organic acids and lost during pretreatment process. It is also concluded that the cellulose and hemicellulose in the corncob particles are mainly responsible for the biosorption of the metal ions.

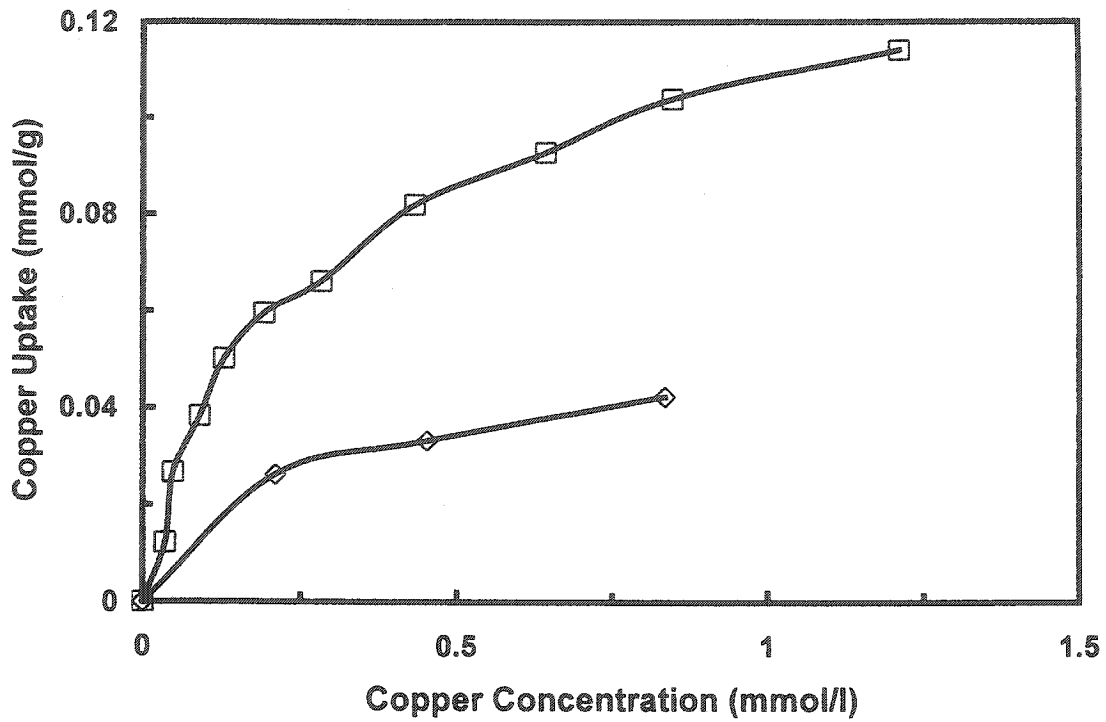


Fig. 6.44: Effect of NaOH pretreatment on adsorption isotherms of copper. ◇ pretreatment, □ no pretreatment.

6.10 The Estimation of Free Energy of Adsorption for Various pH Values at 25°C

Assuming that the various adsorption mechanisms act independently, the free energy of adsorption (ΔG_{ads}) can be expressed as the sum of the contributions of the chemical, solvation, and coulombic mechanisms (James and Healy, 1972), and it is given by the following expression:

$$\Delta G_{ads} = \Delta G_{chem} + \Delta G_{coul} + \Delta G_{solv} \quad (6.13)$$

where

$$\Delta G_{coul} = -RT \ln K_{coul} \quad (6.14)$$

$$\Delta G_{chem} = -RT \ln K_{chem} \quad (6.15)$$

$$\Delta G_{solv} = -RT \ln K_{solv} \quad (6.16)$$

Considering that the equilibrium constants of the adsorption process is:

$$K_e = K_{chem} K_{coul} K_{solv} \quad (6.17)$$

Then the free energy of adsorption is:

$$\Delta G_{ads} = -RT \ln K_e = -RT \ln K_{chem} - RT \ln K_{coul} - RT \ln K_{solv} \quad (6.18)$$

where

$$K_{coul} = \frac{\exp\left(-\frac{2F\Psi_\beta}{RT}\right)}{\left[\exp\left(-\frac{F\Psi_o}{RT}\right)\right]} \quad (6.19)$$

$$K_e = \frac{k_{ads}}{k_{des}} \quad (6.20)$$

The parameters, K_e , K_{coul} , K_{solv} and K_{chem} , represent the apparent adsorption, the coulombic, the solvation, and the specific chemical equilibrium constants, respectively, the constant, F , is the Faraday constant (96485 C/mol), and the parameters, ψ_β and ψ_o , are the surface potentials of the inner Helmholtz plane β and the surface plane o of the electrical double layer.

From equation (6.19), it can be seen that the change of coulombic free energy is related to the surface and inner Helmholtz plane potentials at a constant temperature. The former can be estimated by the difference between the pH_{zcp} and the pH in solutions (Equation (6.1)). The latter needs an electrical double layer model for estimation. Some electrical double layer models, such as the diffusion layer, the constant capacitance, the basic stern, and the triple layer models, have been summarized (Westall, 1980). In present work, the diffusion layer model has been adopted, since the estimation of capacitance in the other models is difficult. According to this model:

$$\sigma_o + \sigma_d = 0 \quad (6.21)$$

$$\Psi_\beta = \Psi_d = \Psi_o \quad (6.22)$$

where σ is the charge density (C/m^2) of the planes. Subscripts o, β , and d denote the surface, inner, and outer Helmholtz planes of the electrical double layer, respectively.

Substituting equations (6.1) and (6.22) into equation (6.19), the following expression for K_{coul} is obtained:

$$K_{coul} = \exp\left(-\frac{F\Psi_o}{RT}\right) = \exp\left[-\frac{0.059F(pH_{zcp} - pH)}{RT}\right] \quad (6.23)$$

The solvation energy term depends on the difference between the inverse of dielectric constant in the bulk solution and the inverse of that on the interface. It can be estimated by equation (6.24) (James and Healy, 1972).

$$\begin{aligned} \Delta G_{solv} = & \left(\frac{z_i^2 e^2 N}{16\pi\epsilon_o}\right) \left[\frac{1}{r_{ion} + 2r_w} - \frac{r_{ion}}{2(r_{ion} + 2r_w)^2} \right] \left(\frac{1}{\epsilon_{int}} - \frac{1}{\epsilon_{bulk}} \right) \\ & + \left(\frac{z_i^2 e^2 N}{32\pi\epsilon_o}\right) \left(\frac{1}{r_{ion} + 2r_w} \right) \left(\frac{1}{\epsilon_{ads}} - \frac{1}{\epsilon_{int}} \right) \end{aligned} \quad (6.24)$$

Using,

$$\epsilon_{int} = \left[\frac{\epsilon_{bulk} - 6}{1 + 1.2 \times 10^{-17} (d\Psi/dx)} \right] + 6 \quad (6.25)$$

$$\frac{d\Psi}{dx} = -2\kappa \frac{RT}{zF} \sinh\left(\frac{zF\Delta\Psi_x}{2RT}\right) \quad (6.26)$$

$$\Delta\Psi_x = \frac{2RT}{zF} \ln \left\{ \frac{\exp\left(\frac{ZF\Psi_o}{2RT}\right) + 1 + \left[\exp\left(\frac{ZF\Psi_o}{2RT}\right) - 1 \right] \exp(-\kappa x)}{\exp\left(\frac{ZF\Psi_o}{2RT}\right) + 1 - \left[\exp\left(\frac{ZF\Psi_o}{2RT}\right) - 1 \right] \exp(-\kappa x)} \right\} \quad (6.27)$$

where

$$\text{Dabye length } \kappa = 0.328 \times 10^{10} I^{1/2}$$

$$x = (r_{ion} + 2r_w)$$

z_i = sign and number of charges on the adsorbed ion.

$z = 1$ (for 1:1 background electrolyte).

The parameters, ϵ_{int} , ϵ_{bulk} , ϵ_{ads} , and ϵ_o , are the dielectric constants of interface, solvent (water), solid (adsorbent) and vacuum (8.85×10^{-12} C/(v.m)), respectively. r_{ion} and r_w are the radii of metal ion and water (m), The constants, N and e , are the Avogadro's constant (6.022×10^{23} mol⁻¹) and the elementary charge (1.60×10^{-19} C), and I and κ are the ionic strength of background electrolyte (mol/l) and the Dabye length (m), respectively. When the pH is equal to the pH_{zcp} , Ψ_o , $\Delta\Psi_x$, and $d\Psi/dx$ are equal to zero. ϵ_{int} in Eq. (6.25) is equal to ϵ_{bulk} (the dielectric constant of water 78.5). The solvation free energy in equation (6.24) is reduced to the solvation free energy at pH_{zcp} :

$$\Delta G_{solv,zcp} = \left(\frac{z_i^2 e^2 N}{32\pi\epsilon_o} \right) \left(\frac{1}{r_{ion} + 2r_w} \right) \left(\frac{1}{\epsilon_{ads}} - \frac{1}{\epsilon_{bulk}} \right) \quad (6.28)$$

The radii of copper and cadmium are 0.72 Å and 0.97 Å, respectively. If the dielectric constant of the corncob is taken 2.4, i. e., equal to that of cellulose (Mizumachi, 2001), because 85 % of the corncob is cellulose and hemicellulose, the solvation free energies of 80.5 kJ/mol for copper and 75.1 kJ/mol for cadmium at the pH_{zcp} are obtained using equation (6.28). The free energies of adsorption ΔG_{ads} can be estimated from equation (6.18) in which K_e is from Table 6.1 and equation (6.8). The values of ΔG_{ads} increase from 1.87 kJ/mol at a pH of 4.5 to 11.0 kJ/mol at a pH of 5.5 for copper, and from 8.28 kJ/mol at a pH of 6.0 to 20.5 kJ/mol at a pH of 8.3 for cadmium. It is noted that ΔG_{coul} and ΔG_{chem} are only a function of the pH of the solution and temperature, respectively. At the pH_{zcp} , the free energy of adsorption will be equal to the sum of the chemical free energy and the solvation free energy. The chemical free energies (-72.6 kJ/mol for copper

and -72.4 kJ/mol for cadmium with mixed particle size) can be estimated from the difference between the adsorption free energy and the solvation free energy at the pH_{zcp} . Furthermore, with an increase of the pH, ΔG_{coul} will decrease from 5.52 kJ/mol at a pH of 4.0 to -3.02 kJ/mol at a pH of 5.5 for copper, and -5.86 kJ/mol at a pH of 6.0 to -19.0 kJ/mol at a pH of 8.3 for cadmium. Once ΔG_{ads} , ΔG_{coul} , and ΔG_{chem} are known, ΔG_{solv} with various pHs can be calculated using equation (6.13). ΔG_{solv} will increase from 69.0 kJ/mol at a pH of 4.0 to 86.6 kJ/mol at a pH of 5.5 for copper, and from 86.5 kJ/mol at a pH of 6.0 to 112 kJ/mol at 8.3 for cadmium. These results are shown in Figs. 6.45 and 6.46. They indicate that the chemical and solvation free energies are major contributions to the adsorption free energy, while the coulombic free energy is smaller. The results also indicate that the chemical free energy is constant, and the solvation free energy and the adsorption free energy increase with an increase of pH during biosorption processes of cupric and cadmium ions on the corncob particles.

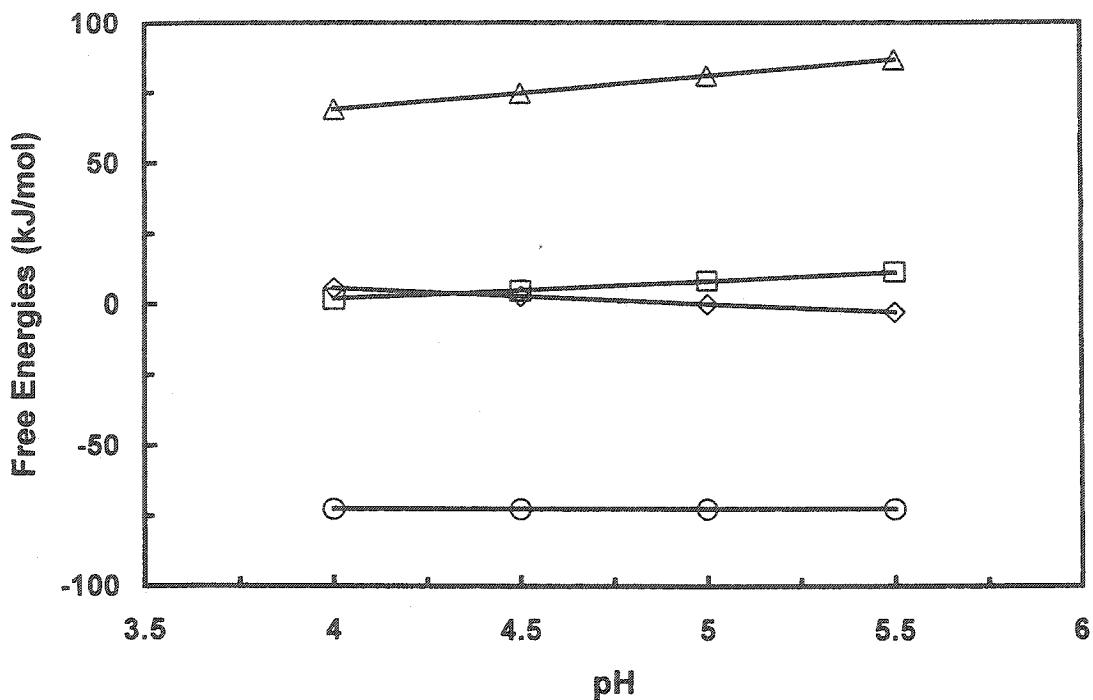


Fig. 6.45: The relationship between free energies and pH for copper. \square changes of adsorption free energies, \diamond changes of coulombic free energies, \triangle changes of solvation free energies, \circ changes of chemical free energies. Symbols are calculated data using Eqs. (6.13-6.16).

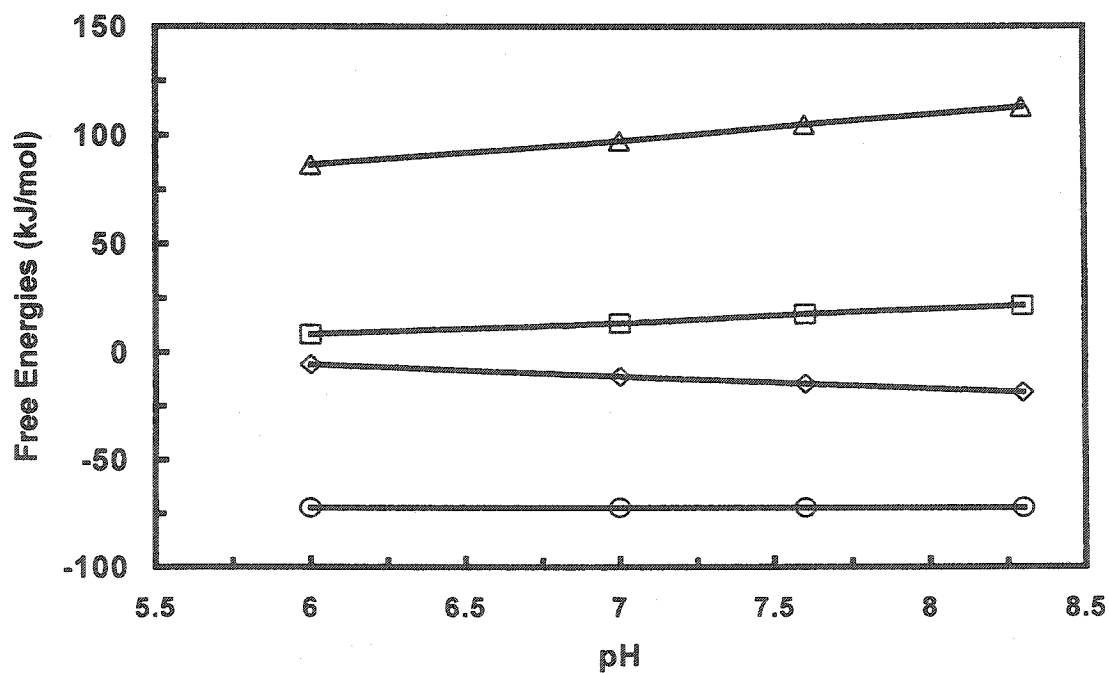


Fig. 6.46: The relationship between free energies and pH for cadmium. \square changes of adsorption free energies, \diamond changes of coulombic free energies, \triangle changes of solvation free energies, \circ changes of chemical free energies. Symbols are calculated data using Eqs. (6.13-6.16).

CHAPTER SEVEN

CONCLUSIONS AND RECOMMENDATIONS

7.1 Conclusions

Corn cob, an agricultural by-product, has a low cost and a good ability for binding metal ions. At a higher initial pH in the range of pH 4.0 - 6.0 for copper and pH 4.0 - 8.3 for cadmium, the corn cob particles have more affinity for the two metal ions. The adsorption characteristic can be described by the Langmuir model in the range of the initial pH 4.0 - 6.0 and below the equilibrium concentration of 1.2 mmol/l of copper in the solution, and pH 6.0 - 8.3 and below 0.65 mmol/l for cadmium. A new equation correlating the maximum adsorption capacity and the equilibrium constant with the pH and the pH_{zcp} can describe the changes of metal ion uptake by the corn cob particles with various pH values. The equilibrium constants in the Langmuir model decrease with an increase of temperature, which shows that biosorption processes of copper and cadmium on the corn cob particles are exothermic.

Several factors on adsorption kinetics, such as agitation speed, particle size, initial pH, concentration of corn cob particles, and initial metal ion concentration, were investigated. A higher uptake of the metal ions by the corn cob particles was found with a higher agitation speed, initial pH, and initial ion concentration, a smaller particle size, and a lower biomass concentration. However, at the initial pH values higher than 6.6 for copper and 7.6 for cadmium, the removal efficiencies for the two ions decrease since some components, which are mainly responsible for biosorption, in the corn cob particles were extracted into the solution. A novel reversible surface reaction model combined

with an effectiveness factor was developed. The model fits the kinetic experimental data well. The intrinsic forward and backward rate constants (1.092 l/(mmol.min) and 0.472 min⁻¹ for copper and 2.88 l/(mmol.min) and 0.184 min⁻¹ for cadmium, respectively) were obtained by the regression under the conditions of the elimination of the external and intraparticle diffusion. The other two parameters, the effectiveness factor and the maximum adsorption capacity, in the model change with the initial pH and particle size. The maximum removal efficiencies are about 70 % for copper and 90 % for cadmium by one treatment.

The chemical, solvation, and coulombic free energy in the Ion-Solvent Interaction (James-Healy) model were estimated by means of the equilibrium constants with the pH and the pH_{zcp}, which was determined by the primary equilibrium method of H⁺ and OH⁻ of the corncob particles. These results indicate that the chemical and solvation free energies are two main factors that affect adsorption, and their effects are opposite. The adsorption free energy increases with the pH value during the biosorption processes of cupric and cadmium ions on the corncob particles.

7.2 Recommendations

Based on the results obtained in this study, the following recommendations are suggested:

- Study the biosorption of the other heavy metal ions, such as lead, cobalt, and chromium, by the corncob particles to investigate the possibilities of treating the wastewater containing these metal ions.

- Measure the surface area of the corncob particles and their porous size distribution to estimate the diffusivities in the intraparticle diffusion model.
- Compare the simulated results of the three kinds of models, the external diffusion model, the intraparticle diffusion model, and the surface reaction model, to determine the rate-controlling step during the biosorption processes.
- Research the other binary metal ion systems to find more inversed U-shaped isotherms.
- Modify the corncob particles by chemicals to enhance their adsorption capacity.

REFERENCES

- Adamson, A. W. and Gast, A. P., *Physical Chemistry of Surface*, 6th Ed., p393 John Wiley & Sons, New York (1997).
- Ahmed, S. M., "Studies of the dissociation of oxide surfaces at the liquid-solid interface", *Canadian Journal of Chemistry*, **44**, 1663-1670 (1966).
- Aksu, Z., and Kutsal, T., "A bioseparation process for lead(II) ions from waste water by using *C. vulgaris*", *J. Chem. Tech. Biotechnol.*, **52**, 109-118 (1991).
- Al-Asheh, S. and Duvnjak, Z., "Adsorption of copper by canola meal", *Journal of Hazardous Materials*, **48**, 83-93 (1996).
- Al-Asheh, S and Duvnjak, Z., "Binary metal sorption by pine bark: study of equilibria and mechanisms", *Separation Science and Technology*, **33**(9), 1303-1329 (1998).
- Akratopulu, K. Ch., Vordonis, L., and Lycourghiotis, A., "Effect of temperature on the point of zero charge and surface dissociation constants of aqueous suspensions of γ - Al_2O_3 ", *J. Chem. Soc., Faraday Trans., I*, **82**, 3697-3708 (1986).
- Ash, S. G., and Bonn, R., and Everett, D. H., "A high-precision apparatus for the determination of adsorption at the interface between a solid and a solution", *J. Chem. Thermodynamics*, **5**, 239-246 (1973).
- Azab, M. S. and Peterson, P. J., "The removal of cadmium from water by the use of biological sorbents", *Water Science and Technology*, **21**, 1705-1706 (1989).
- Bellot, J. C. and Condoret, J. S., "Modeling of liquid-chromatograph equilibria", *Process Biochem.*, **28**(6), 365-376 (1993).
- Biermann, C. J., *Handbook of Pulping and Papermaking*, 2nd Ed., p407, Academic Press, Inc., San Diego, California, USA (1996).
- Benjamin, M. M., and Leckie, J. O., "Competitive adsorption of Cd, Cu, Zn, and Pb on amorphous iron oxyhydroxide", *J. Colloid and Interface Sci.*, **82**, 410-419 (1981).
- Bosinco, S., Roussy, J., Guibal, E., and Cloirec, P., Le, "Interaction mechanisms between hexavalent chromium and corncob", *Environmental Technology*, **17**, 55-62 (1996).
- Boyd, G. E., Adamson, A. W., and Myers, L. S. Jr., "The exchange adsorption of ions from aqueous solutions by organic zeolites II", *Am. Chem. Soc.*, **69**, 2836-2848 (1947).
- Butler, J. A. V. and Ockrent, C. J., "Studies in electrocapillarity. III The surface tensions of solutions containing two surface-active solutes", *J. Phys. Chem.*, **34**, 2841-2859 (1930).

Chien, S. H., and Clayton, W. R., "Application of Elovich equation to the kinetics of phosphate release and sorption in soils", *Soil Soc. Amer. J.*, **44**(2), 265-268 (1980).

Chong, K. H., and Volesky, B., "Metal biosorption equilibria in a ternary system", *Biotechnol. Bioeng.*, **49**(6), 629-638 (1996).

Christophi, C. A. and Axe, L., "Competition of Cd, Cu, and Pb adsorption on goethite", *J. Environmental Engineering*, Jan., 66-74 (2000).

Cowan, E. C., Zachara, J. M., and Resch, C. T., "Cadmium adsorption on iron oxides in the presence of alkaline-earth elements", *Envir. Sci. and Technol.*, **25**, 437-446 (1991).

Corapcioglu, M. O., and Huang, C. P., "The adsorption of heavy metals onto hydrous activated carbon", *Water Research*, **21**, 1031-1044 (1987).

Coulson, J. M., and Richardson, J. F., *Chemical Engineering*, sixth edition, Vol. 1, a p604, b p282, Butterworth-Heinemann, Linacre House, Jordan Hill, Oxford, (1999).

Crank, J., *The Mathematics of Diffusion*; 2nd Ed. p94, University Press: Oxford, U. K. (1975).

David, L. D., *CRC Handbook of Chemistry and Physics*, Frederikse H. P. R. 78th Ed., CRC, Boca Raton, Fla., a p1-7, b p9-74, c p10-201, d p5-93 (1998).

Ebihara, K., and Takeuchi, M., "Effect of particle size on the cation-exchange capacity, surface area and zinc-binding capacity of refined corn hull", *Agric. Biol. Chem.*, **55**(6), 1455-1458 (1991).

Esposito, A., Pagnanelli, F., and Veglio, F., "pH-related equilibria models for biosorption in single metal systems", *Chemical Engineering Science*, **57**, 307-313 (2002).

Faust, S. D. and Aly, O. M., *Chemistry of Water Treatment*, Butterworths, a p513, b p14, c p503, d p9 Woburn, MA (1983).

Friedman, M. and Waiss, A. C. Jr., "Mercury uptake by selected agricultural products and by-products", *Environmental Science and Technology*, **6**(5), 457-458 (1972).

Fritz, W., "Competitive Adsorption of Dissolved Organics on Activated Carbon", p283, Chapter 9 in *Activated Carbon Adsorption of Organics from the Aqueous Phase*, Vol. 1, Suffet, I. H. and McGuire, M. J., Eds., Ann Arbor Science Publishers, Ann Arbor, Mich. (1980).

Fokkink, L. G. J., DeKeizer, A., and Lyklema, J., "Temperature dependence of the electrical double layer on oxides: rutile and hematite", *J Colloid Interface Sci.*, **127**, 116-131 (1989).

Furusawa, T. and Smith, J. M., "Intraparticle mass transport in slurries by dynamic adsorption studies", *AIChE J.* **20**, 88-93 (1974).

Gadde, R., and Laitinen, H. A., "Studies of heavy metal adsorption by hydrous iron and manganese oxides", *Analytical Chemistry*, **46**, 2022-2026 (1974).

Good, N. E., Winget, D., Winter, W., and Connolly, T. N., "Hydrogen ion buffers for biological research", *Biochemistry*, **5**(2), 467-477 (1966).

Grathwohl, Peter *Diffusion in Natural Porous Media*; p44, Kluwer Academic Publishers: Norwell, MA (1998).

Guibal, E., Milot, C., and Tobin, J. M., "Metal-anion sorption by chitosan beads: equilibrium and kinetic studies", *Ind. Eng. Chem. Res.*, **37**, 1454-1463 (1998).

Guibal, E., Jansson-Charrier, M., Saucedo, I., and Le Cloirec, P., "Enhancement of metal ion sorption performances of chitosan: effect of the structure on the diffusion properties", *Langmuir*, **11**, 591-598 (1995).

Hanasen, A., M., Leckie, J. O., and Mee, L., D., "Cobalt (II) interactions with Near-coastal marine sediments", *Environ. Geol. Water Sci.*, **19**(2), 97-111 (1992).

Haynie, Donald, *Biological Thermodynamics*, p195, Cambridge University Press, New York, NY, USA (2001).

Helferich, F, *Ion Exchange*, p5, McGraw-Hill Book Company, Inc. (1962).

Higbie, R., "The rate of absorption of pure gas into a still liquid during short periods of exposure", *Trans. Am. Inst. Chem. Eng.*, **31**, p365-389 (1935)

Hill, C. G., *An Introduction to Chemical Engineering Kinetics and Reaction Design*, p26, John Wiley & Sons, Inc. (1977).

Holleman, A. F., *Inorganic Chemistry*, a p195, b p1129 Academic Press, San Diego, California, USA (2001).

Holtzclaw, H. F. Jr., Robinson, W. R., and Nebergall, W. H., *General Chemistry*, 6th Ed., p102, D. C. Heath and Company, Lexington, Mass. (1984).

Itoh, M., Yuasa, M., and Kobayashi, T., "Adsorption of metal ions on yeast cells at varies cell concentrations", *Plant Cell Physio.*, **16**, 1167-1169 (1975).

James, R. O., and Healy, T. W., "Adsorption of hydrolysable metal ions at the oxide-water interface", *J. Colloid Interface Sci.*, **40**(1), 65-81 (1972).

- Jha, I. N., Iyengar, L., and Rao, A., "Removal of cadmium using chitosan", *J. Environ. Eng.-ASCE*, **114**, 962-974 (1988).
- Johnson, B. B., "Effect of pH, temperature, and concentration on the adsorption of cadmium on goethite", *Environ. Sci. Technol.*, **24**, 112-118 (1990).
- Johnson, R. D., and Arnold, F. H., "The Temkin isotherm describes heterogeneous protein adsorption", *Biochemica et Biophysica Acta*, **1247**, 293-297 (1995).
- Kipling, J. J., "Adsorption of nonelectrolytes from solution", *Quart. Revs.*, **5**, 60-71 (1951).
- Keinath, T. M. and Weber, W. J. Jr., "A predictive model for the design of fluid-bed adsorbers", *J. Water Pollut. Cont. Fed.*, **40**, 741-765 (1968).
- Kuyucak, N., and Volesky, B., "Biosorbent for recovery of metals from industrial solutions", *Biotechnology Letters*, **10**(2), 137-142 (1988).
- Lehrfeld, J., "Conversion of agricultural residues into cation exchange materials", *Journal of Applied Polymer Science*, **61**, 2099-2105 (1996).
- Leusch, A. and Volesky, B., "The influence of film diffusion on cadmium biosorption marine biomass", *Journal of Biotechnology*, **43**, 1-10 (1995).
- Liu, K. T. and Weber, W. J. Jr., "Characterization of mass transfer parameters for adsorber modeling and design", *J. Water Pollut. Cont. Fed.*, **53**, 1541-1550 (1981).
- Low, M. J. D., "Kinetics of chemisorption of gases on solids", *Chem. Reviews*, **60**, 267-312 (1960).
- Maliou, E., Malamis, M., and Sakellarides, P. O., "Lead and cadmium removal by ion exchange", *Water Sci. Technol.*, **25**, 133-138 (1992).
- Markham, E. C. and Benton, A. F., "The adsorption of gas mixtures by silica", *J. Am. Chem. Soc.*, **53**, 497-507 (1931).
- Marshall, W. E., Evans, W. J., and Champagne, E. T., "Use of rice milling byproducts (hulls & bran) to remove metal ions from aqueous solution", *J. Environ. Sci. Health*, **A28**(9), 1977-1992 (1993).
- Marshall, W. E., and Champagne, E. T., "Agricultural byproducts as adsorbents for metal ions in laboratory prepared solutions and in manufacturing wastewater", *J. Environ. Sci. Health*, **A30**(2), 241-261 (1995).
- McKay, G., and Allen, S. J., "Surface mass transfer process using peat as an adsorbent for dyestuffs", *Canadian Journal of Chemical Engineering*, **58**, 521-526 (1980).

McKay, G., and Bino, M. J., "Application of two resistance mass transfer model to adsorption systems", *Chem. Eng. Res. Des.*, **63**, 168-174 (1985).

Mizumachi, H, "Wood-polymer composites", *Wood and Cellulosic Chemistry*, p717, Edited By Hon, D., N.-S. and Shiraishi, N. (2001).

Mohamad, S., E. and Akl, M. M. "Evaluation of surface diffusion and external mass transfer coefficients for maize cob adsorption", *Trans. Egypt. Soc. Chm. Eng.*, **17**(1), 52-66 (1991a).

Mohamad, S., E. and Akl, M. M. "Evaluation of effective pore diffusion and external mass transfer coefficients for maize cob adsorption", *Trans. Egypt. Soc. Chm. Eng.*, **17**(1), 31-51 (1991b).

Morris, J. C., and Weber, W. J., "Adsorption of biochemically resistant materials from solution", *Environmental Health Series AWTR-0*, May (1964).

Netzer, A., and Hughes, D. E., "Adsorption of copper, lead, and cobalt by activated carbon", *Water Research*, **18**(8), 927-933 (1984).

Odozi, T. O., Okeke, S., and Lartey, R. B., "Studies on binding metal ions with polymerizes corn cob and a composite resin with sawdust and onion skin", *Agricultural Wastes*, **12**, 13-21 (1985).

Odozi, T. and Emelike, R., "The sorption of heavy metals with corncob hydroxylate-red onion skin resins", *Journal of Applied Polymer Science*, **30**, 2715-2719 (1985).

Periasamy, K. and Namasivayam, C., "Process development for removal and recovery of cadmium from wastewater by a low-cost adsorbent: adsorption rate and equilibrium studies", *Ind. Eng. Chem. Res.* **33**, 317-320 (1994).

Perrin, D. D., and Dempsey, Boyd, *Buffers for pH and Metal Ion Control*, p43, Chapman and Hall, New York, USA (1974).

Randall, J. M., Hautala, E., and McDonald, G., "Binding of heavy metal ions by formaldehyde polymerized peanut skins", *J. Appl. Polym.*, **22**, 379-387 (1978).

Richie, A. G., "Alternative to the Elovich equation for the kinetics of adsorption of gases on solids", *J. Chem. Soc. Faraday Trans. 1*, **73**, 1650-1653 (1977).

Robertson, A. P., and Leckie, J. O., "Cation binding predictions of surface complexation models: effects of pH, ionic strength, cation loading, surface complex, and model fit", *J. Colloid Interface Sci.*, **188**, 444-472 (1997).

- Sag, Y., and Kutsal, T., "Determination of the biosorption heats of heavy metal ions on *Zoogloea ramigera* and *Rhizopus arrhizus*", *Biochemical Engineering Journal*, **6**, 145-151 (2000).
- Schwuger, M. J., and Smoka, H. G., "Mixed adsorption of ionic and nonionic surfactants on active carbon", *Colloid & Polymer Sci.*, **255**, 589-594 (1977).
- Sengupta, M., and Paul, T. B., "Multicomponent ion exchange equilibria I Zn^{2+} - Cd^{2+} - H^+ and Cu^{2+} - Ag^+ - H^+ on Amberlite IR 120", *Reac. Pol.*, **3**, 217-229 (1985).
- Smith, J. M., *Chemical Engineering Kinetics*, 2nd, a p428, b p17, c p439, McGraw-Hill, Inc. (1970).
- Smith, J. M., *Kinetics of Adsorption*, Chapter 2 in *Adsorption from Aqueous Solution*, *Advances in Chemistry Series 79*, American Chemistry Society, Washington, D. C. (1968).
- Singh, D. K., Tinari, D. P., and Saksena, D. N., "Removal of lead from aqueous solutions by chemically treated used tea leaves", *Indian J. Environ. Health*, **35**(3), 169-177 (1993).
- Sorg, T. J., Csanady, M., and Gary, S., "Treatment technology to meet the interim drinking water regulations for inorganics: Part 3", *J. Amer. Waters Assoc.*, **70**(12), 680-691 (1978).
- Sun, G., and Shi, W., "Sunflower stalks as adsorbents for the removal of metal ions from wastewater", *Ind. Eng. Chem. Res.*, **37**, 1324-1328 (1998).
- Tewari, P. H., and Campbell, A. B., "Temperature dependence of point of zero charge of cobalt and nickel oxides and hydroxides", *J. Colloid and Interface Science*, **55**(3), 531-539 (1976).
- Tewari, P. H., and Lee, Won, "Adsorption of Co(II) at the oxide-water interface", *J. Colloid Interface Sci.*, **52**, 77-88 (1975).
- Tien, Chi *Adsorption Calculations and Modeling*, p79, Butterworth-Heinemann: Newton, MA (1994).
- Tobin, J. M., Copper, D. G., and Neufeld, N. J., "Uptake of metals by *Rhizopus arrhizus* biomass", *Appl. Environ. Microbiol.*, **47**, 821 (1984).
- Valsaraj, K. T., *Elements of Environmental Engineering Thermodynamics and Kinetics*, 2nd Ed., p150-154, CRC Press LIC (2000).
- Vaughan, T. Seo, C. W. and Marshall, W. E. "Removal of selected metal ions from aqueous solution using modified corncobs", *Bioresource Technology*, **78**, 133-139 (2001).

Volesky, B., "Biosorbents for metal recovery", *Trends in Biotechnology*, **5**, 96-101 (1987).

Volesky, B. "Removal and recovery of heavy metals by biosorption", a p38, b p13, *Biosorption of Heavy Metals*, Ed by Volesky, B., CRC Press, Inc., Boca Raton, Florida (1990).

Wartelle, L. H. and Marshall, W. E. "Citric acid modified agricultural by-products as copper ion adsorbents", *Advances in Environmental Research*, **4**, 1-7 (2000).

Weber, W. J. Jr., *Physicochemical Processes for water Quality Control*, Wiley-Interscience, New York (1972).

Weber, W. J. Jr., and Rumer, R. R. Jr., "Intraparticle transport of surfonated alkylbenzenes in a porous solid: diffusion with nonlinear adsorption", *Water Resources Res.*, **1**(3), 361-373 (1965).

Weber, W. J. Jr. and Morris, J. C., "Kinetics of adsorption on carbon from solution", *J. Sanit. Eng. Div. ASCE SA2*, 31-59 (1963).

Westall, J and Hohl, H., "A comparison of electrostatic models for the oxide/solution interface", *Advances in Colloid and Interface Science*, **12**, 265-294 (1980).

Wing, R. E., "Corn fiber citrate: Preparation and ion exchange properties", *Ind. Crops Prod.*, **5**, 301-330 (1996).

Zasoski, R. J. and Burau, R. G., "Sorption and sorptive interactions of cadmium and zinc on hydrous manganese oxide", *Soil Sci. Soc. Am. J.*, **52**, 81-87 (1988).

Zhou, J. L., and Kiff, R., J., "The uptakes of copper from aqueous solution by immobilized fungal biomass", *J. Chem. Tech. Biotechnol.*, **52**, 317-340 (1991).

APPENDIX

One Example of Determination of Parameters in Eq. (4.19)

From Fig. 6.2, the Langmuir model parameters, the equilibrium constant of K_i and the maximum adsorption capacity of q_m , at 0.21 mm particle size at the various pH values can be obtained (Table 6.1). These q_m will be applied in the kinetic simulation.

From the curve of particle size of 0.21 mm in Fig. 6.24, which is supposed that the intraparticle diffusion has been eliminated ($\eta = 1$), and using equation (4.23), the intrinsic rate constants k_{ads} (1.082 l/(mmol.min)) and k_{desH} (0.472 min⁻¹) for copper can be determined.

It is noted that in Fig. 6.24, the uptakes, q , at the final contact time (i. e., approaching equilibrium point) increase with decreasing the corncob particle size, which is different from the normal cases where the uptakes at a final time should not change with the particle size. This may suggest that the maximum adsorption capacity, q_m , obtained from the finest size (0.21 mm) in the Langmuir model cannot be fully used in the cases of larger particle sizes (i. e., effective maximum adsorption capacities decrease with an increase of the particle size). Therefore, the (effective) maximum adsorption capacities, q_m , in equation (4.19) are regressed as an adjustable parameter for other three curves in Fig. 6.24, similar to the effectiveness factor η

For Figs. 6.28 and 6.34 that show the effects of the pH and the corncob concentration on adsorption kinetics, respectively. Since the intrinsic rate constants k_{ads} (1.082 l/(mmol.min)) and k_{desH} (0.472 min⁻¹) are known, which do not change with

operating conditions, the other two parameters, η and q_m , in equation (4.19) are regressed because both parameters are a function of the pH and the biomass concentration.

The similar approach was also applied to cadmium adsorption kinetics on the corn cob particles.